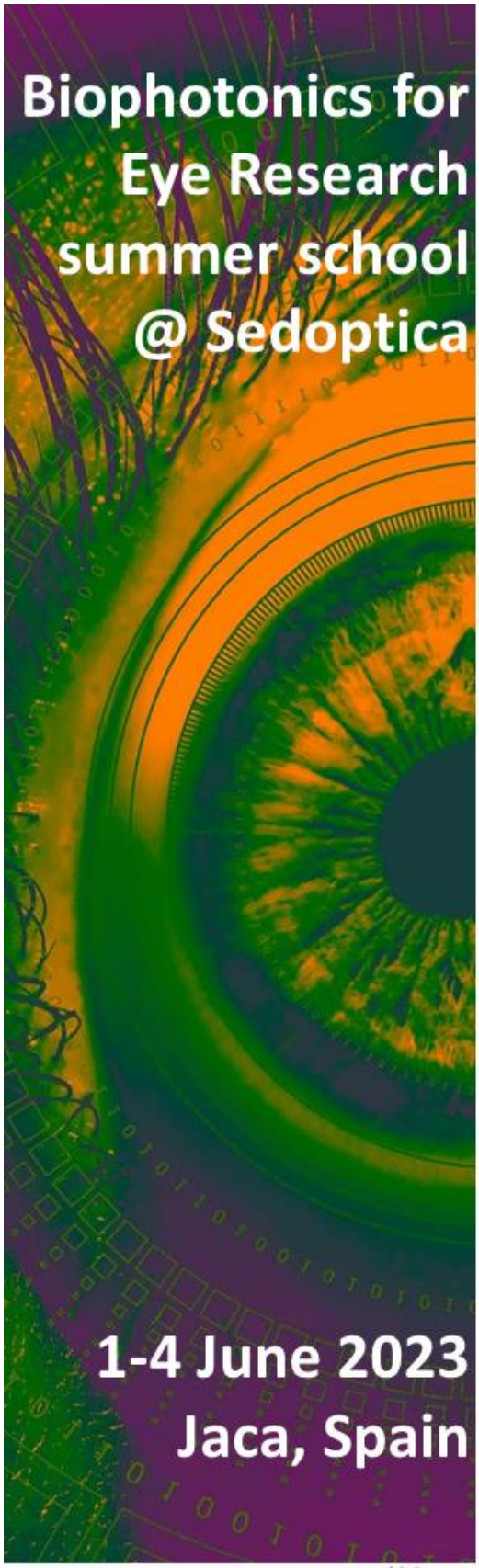

Biophotonics for Eye Research
BER2023
JACA 1-4 JUNE

The Biophotonics for Eye Research summer school @Sedoptica is a scientific meeting dealing with aspects of the Physics and Engineering of the human eye.

This meeting aims to follow on from the summer schools organized previously by the Visual Sciences committee @SEDOPTICA. In this meeting, we shall focus on new results and techniques in imaging technology and optics of vision.

The format of the meeting is a series of classes, invited lectures with ample time for discussion and interaction, and scientific contributions presentations. The interaction of basic science and cutting edge technology to develop future solutions for better vision will be at the center of the workshop.

Young researchers and doctoral students will present their research in dedicated sessions.

The meeting will be hosted in University of Zaragoza residence in Jaca, the Aragonese Pyrenees (1-4 June 2023).

SEDOPTICA
SOCIEDAD ESPAÑOLA DE ÓPTICA

COMITÉ de CIENCIAS de la VISIÓN

Universidad Zaragoza
1542

SPIE.

OPTICA
Advancing Optics and Photonics Worldwide

BER2023

Biophotonics for Eye Research summer school @Sedoptica

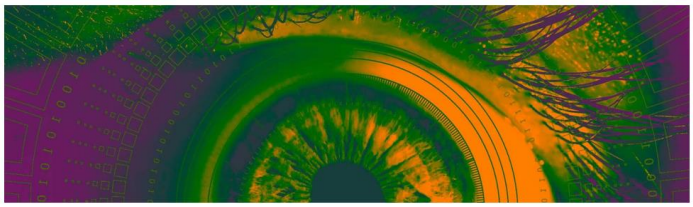

ISBN	978-84-09-53100-4 / No commercial
Publisher	Sociedad Española de Óptica
Title	Proceedings of the Biophotonics for eye research summer school 2023 of the Spanish Optical Society
Peer reviewed by	Sociedad Española de Óptica
Conference	Biophotonics for eye research summer school 2023 of the Spanish Optical Society nº 1, Jaca 2023
Format	Digital: download; PDF
Collection	Proceedings of the Biophotonics for eye research summer school of the Spanish Optical Society
Nr. / Edition Nr.	1/1
Language	English
Publishing date	01/08/2023
Place of publication	Spain
Main Topic Thema	TTB : Applied Optics
Topic Thema	PHJ : Applied Physics
Main Topic IBIC	TTB : Applied Optics

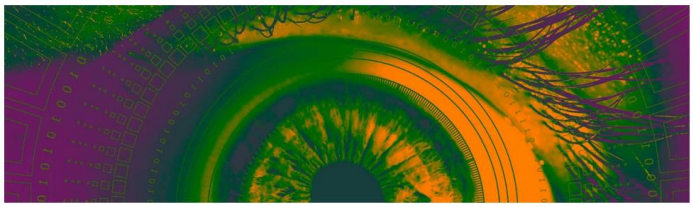

ORGANIZING & SCIENTIFIC COMMITTEE

María Viñas	Institute of Optics-CSIC (Spain)
Francisco Ávila	University of Zaragoza (Spain)
Mikel Aldaba	Technical University of Catalonia-UPC (Spain)
Justo Arines	University of Santiago de Compostela-USC (Spain)
José Juan Castro	University of Granada (Spain)
Carmen Martínez	University of Valladolid (Spain)
María S. Millán	Technical University of Catalonia-UPC (Spain)
E. Josua Fernández	University of Murcia (Spain)
Juanma Bueno	University of Murcia (Spain)
Pablo Artal	University of Murcia & VOPTICA (Spain)
Susana Marcos	University of Rochester (USA)
Carlos Dorronsoro	Institute of Optics-CSIC & 2EyesVision (Spain)
Jaume Pujol	Technical University of Catalonia-UPC (Spain)
Rafael Navarro	Spanish National Research Counil (CSIC) (Spain)
Brian Vohnsen	University College Dublin (Ireland)
Christina Schwarz	University of Tübingen (Germany)
Carmen Canovas	Johnson & Johnson Surgical Vision (The Netherlands)
Andrea Curatolo	Int. Centre for Translational Eye Research-ICTER (Poland)
Sabine Kling	ETH Zurich & University of Bern (Switzerland)
Linda Lundström	KTH Royal Institute of Technology (Sweden)

LOCAL COMMITTEE

Francisco Ávila	University of Zaragoza (Spain)
Laura Remón	University of Zaragoza (Spain)
Óscar del Barco	University of Zaragoza (Spain)

INSTITUTIONAL SPONSORS

SPIE.

OPTICA Advancing Optics and Photonics Worldwide

SEDOPTICA SOCIEDAD ESPAÑOLA DE ÓPTICA

COMITÉ de CIENCIAS de la VISIÓN

Universidad Zaragoza 1542

BER2023

Biophotonics for Eye Research summer school @Sedoptica

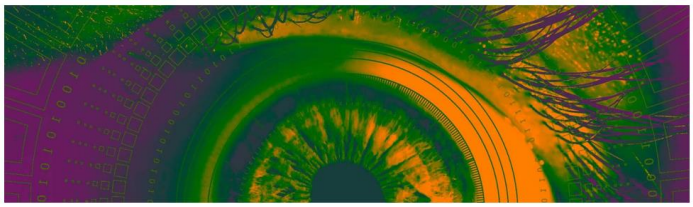

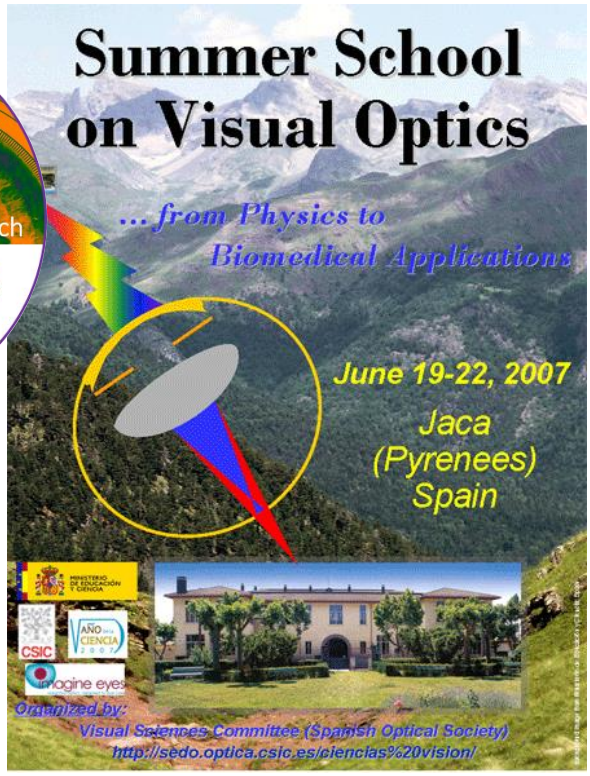

GOLD SPONSORS

LASING

NKT Photonics

SILVER SPONSORS

SmarThings4Vision

2EYESVISION

THORLABS

imagine eyes

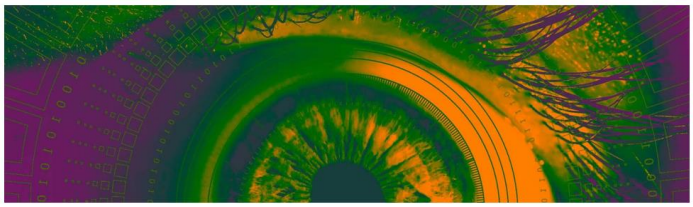

BER2023 will gather students, researchers, and renowned scholars in an international forum on Biophotonics for eye research, with a series of classes, invited lectures with ample time for discussion and interaction, and scientific contributions presentations. The interaction of basic science and cutting-edge technology to develop future solutions for better vision will be at the center of the workshop.

TECHNICAL PROGRAM

	1 June-Thursday	*2 June-Friday*	*3 June-Saturday*	*4 June-Sunday*
Morning		***SESSION I*** Optics and vision	***SESSION IV*** New horizons in refractive, cataract and eye surgery	***YOUNG RESEARCHERS SESSION***
		SESSION II Structure and Biomechanics of the eye	***SESSION V*** Diagnostics tools & Visual Function	***AWARDS CEREMONY & CLOSING REMARKS***
Afternoon	***MINI COURSE*** Early career skills for a career in Optics & Photonics	***SESSION III*** Novel technologies for unsolved problems in Visual Optics	***SOCIAL EVENT*** Pyrenee mountains	
Evening	***KEYNOTE TALK*** Biophotonics for eye research ***WELCOME RECEPTION BER2023***	***SOCIAL EVENT*** Dinner with the experts		

1 JUNE		**THURSDAY**		
	3:00-6:00 pm	**MINI COURSE.** ***Early career skills for a career in Optics & Photonics***		
	3:00-4:15	**Workshop**. Career development. Soft skills and Networking **Hands-on**. Grants & fellowships preparation		
	4:15-4:45	**Break**		
	4:45-5:15	**Session**. Career development opportunities: OPTICA & SPIE		
	5:15-6:00	**Round table**. Academia vs Research vs. Industry. Everything Everywhere All at Once.	Pablo Artal Carlos Dorronsoro Valentín Guadaño Yaiza García Moderator: Mikel Aldaba	| UMU & VOPTICA | CSIC & 2EyesVision | Lasing | Bausch & Lomb
	7:00-8:00 pm	**KEYNOTE TALK**		
		Prof. Pablo Artal University of Murcia (Spain)	*Biophotonics for eye research*	
	8:00-10:00 pm	**WELCOME RECEPTION**		

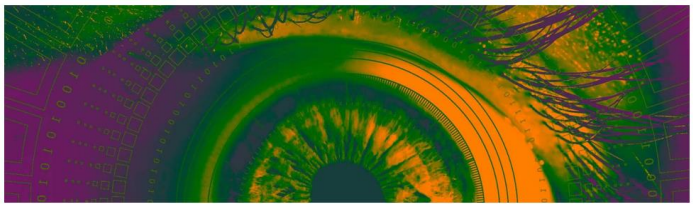

2 JUNE		**FRIDAY**	
	9:00-11:00 am	**SESSION I. Optics and vision**	
	9:00-9:20	**Prof. Susana Marcos** Univ. Rochester (USA)	*Aberrations, modified optics and neural adaptation*
	9:20-9:40	**Prof. Linda Lundstron** KTH Royal Institute of Technology (Sweden)	*Focus on the periphery: Optical and neural factors*
	9:40-10:00	**Prof. E. Josua Fernández** Univ. Murcia (Spain)	*Chromatic aberration in the human eye and its impact in vision and imaging*
	10:00-10:20	**Prof. Brian Vohnsen** Univ. College Dublin (Ireland)	*What is the Stiles-Crawford effect?*
	10:20-10:40	**Prof. Justo Arines** Univ. Santiago de Compostela (Spain)	*Hartmann-Shack: from the base to the application*
	10:40-11:00	**Discussion**	*Moderator: Mikel Aldaba*
	11:00-11:30	**Break**	
	11:30-1:30	**SESSION II. Structure and Biomechanics of the eye**	
	11:30-11:50	**Sabine Kling** Swiss Federal Inst. Tec.-ETH (Switzerland)	*Ocular Biomechanics*
	11:50-12:10	**Judith Birkenfeld** Institute of Optics-CSIC (Spain)	*Optical Coherence Tomography for the investigation of ocular biomechanics: An overview of different excitation methods and their applications*
	12:10-12:30	**Prof. Juan Manuel Bueno** University of Murcia (Spain)	*In Vivo Multiphoton Imaging of Ocular Structures*
	12:30-12:50	**Prof. Carmen Martínez** University of Valladolid (Spain)	*Corneal regeneration: Biological and optical studies*
	12:50-1:15	**Discussion**	*Moderator: Francisco Ávila*
	1:30-2:30	**Lunch**	
	2:30-4:30 pm	**SESSION III. Novel technologies for unsolved problems in Visual Optics**	
	2:30-2:50	**Pablo Pérez-Merino** University of Ghent (Belgium)	*New intraocular lens technologies: Ray Tracing optimization & Bio-interfaced pressure sensors*
	2:50-3:10	**Zhijian Zhao** University of Tübingen (Germany)	*Developing multiphoton imaging of the living retina to understand the visual cycle*
	3:10-3:30	**Andrea Curatolo** International Centre for Translational Eye Research (Poland)	*Structural and functional imaging of the retina with Spatio-Temporal Optical Coherence Tomography*
	3:30-3:50	**María Viñas-Peña** Institute of Optics-CSIC (Spain)	*Investigating the ocular optics, biomechanics and structure using light-based technologies*
	3:50-4:10	**James Germann** Institute of Optics-CSIC (Spain)	*Multi-Photon Microscopy: How the microscale affects the macro-world*
		Discussion	*Moderator: Alejandra Consejo*
	8:00-10:00 pm	**SOCIAL EVENT. Dinner with the experts**	

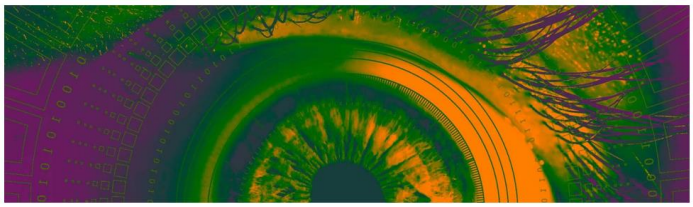

3 JUNE		**SATURDAY**	
	8:00-9:00 am	**BREAKFAST REDES TEMÁTICAS** **Hybrid event by invitation**	
	9-11 am	**SESSION IV. New horizons in refractive, cataract and eye surgery**	
	9:00-9:20	**Prof. Maria S. Millán** Technical University of Catalonia-UPC (Spain)	*Presbyopia-correcting intraocular lens with diffractive profile. Chromatic considerations*
	9:20-9:40	**Carlos Dorronsoro** Institute of Optics-CSIC & 2EyesVision (Spain)	Simulation and validation of multifocal lenses with SimVis technology
	9:40-10:00	**Prof. JM Meijomé** University of Minho (Portugal)	*Multifocal Contact Lenses for Myopia Control*
	10:00-10:30	**Discussion**	*Moderator: Laura Remón*
	10:30-11:00	**Break**	
	11:00-1:30 pm	**SESSION V. Diagnostics tools & Visual Function**	
	11:00-11:20	**Prof. Alejandra Consejo** University of Zaragoza (Spain)	*Diagnostic Tools for Keratoconus*
	11:20-11:40	**Prof. Mikel Aldaba** Technical University of Catalonia-UPC (Spain)	*New technologies in visual refraction*
	11:40-12:00	**Prof. Meritxell Vilaseca** Technical University of Catalonia-UPC (Spain)	*Clinical applications of a visible and near-infrared multispectral camera for reflectance evaluation of eye fundus structures*
	12:00-12:20	**Prof. Miriam Casares** University of Granada (Spain)	*Alcohol, driving, and visual performance*
	12:20-1:00	**Discussion**	*Moderator: Oscar del Barco*
	1:00-2:00	**Lunch**	
	5:30-7:30 pm	**SOCIAL EVENT. Trekking on the Pyrenee mountains**	
	8:00-10:00 pm	**CONFERENCE DINNER**	

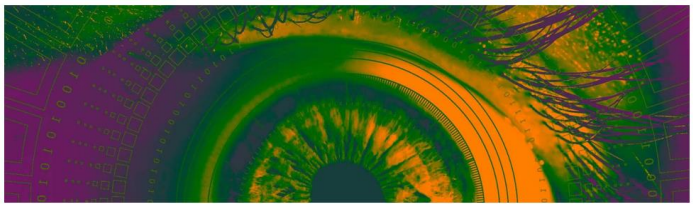

	SUNDAY		
9-12 am	**YOUNG RESEARCHERS SESSION: PAPERS & POSTERS**		
9-10:30 am	**Paper session**		
	T1	**Aina Turull-Mallofré**	*Prediction of the spherical subjective refraction using accommodation data in machine learning models*
	T2	**Rosa Vila-Andrés**	*In-line characterization of toric contact lens permanent marks using a lensless microscope*
	T3	**Eduardo Esteban-Ibañez**	*Clinical validation of daily soft multifocal contact lens simulations using SimVis Gekko based on in-vitro measurements*
	T4	**André Amorim**	*Age and gender contribution to refraction and keratometry based axial length estimates derived using a support vector regression algorithm*
	T5	**Alba M. Paniagua-Díaz**	*Straylight and Optical Memory Effect characterization of ex-vivo cataractous crystalline lenses*
	T6	**Alejandro Martínez Jiménez**	*Dual Ultrahigh Speed Swept-Source & Time Domain Optical Coherence Tomography system using a time-stretch laser and a KTN deflector*
		Discussion	*Moderator: María Viñas-Peña*
10:30-12 am	**Poster session + coffee break**		
4 JUNE	**P1**	**Ebrahim Safarian Baloujeh**	*Effect of small angle misalignments on ocular wavefront Zernike coefficients*
	P2	**Francesco Martino**	*Do interocular differences affect binocular visual performance after inducing forward scattering?*
	P3	**Joan Goset**	*Eye movements inPost-COVID-19 condition patients*
	P4	**PaulaGarcía**	*Colorimetric screen characterization based on a non-primary constancy colour model*
	P5	**Diana Gargallo**	*Using a clinical OCT to characterize the edge shape of Contact Lenses (CL)*
	P6	**Pilar Casado**	*Exploring the relationship between axial length and disability glare vision*
	P7	**Lourdes Camblor**	*Caracterización del color percibido en visión con luz infrarroja pulsada*
	P8	**Danielle Viviana Ochoa**	*Effects of optical irradiation with laser and LED light sources on cell cultures of leukemia*
	P9	**João M.M Linhares**	*A Color Vision Test – comparing results between computer screens*
	P10	**José A.R. Monteiro**	*A Color Vision Test Assessed by Neural Networks*
	P11	**Laura Clavé**	*Colour vision change after multifocal diffractive IOL implantation*
	P12	**Victor Rodriguez-Lopez**	*Direct Subjective Refraction: a new approach for refractive error measurements and the impact of accommodation*
	P13	**Sara F.Lima**	*Impact of refractive error compensation methods on a webcam eyetracking system*
	P14	**Alba Herrero-Gracia**	*Comparison of the Farnsworth Munsell 100 Hue and MUC tests in the over 50s*
	P15	**Anabel Martínez-Espert**	*Assessment of the optical performance of presbyopic intraocular lenses by measuring of the Through the Focus Point Spread Function*
	P16	Withdrawn	

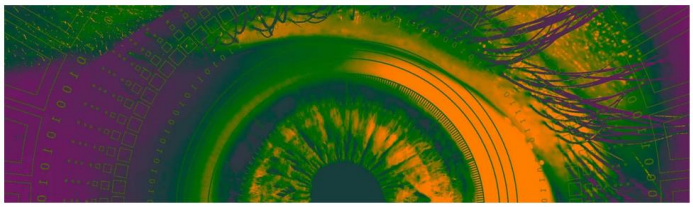

P17	**IñakiBlanco-Martínez**	*Contribution of the anterior corneal topography to off-axis wavefront aberration: a pilot study*
P18	**Inas Baoud Ould Haddi**	*Effect of aberrometry in intraocular lenses on visual quality*
P19	**Raquel Salvador-Roger**	*Calibration of a tunable Lens for optometric applications*
P20	**Sara Ferrer-Altabás**	*Low-cost manually tunable lens for astigmatic compensation in optical instruments*
P21	**Fátima Cuéllar**	*Optical imaging quality and expected range of vision of two presbyopia-correcting intraocular lens designs*
P22	**Marina Bou**	*Development of a portable and low-cost multispectral fundus camera*
P23	**María Mechó-García**	*Repeatability in wavefront measurement at different pupil sizes in Young subjects*
P24	**Santiago Sager**	*A compact binocular adaptive optics visual simulator for clinical use in highly aberrated patients*
P25	**Sara Silva-Leite**	*Visual Function of Myopic Young Adult swith a Novel Ophthalmic Lens for the Control of Myopia Progression*
P26	**Jessica Gomes**	*Dynamic accommodation from wavefront aberrometry in symptomatic and asymptomatic subjects*
P27	**XinyuWang**	*Adaptive Optics vision simulator for 2-photon visión*
P28	**ErikM.Barrios**	*Restoration of retinal images using dictionary learning-based methodology*
P29	**María Pilar Urizar**	*Towards a low-cost optical biometer: development of a low-cost optical delay line for axial scans and a whole-eye beam scanner for fixation checks*
P30	**Elena Moreno**	*Wavefront shaping and optical memory effect of ex-vivo cataractous crystalline lenses*
P31	**Pilar Granados-Delgado**	*Eye dominance and visual quality*
P32	**Amal Zaytouny**	*Clinical validations of the SimVis binocular visual simulator*
	Moderators: María Viñas-Peña, Francisco Ávila, Mikel Aldaba	
12 -12:15 pm	**CLOSING REMARKS. AWARDS CEREMONY**	

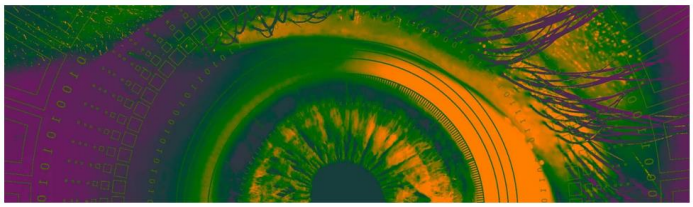

KEYNOTE TALK

Biophotonics for eye research

Pablo Artal Soriano

LOUM. University of Murcia (Spain)

This presentation will cover in a tutorial-style several of the recent topics of research in visual optics carried out in my laboratory. This will include, wearable adaptive optics for the eye, the importance of the eye's peripheral vision and vision under pulsed infrared light.

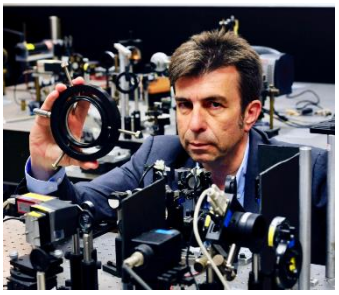

Pablo Artal *was born in Zaragoza (Spain) where I studied Physics at the University of Zaragoza. He was a pre-doctoral fellow at the Madrid-CSIC "Instituto de Optica" under the supervision of Javier Santamaria, a post-doctoral research fellow, first at Cambridge University (UK) and later at the Institut d'Optique in Orsay, France. After returning to Spain, he obtained a permanent researcher position at the Instituto de Optica. In 1994, he became the first full Professor of Optics at the University of Murcia, Spain founding the "Laboratorio de Optica". He spent sabbatical years in Rochester (USA) and Sydney (Australia). He is currently a distinguished visiting professor at the Central South University in Changsha, China.*

Pablo Artal's *research interests are centered on the optics of eye and the retina and the development of optical and electronic imaging techniques to be applied in Vision, Ophthalmology and Biomedicine. He pioneered highly innovative and significant advances in the methods for studying the optics of the eye and contributed substantially to our understanding of the factors that limit human visual resolution. In addition, several of my results and ideas in the area of ophthalmic instrumentation over the last years have been introduced in instruments and devices currently in use in clinical Ophthalmology. He has published more than 350 reviewed papers that received more than 24600 citations (h-index of 80) in Google Scholar, presented more than 200 invited talks in international meetings and around 150 seminars in research institutions around the world.*

He was elected fellow member of the Optical Society of America (OSA) in 1999, fellow of the Association for research in Vision and Ophthalmology (ARVO) in 2009 and 2013 (gold class), fellow of the European Optical Society (EOS) in 2014 and fellow of the SPIE in 2016. In 2013, he received the "Edwin H. Land Medal" for scientific contributions to the advancement of diagnostic and correction alternatives in visual optics. This award was established by the Optical Society of America (OSA) and the Society for Imaging Science and Technology (IS&T) to honor Edwin H. Land. This medal recognizes pioneering work empowered by scientific research to create inventions, technologies, and products. In 2014, he was awarded with an Advanced Research grant of the European Research Council. In 2015, he received the "King Jaime I" award in New Technologies. In 2018, he was awarded the Spanish National Research award "Juan de la Cierva" and in 2019 the "Edgar D. Tillyer" award of the Optical Society of America for "the pioneering use of optics and photonics technologies to unravel the human visual system and to improve eye diagnostics and correction". In 2021, he was awarded the medal of the Spanish Royal Physics Society. I am a co-inventor of 30 international patents in the fields of Optics and Ophthalmology and the co-founder of four spin-off companies developing my concepts and ideas.

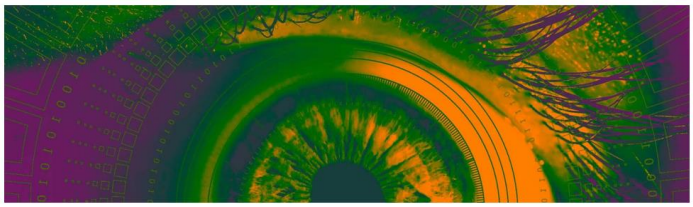

SESSION I Optics and vision

Aberrations, modified optics and neural adaptation

Susana Marcos

Center for Visual Science. University of Rochester (US)

Aberrations degrade the quality of the images projected on the retina. The optical quality of the eye is driven by the geometry and structure of the ocular components of the eye. Changes in cornea or lens occur with age, accommodation, corneal disease or conditions such as cataract, presbyopia and myopia results in changes in the optical quality of the eye. Quantifying the contributions of the structure of cornea and lens on the optical aberrations of the eye is important to improve the treatment strategies in the eye. These treatments may entail modifying the corneal shape, replacing the crystalline lens by an intraocular lens, or fitting a contact lens.

Adaptive Optics (AO) is an excellent way to manipulate the optics of the eye and simulate vision with these corrections prior to a more invasive procedure. State-of-the-art head-mounted see-through devices that allow testing different lens designs AO can also provide full correction of the aberrations of the eye, leaving the eye diffraction-limited, opening possibilities to investigate the spatial limits to spatial resolution.

Perceived visual quality is not only determined by optical blur produced by the aberrations, but also to perceptual aspects, including neural adaptation. Adaptive Optics is also an ideal tool to measure after-effects associated to sharpening on blurring the image (with the deformable mirror).

Susana Marcos *es David R Williams Director of The Center for Visual Science, Nicholas George Professor of Optics at the Institute of Optics and Professor of Ophthalmology at the Flaum Eye Institute. She is Professor of Research Founder of the VioBioLab and past director at the Instituto de Optica-CSIC. She has pioneered multiple technologies for diagnostics and treatment in the eye, protected in 24 patents, many licensed to industry. She is co-founder of spin outs Plenoptika and Quicksee. She has served in numerous professional organizations, including as President of the Spanish Research Agency Advisory committee, Optica Chair of Publications Council and Board of Directors. She has won many awards including Optica Adolph Lomb Medal, Optica Edwin Land Medal, ICO Prize, Jaime I Award in New Technologies, Ramon y Cajal Medal by the Royal Academy of Science, National Award in Engineering.*

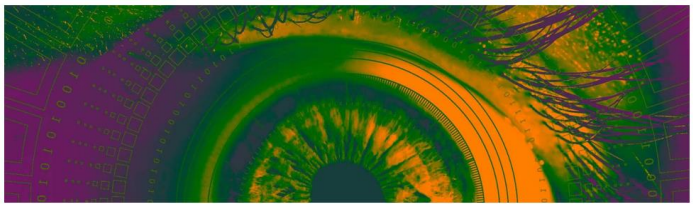

Focus on the periphery: Optical and neural factors

Linda Lundström

Department of Applied Physics, Royal Institute of Technology (KTH) (Sweden)

We investigate how peripheral optical errors affect vision with the aim to design better peripheral corrections to (1) reduce the ocular growth in myopia and (2) improve the remaining vision for individuals with large central visual field loss. Compared to central vision, peripheral visual function depends on a complex interaction of optical and neural limitations. The optical aberrations, both chromatic and monochromatic, are considerably larger in the periphery and the neural sampling density is lower. Hence, visual functions such as high contrast resolution, which are limited by the optical image quality for central vision, can be sampling limited off-axis. We therefore investigate the influence of chromatic and monochromatic aberrations on different peripheral visual functions.

Peripheral vision is evaluated with our adaptive optics visual simulator under well-controlled optical conditions for both monochromatic and polychromatic aberrations. Different visual functions are evaluated with sinusoidal Gabor gratings of different orientations presented on a calibrated monitor in 10-bit grayscale, utilizing alternative forced choice in Bayesian psychophysical procedures. Generally, high contrast peripheral resolution acuity is relatively insensitive to optical errors whereas low contrast sensitivity and detection acuity depend more on the peripheral image quality. Additionally, peripheral vision shows asymmetries both regarding the orientation of the stimuli and the sign of defocus.

ACKNOWLEDGEMENTS: Peter Unsbo, Abinaya Priya Venkataraman, Dmitry Romashchenko, Petros Papadogiannis, Simon Winter, Charlie Börjeson and Anna-Caisa Söderberg. Research funding from the European Commission and the Swedish Research council.

Linda Lundström *is a professor in Applied Physics at KTH specialized on the peripheral human eye. I have a MSc in Engineering Physics and I did my PhD in Visual Optics at KTH on building and programming a Hartmann-Shack wavefront sensor for peripheral measurements with the aim to improve the remaining vision for people with large central visual field loss. After that, I held a postdoc position with Pablo Artal at LOUM in Spain, working on instrumentation to decipher the progression of myopia. In 2009, I returned to KTH and am now leading the research in the Visual Optics group, which consists of two senior scientists and 2-3 doctoral students/postdocs. Our research concerns the formation of the retinal image and the optical limits to vision. We develop techniques in wavefront sensing, adaptive optics, and psychophysics specially to investigate the peripheral visual field and the effects of optical manipulation. Applications span from basic research to central visual field loss due to AMD and myopia development. Apart from research, I teach basic optics courses, mainly for students on the optometry education offered at Karolinska Institutet. I am also head of the division for Biomedical and X-Ray Physics at KTH.*

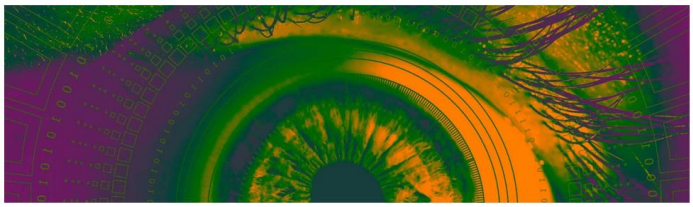

Chromatic aberration in the human eye and its impact in vision and imaging

Enrique Josua Fernandez

Laboratorio de Óptica, Centro de Investigación en Óptica y Nanofísica (CiOyN), Universidad de Murcia (Spain)

In this course several aspects of the chromatic aberration will be presented. It will start with the origins and the geometrical optics characterization of the chromatic aberration, to later show some of the most successful chromatic eye models currently used in the field[1]. Experimental methods for the determination of the chromatic aberration in the eye will be shown, discussing some of the practical issues associated to the existing techniques[2]. Both subjective and objective methods will be described and compared to gain a deep understanding of the limitations of each modality.

The impact of chromatic aberration in vision will be presented[3]. In this regard, its role in accommodation will be discussed. The apparent paradox of the correction of chromatic aberration for visual enhancement in normal vision, exhibiting a modest benefit when any, will be reviewed and discussed[4].

Finally, the role of chromatic aberration for retinal imaging will be presented. The only ophthalmic technique that uses inherently polychromatic light is optical coherence tomography (OCT). An introduction to this imaging modality will be given, together with some experimental methods for the correction of chromatic aberration in this context[5,6,7]. To conclude, limits to the performance and benefits of the chromatic aberration correction in OCT will be presented.

---

[1]D. A. Atchison and G. Smith; J. Opt. Soc. Am. A 22(1), 29 (2005).
[2]M. Vinas, C. Dorronsoro, D. Cortes, D. Pascual, and S. Marcos; Biomed. Opt. Express 6(3), 948 (2015).
[3]N. Suchkov, E. J. Fernandez, and P. Artal; Opt. Express 27, 35935 (2019).
[4]E. J. Fernandez, N. Suchkov, and P. Artal; Opt. Express 28, 37450 (2020).
[5]E. J. Fernandez and W. Drexler; Opt. Express 13, 8184 (2005).
[6]E. J. Fernandez, A. Unterhuber, B. Považay, B. Hermann, P. Artal, and W. Drexler; Opt. Express 14, 6213 (2006).
[7]E. J. Fernandez, B. Hermann, B. Považay, A. Unterhuber, H. Sattmann, B. Hofer, P. K. Ahnelt, and W. Drexler; Opt. Express 16, 11083 (2008).

Enrique Josua Fernandez *received the M.S. degree in Physics, specialty in Astrophysics, and the International Student Diploma in 1999 from the University of La Laguna, Spain, and Imperial College, London, UK, respectively. In 2004 he received his Ph.D. degree in Physics from University of Murcia, Spain, applying adaptive optics (AO) techniques to the human eye. From 2004 to 2006, he was Associate Researcher at University of Vienna, Austria, where he worked in ophthalmic optical coherence tomography (OCT). Since 2007, he is Associate Professor (tenured) at Physics Department, University of Murcia. He is the author of more than 50 articles, and more than 10 inventions, most of them licensed to the industry. He has been the cofounder of the spin-off company Voptica, being the first author of several patents of ophthalmic instruments for diagnosis and visual simulation based on AO technology, and several types of intraocular lenses. He has chaired the sections of Vision and Applications in the Spanish Optical Society (SEDOPTICA) and in OPTICA, formerly OSA. Among other distinctions, Dr. Fernandez was the recipient of the International Pascal Rol Award in 2006, SPIE; and the recipient of Young Researcher Award, Royal Spanish Physic Society and Spanish Optical Society in 2003. Currently he serves as vice-dean of Physics at the University of Murcia. His current research interests include new and efficient forms to generate high photon-bunching light sources for biomedical optics applications and quantum imaging.*

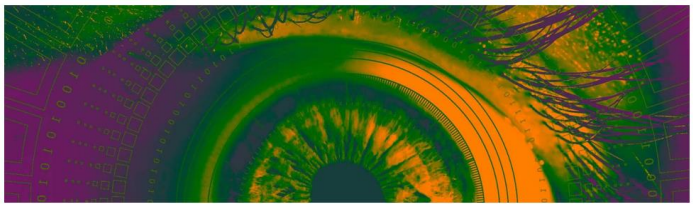

What is the Stiles-Crawford effect?

Brian Vohnsen

School of Physics, University College Dublin (Ireland)

The Stiles-Crawford effect (SCE) has remained an enigma in visual optics since its discovery 90 years ago by Walter Stiles and Brian Crawford.[1] Together, they quickly recognized that it has its origin in the retina that dampen the impact of oblique light. Yet, its true cause has eluded a satisfactory understanding for decades. Undoubtedly this is due to the time-consuming and challenging psychophysical techniques employed when analysing it point-by-point with Maxwellian light as well as a concurrent interest in waveguide optics.[2] At times, it has also been confused with an optical directionality in backscattered light, better known as the optical SCE. Both give rise to Gaussian-like distributions in the pupil plane, that can be confounded with the SCE. Only in the past decade has leakage of light been identified as the principal cause of the SCE,[3,4] deviating from the widespread assumption of imperfect waveguide coupling to the retinal photoreceptors.

Here, I will review the current understanding of the SCE (see Fig. 1) and report on how it impacts vision when integrated across the natural pupil providing a photopic apodization that is nearly an order-of-magnitude higher than with Maxwellian light while largely absent in scotopic conditions.[5] I will discuss how the same optics may have an impact on emmetropization and, therefore, on why being outdoors is vital to prevent the onset of myopia.[6] This suggests a delicate balance between the refractive optics of the anterior eye with the elementary light-capturing cones and rods of the retina to obtain good vision throughout life.

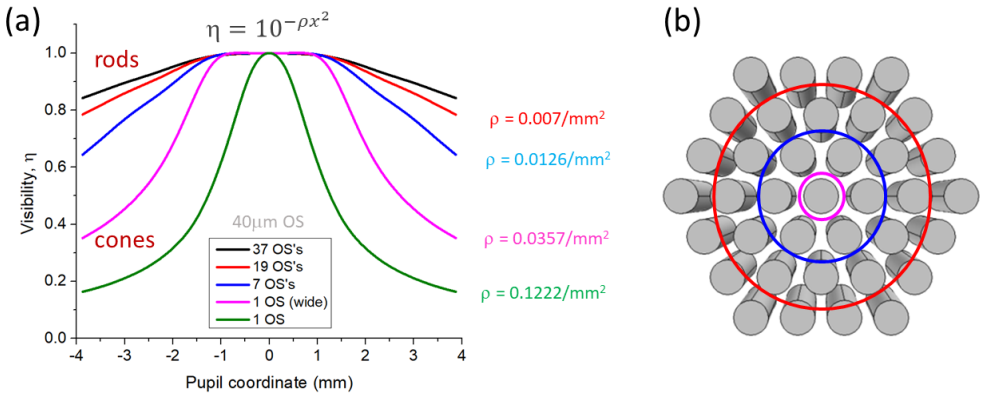

Figure 1: Model of light leakage between adjacent cells and corresponding effective SCE visibility plot.

[1]W. S. Stiles and B. H. Crawford, *Proc. R. Soc. London* **112,** 428 (1933).
[2]B. Vohnsen, *Handbook of Visual Optics (Ed. P. Artal)* **Vol. I**, 257 (2017).
[3]B. Vohnsen, *Biomed. Opt. Express* **5,** 1569 (2014).
[4]J. M. Ball, S. Chen, and W. Li, *Science Adv*. **8**, eabn2070 (2022)
[5]B. Vohnsen, A. Carmichael, N. Sharmin, S. Qaysi, and D. Valente, *J. Vision* **17**, 18:1 (2017).
[6]B. Vohnsen, *Vision Res*. **189,** 46 (2021).

Brian Vohnsen *is an associate professor at University College Dublin, where he is Chair of EDI in the School of Physics and Head of Postgraduate studies in Physics. He has a PhD from Aalborg University in Denmark, and has also been Marie Curie and Ramon y Cajal Fellow at LOUM in Murcia. He is Fellow of Optica and Chair of Optica Vision & Color in the Meetings Committee. He is on the ARVO annual meeting committee for VI and the ARVO publications committee.*

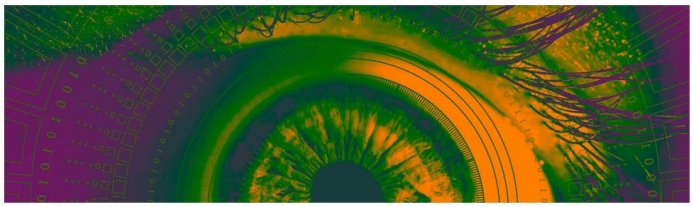

Hartmann-Shack: from the base to the application

Justo Arines

Department Applied Physics, Photonics4Life research Group, Faculty Optics & Optometry, University of Santiago de Compostela (Spain)

The Hartmann-Shack is probably the most used wavefront sensor in visual optics. It is present in most of the Optics laboratories in the world. However, now it is just a tool for most of the scientists. Despite its simplicity in terms of hardware (just a microlens array and a detector) the estimation of the wavefront with a Hartmann-Shack involves different optical concepts, engineering and computational aspects. This talk is planned to describe in detail the concepts and questions related with the bases and uses of the Hartmann-Shack[1]. We will start with some history, from the Hartmann sensor to the Hartmann-Shack. We will deal with the exact equations and the approximations that relates centroid displacements with wavefront gradients[1]. We will learn that the Hartmann-Shack can be used with point and extended sources[1], that can be used to center deformable mirrors or Spatial Light modulators[2]. That there is an optimum number of Zernike polynomials to be estimated, and the different sources of error involved on the estimation error[3]. We will understand the rules of Zernike scaling and transformation[4], the influence of the microlens distribution[5], the way in which ocular movements can be used to develop a synthetic Aperture Hartmann-Shack sensor[6], how to increase its dynamic range and sensitivity.

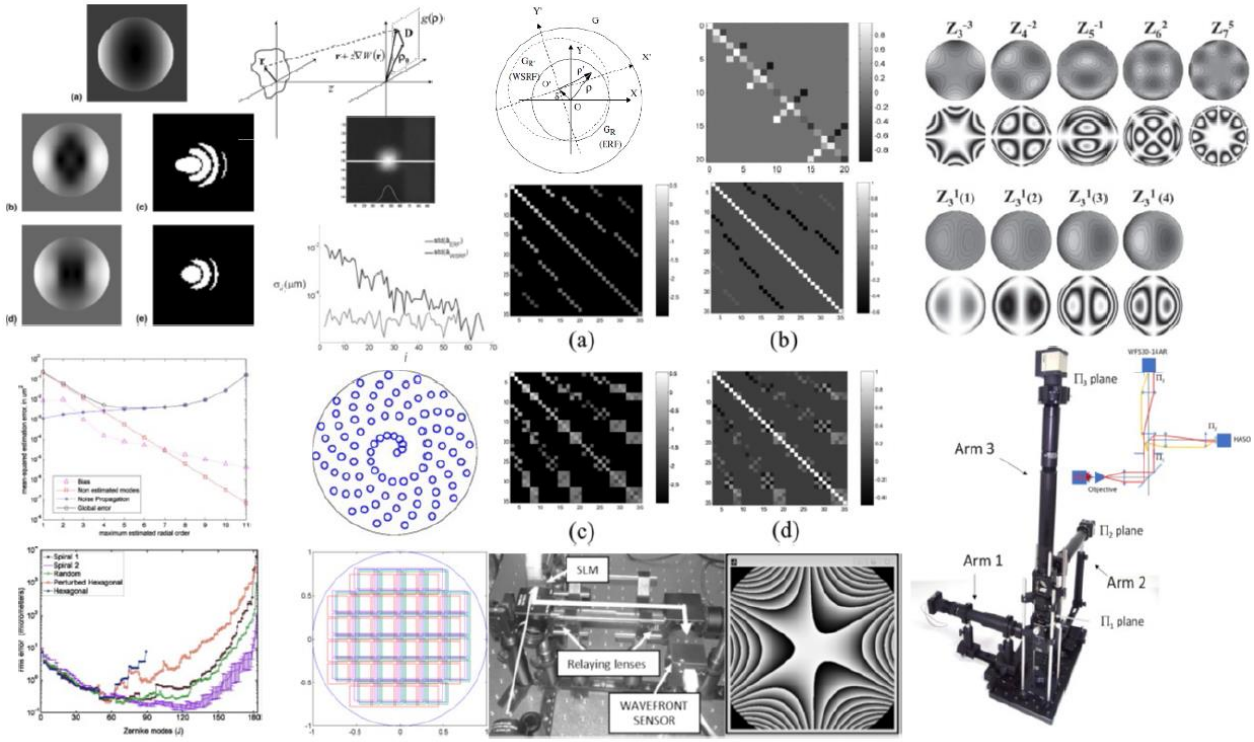

Figure 1: Collage of different studies related with Hartmann-Shack sensor

ACKNOWLEDGEMENTS: Ministerio de Ciencia e Innovación PID2020-115909RB-I00, and to S. Bará, J. Ares, E. Pailos, P. Prado, E. Acosta, and R. Navarro.

[1]J. Arines, TESIS DOCTORAL. (2006)
[2]J. Arines and A. García, (2020); *Optical Engineerin*, ***59***(4), 041206-041206 (2020).
[3]S. Bará, E. Pailos, and Justo Arines; *Optics Letters* **37**(12) 2427-2429, (2012).
[4]S. Bará, J. Arines, J. Ares, P. Prado; *J. Opt. Soc. Am. A,* **23**, 2061-2066 (2006).

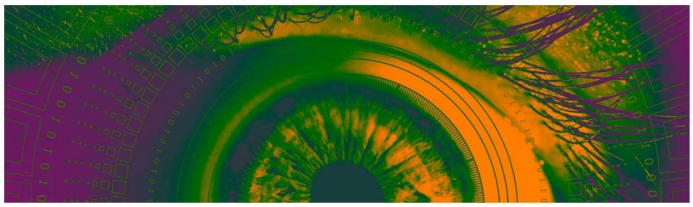

[5]R. Navarro, J. Arines, and R. Rivera; *Optics letters* **36**(4) 433-435, (2011).
[6]S. Bara, J. Arines, and E. Pailos; *Optical Engineering,* **53**(6) 061703-061703, (2014).

Justo Arines *is Associate Professor at the Faculty of Optics and Optometry of the University of Santiago de Compostela. Previously, he was hired by the University of Vigo and the University of Zaragoza. His teaching experience focuses on degrees in Physics and Optics and Optometry, as well as master's degrees associated with these topics. His main line of research is Visual Optics with special emphasis on the measurement and correction of aberrations to improve the retinal image, also participating in other fields such as microprocessing of surfaces with lasers, the circadian effects of light, or the inactivation of microorganisms with UVC radiation.*

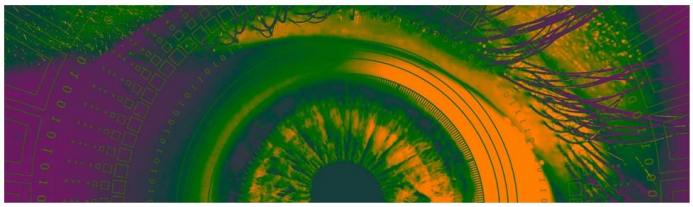

SESSION II Structure and Biomechanics of the eye

Ocular Biomechanics

Sabine Kling[1,2]

[1] Institute for Biomedical Engineering, Department of Information Technology and Electrical Engineering, ETH Zurich, (Switzerland)
[2] ARTORG Center for Biomedical Engineering Research, Medical Faculty, University of Berne (Switzerland)

As a determinant of its geometrical shape, mechanical tissue properties are an important factor to consider when evaluating the refractive power and optical performance of the eye.

The cornea forms the anterior transparent shell of the eye and represents its most important refractive component. Already minor deviations from its ideal aspheric shape deteriorate the visual acuity. Moreover, there are several degenerative diseases that induce localized progressive tissue weakening (e.g. iatrogenic ectasia, keratoconus), which severely reduces the eye's optical quality. These conditions may be addressed with photochemical corneal cross-linking (CXL), which locally increases corneal stiffness and induces refractive changes[1] at the same time. Consequently, modifying mechanical properties has been proposed as a more flexible alternative to glasses promising the correction of asymmetric refractive errors. The second most important refractive component of the eye is the crystalline lens. It is the only ocular component that permits steady accommodation and provides the eye with a wide range of focus. With increasing age, the crystalline lens loses this capability as it turns stiffer making it less responsive to the accommodative mechanical stimulus exerted by the ciliary muscle. The gradual loss of visual accommodation starts at age 40 years and is known as presbyopia. Up to date, neither the precise mechanism of accommodation, nor the origin of presbyopia is fully understood. This knowledge however is critical when developing novel treatment solutions for presbyopia, be it functional artificial lenses for implantation that mimic the natural behavior of a young crystalline lens[2], or laser surgery creating microincisions into the lens re-establishing its deformability[3–5]. In this talk, the involved biomechanics in corneal ectasia, refractive surgery, CXL treatment and accommodation will be discussed and the diagnostic potential of in vivo elastography[6] will be explored.

ACKNOWLEDGEMENTS: This work received funding from the European Union's HORIZON 2020 research and innovation programme under grant agreement No 956720, and from the AMBIZIONE career grant PZ00P2_174113 from the Swiss National Science Foundation.

[1] Lim, W. K., Da Soh, Z., Choi, H. K. Y. & Theng, J. T. S.; *Clinical Ophthalmology (Auckland, NZ)* **11,** 1205 (2017).
[2] Findl, O. & Leydolt, C.; *Journal of Cataract & Refractive Surgery* **33,** 522–527 (2007).
[3] Teuma, V., Gray, G., Bielitzki, J., Bott, S., Frey, R. & Kuszak, J. FEA; *Investigative Ophthalmology & Visual Science* **50,** 6132–6132 (2009).
[4] Ripken, T., Oberheide, U., Fromm, M., Schumacher, S., Gerten, G. & Lubatschowski, H.; *Graefe's archive for clinical and experimental ophthalmology* **246,** 897–906 (2008).
[5] Holzer, M. P., Mannsfeld, A., Ehmer, A. & Auffarth, G. U.; *Journal of Refractive Surgery* **25,** 855–861 (2009).
[6] Kling, S.; *Journal of The Royal Society Interface* **17,** 20190786 (2020).

Sabine Kling *is currently a junior group leader at the Biomedical Engineering Institute at ETH Zurich and at the ARTORG Center for Biomedical Engineering Research at the University of Bern. She obtained her PhD on the topic of corneal biomechanics at the University of Valladolid and has spent her postdoctoral time at the Universities of Geneva and Zurich. Her current research is focused on the anterior eye and the relation between structural and functional tissue properties. She is an author of over 56 peer-review publications, five book chapters and has contributed to over 64 International and National conferences.*

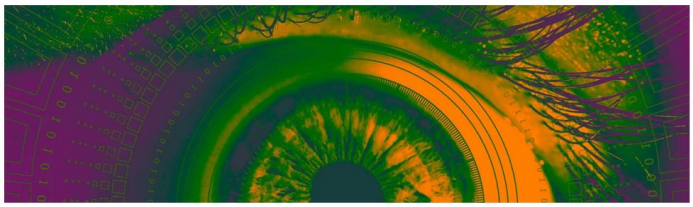

Optical Coherence Tomography for the investigation of ocular biomechanics: An overview of different excitation methods and their applications

Judith S. Birkenfeld[1], Ahmed Abass[2], Sergey Alexandrov[3], David Bronte-Ciriza[4], Andrea Curatolo[5], Ashkan Eliasy[2], James A. German[1], Andrés de la Hoz[1], Karol Karnowski[5], Bernardo Lopes Teixeira[2], Eduardo Martinez-Enriquez[1], Ryan McAuley[3], Andrew Nolan[3], Alejandra Varea[1], Lupe Villegas[1], Ahmed Elsheikh[2], Martin Leahy[3], Jesus Merayo-Lloves[6], Maciej Wojtkowski[5], Fernando Zviertcovich[1], Susana Marcos[7]

[1] Instituto de Óptica "Daza de Valdés", Consejo Superior de Investigaciones Científicas (Spain)
[2] Biomechanical Engineering Group, University of Liverpool (United Kingdom)
[3] Tissue Optics and Microcirculation Imaging Facility, School of Physics, NUIG (Ireland)
[4] CNR – IPCF, Istituto per i Processi Chimico-Fisici (Italy)
[5] International Centre for Translational Eye Research (Poland)
[6] Instituto Universitario Fernandez-Vega, Fundación de Investigacion Oftalmologica, Universidad de Oviedo (Spain)
[7] Center for Visual Science, The Institute of Optics, Flaum Eye Institute, University of Rochester (US)

Ocular biomechanics play an important role in maintaining the eye´s form and function. Abnormal biomechanical properties may be an indicator of ocular pathology or structural deterioration of the eye. Localized biomechanical weakening of corneal tissue, for example, is thought to precede keratoconus (KC), a progressive non-inflammatory corneal disorder that results in thinning and protrusion of the cornea into a conical shape[1]. Corneal alterations are usually detected when the vision is already irreversibly affected, but the changes in the biomechanical properties take place before these morphological features occur[2]. For the more common eye condition myopia, which results from a mismatch between the focal length of the ocular components and the axial length of the eye, studies have shown an alteration of the scleral biomechanical properties in the equatorial and posterior scleral regions[3]. The ability to quantify biomechanical changes in the ocular tissue could enable earlier detection of disease progression, more individualized treatment options, and avoid irreversible vision loss, corneal transplants, or retinal detachment. Non-contact approaches that quantify biomechanical properties in vivo include Optical Coherence Elastography (OCE)[4-6], Brillouin microscopy[8], and air-puff deformation Scheimpflug imaging[9, 10]. Recently, Optical Coherence Tomography (OCT) devices have been coupled to air-puff excitation sources to capture the deformation event at the corneal apex or on the horizontal meridian[10-11].

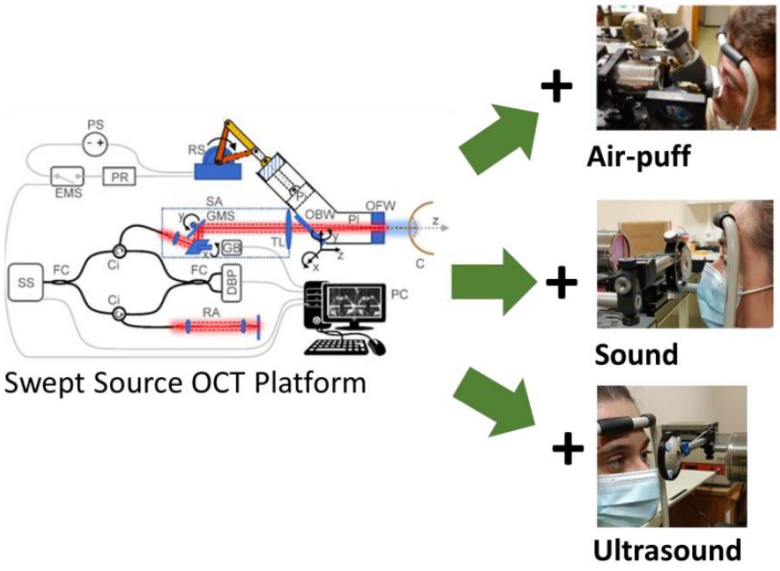

Figure 1: Overview of the developed OCT-based methods for the investigation of corneal and scleral biomechanics at the Visual Optics and Biophotonics laboratory, including a swept-source OCT coupled to cross-meridian air-puff deformation OCT, sound excitation, and ultrasound excitation.

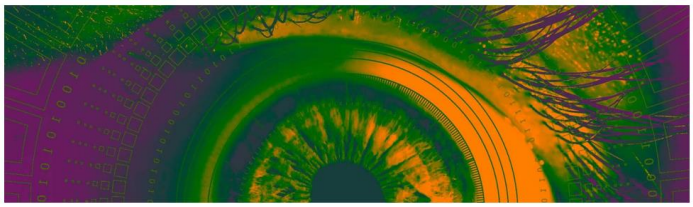

In this talk, we present our recently developed OCT-based methods for the investigation of corneal and scleral biomechanics (fig. 1), including cross-meridian air-puff deformation OCT[12, 13, 14], ultrasonic wave-based OCE[15, 16], and co-axial acoustic-based optical coherence vibrometry (CoA-OCV)[17], and their applications. We will present current results from a patient study that include KC patients and healthy subjects, and from several animal model studies for the investigation of corneal and scleral biomechanics. We will introduce several deformation parameters and biomarkers for the cornea and the sclera and their use to retrieve actual biomechanical parameters, by means of Finite Element modelling (estimation of the Young´s Modulus) and a modified Rayleigh-Lamb wave model[18] (estimation of the Shear Modulus).

ACKNOWLEDGEMENTS: ERC (2018-ADG-SILKEYE-833106); H2020 European Project Imcustomeye and Multiply (H2020-ICT-2017 Ref. 779960, H-2020-MSCACOFUND-2015 Ref. 713694); Spanish Government (FIS2017-84753-R, IJC2018-037508-I and CSIC JAE Intro Fellowship); L'Oréal-UNESCO "For Women in Science" Spain; Fundacja na rzecz Nauki Polskiej (MAB/2019/12); Polish Government (NAWA ULAM/2020/1/00176).

---

1 H. R. Vellara and D. V. Patel, *Clin. Exp. Optom*. **98**(1), 31–38 (2015)
2 C. J. Roberts and W. J. Dupps, *J.Cataract Refractive Surg.* **40**(6), 991–998 (2014).
3 J. R. Phillips, M. Khalaj, and N. A. McBrien, *IOVS*, **41**, 2028–2034 (2000)
4 K. Larin and D. D. Sampson, *Biomedical Optics Express,* **8** (2), 1172-1202 (2017)
5 Z. Jin et al., *Journal of biophotonics,* 13.8, e202000104 (2020)
6 A. Ramier et al., *Scientific reports,* **10** (1), 1-10 (2020)
8 G. Scarcelli et al., *IOVS*, **53**(1), 185-190 (2012)
9 C.J. Roberts, et al., *Journal of refractive surgery,* **33** (4), 266-273 (2017)
10 A. Eliasy et al., *Frontiers in bioengineering and biotechnology* **7,** 105 (2019)
11 D. Alonso-Caneiro, et al., *Optics express,* **19** (15), 14188-14199 (2011)
12 A. Curatolo, *Biomedical optics express,* **11** (11), 6337-6355 (2020)
13 J.S. Birkenfeld et al., *SPIE Photonics West,* 11962-11962 (2022)
14 D. Bronte-Ciriza et al., *Biomedical Optics Express*, ***12***(10), pp.6341-6359
15 F. Zvietcovich et al., *SPIE Ophthalmic Technologies XXXIII* (p. PC123600O) (2023)
16 F. Zvietcovich et al., *Optics Letters*, ***45***(23), pp.6567-6570 (2020)
17 R. McAuley et al., *Scientific Reports*, ***12***(1), p.1883 (2022)
18 Z. Han et al., *Journal of biomedical optics*, ***21***(9), pp.090504-090504 (2016.

Judith S. Birkenfeld *is a Juan de la Cierva researcher at the Institute of Optics of the Spanish National Research Council (IO-CSIC). She obtained an M.Sc. in physics, an M.Sc. in medical physics, and a certificate in business administration from the University of Heidelberg, Germany. She then moved to Spain to pursue her Ph.D. at the Visual Optics & Biophotonics Lab (IO-CSIC) with Prof. S. Marcos and received her Ph.D. in physics from Complutense University. Birkenfeld received several postdoctoral fellowships at the Massachusetts Institute of Technology (MIT), Harvard Medical School, and the Wellman Center for Photomedicine, USA before returning to Spain. Her research is motivated by solving currently unmet medical needs and focuses on applications in eye and skin research, using state-of-the-art techniques from optics, photonics, and artificial intelligence. From 2020-2023, she was the local coordinator of the EU Horizon 2020 project Imcustomeye, a multinational consortium developing novel technologies based on photonics and modeling approaches to detect changes in ocular biomechanics, a promising biomarker for the early detection of various eye conditions.*

Birkenfeld won the prestigious Spanish L'Oréal-UNESCO "For Women in Science" award in 2021 and was included in the EVI TOP LIST of Women in European Vision Research. She is chair-elect of Optica's Microscopy and OCT Technical Group and co-founder and faculty of MITlinQ, an MIT-based program to accelerate innovation technology.

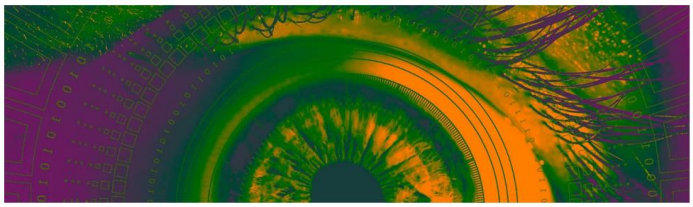

In Vivo Multiphoton Imaging of Ocular Structures

Juan M. Bueno

Laboratorio de Óptica, Instituto Universitario de Investigación en Óptica y Nanofísica, Universidad de Murcia (Spain)

For more than 20 years, multiphoton (MP) microscopy (both Two Photon Excitation Fluorescence [TPEF] and Second Harmonic Generation [SHG]) has become a powerful tool for ex vivo assessment of ocular tissues.[1,2] It provides high resolution images, without the need of external markers and absence of photodamage. In particular, the visualization of individual collagen fibers within the cornea and the sclera are of relevant clinical interest to potentially differentiate healthy from diseased conditions.[3] However, the implementation into in vivo human eyes has been challenging with only a few attempts performed in animal models.[4] Limitations have been imposed by the maximum permissible exposure (MPE), the presence of aberrations and scattering (especially at deeper locations within the tissues) and uncontrolled involuntary movements.

Here we report MP images of the living human eye obtained with a clinically-oriented MP microscope.[5] This is a compact prototype with a mode-locked infrared laser (l = 800 nm) being used as illumination source. The beam is scanned across the ocular structures of interest and the MP signals are acquired in the backward direction, travelling through appropriate spectral filters and reaching a photon-counter unit. The whole system was controlled by a custom software that allows freely modifying each acquisition parameter.

Results show that useful MP images can be acquired in ~0.5 s using an average laser power of 20 mW (at the corneal plane). These experimental settings are about one order of magnitude below the MPE limits. The instrument was successfully employed to obtain non-contact and non-invasive MP images at several locations from different ocular structures. As an example, Figure 1a shows a SHG image from the sclera of one of the volunteers involved in the experiment. For the sense of completeness Figure 1b depicts an ex vivo SHG image from the sclera of a human donor. It can be observed that both images present a similar collagen distribution and individual collagen fibers are visualized. This instrument might become an important tool in Ophthalmology for early diagnosis and tracking of ocular pathologies.

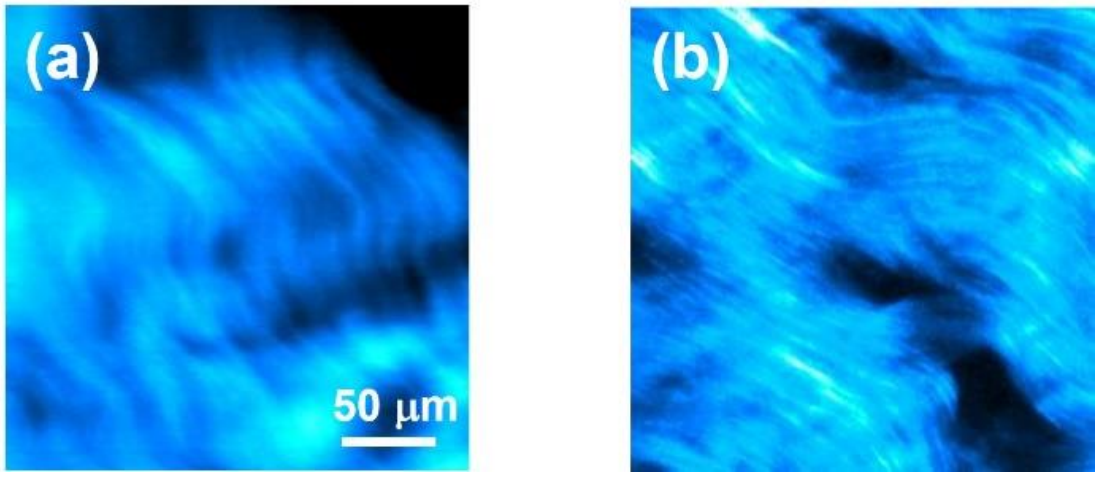

Figure 1: Comparison of SHG images of the human sclera recorded in in vivo (a) and ex vivo (b) conditions.

ACKNOWLEDGEMENTS: This work was supported by the Agencia Estatal de Investigación, Spain (grant PID2020-113919RB-I00/AEI/10.13039/501100011033).

[1]A. T. Yeh, N. Nassif, A. Zoumi and B. Tromberg; *Opt. Lett.* **27**, 2082 (2002).
[2]Y. Imanishi, M. L. Batten, D. W. Piston, W. Baehr, and K. Palczewski; *J. Cell. Biol.* **164**, 373 (2004).
[3]F. J. Ávila, P. Artal and J. M. Bueno; *Trans. Vis. Sci. Tech.* **8**, 51 (2019).
[4]G. Latour, I. Gusachenko, L. Kowalczuk, and M. C. Schanne-Klein; *Biomed. Opt. Express* **3**, 1 (2012).
[5]F. J. Ávila, A. Gambín, P. Artal, and J. M. Bueno; *Sci. Rep.* **9**, 10121 (2019).

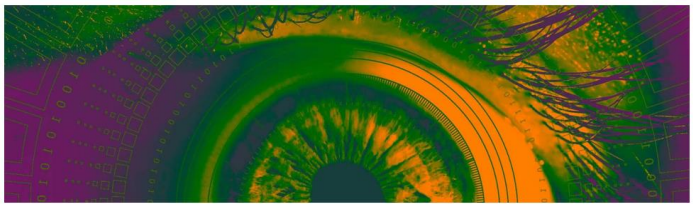

JUAN M. BUENO (PhD in Physics 1999, Doctorate Extraordinary Award) has been a faculty member since 1994 at the University of Murcia in Spain, where he currently holds a position as Full Professor of Optics. He has been Director of the Department of Physics and President of the Vision Science Division of the Spanish Optical Society. In 2017 he was elected Senior Member of the Optical Society of America (formerly OSA, now OPTICA). Dr. Bueno performs his research at the Center for Research in Optics and Nanophysics, leading the biomedical imaging section. Prof. Bueno's research focuses on biophotonics, with special emphasis on multiphoton microscopy of collagen-based structures and polarization properties of tissues. A number of his publications are considered as landmark works. Since 2017 he is Senior Member of OSA (now OPTICA). He is also inventor/co-inventor in a number of patents in the field of Visual Optics and co-founder of Voptica SL a spin-off company.

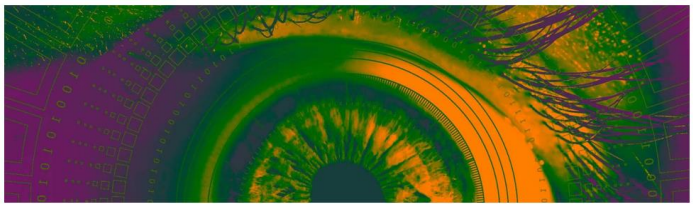

Corneal regeneration: Biological and optical studies

M. Carmen Martínez García and Patricia Gallego Muñoz

Cell Biology, Genetics, Histology and Pharmacology Department, Faculty of Medicine, University of Valladolid (Spain)

La córnea histológicamente está formada por un epitelio superficial poliestratificado, conjunto de células poligonales que descansa sobre una membrana basal. Una gruesa capa de tejido conectivo formada esencialmente por células muy diferenciadas, los queratocitos, y numerosas fibras de colágeno denominada estroma. La diferenciación (especialización) de estas células hace que sus citoplasmas tengan escasos orgánulos y numerosas prolongaciones. Por otra parte, estas células se encargan de sintetizar colágeno y proteoglicanos (PGs) de la matriz extracelular. El colágeno está dispuesto en láminas paralelas y ortogonalmente dispuestas en el centro de la córnea. El colágeno más abundante es el colágeno tipo I que forma complejos heterodiméricos con el colágeno tipo V. Entre las fibras de colágeno se encuentran los PGs que juegan un papel esencial en el espaciamiento de las fibras de colágeno y en la distribución de estas. Finalmente, la córnea tiene una gruesa membrana basal, la membrana de Descemet, y un epitelio simple plano en contacto con el humor acuoso cuyas funciones son la nutrición y el mantenimiento del equilibrio hídrico de la córnea, fundamental para su transparencia. Cuando se produce un daño en la córnea se rompe el equilibrio entre sus componentes, los cuales, como hemos dicho, se encuentran muy ordenados y especializados para conseguir la transparencia.

Los modelos estudiados, han sido modelos de procedimientos quirúrgicos o daños que se pueden observar en la clínica y que nos han servido para el estudio de cómo las córneas dañadas pierden la transparencia y la recuperan en el proceso de cicatrización. Para ello hemos unido estudios ópticos, en diferentes etapas del proceso de regeneración, estudios y hemos relacionado, algunos de ellos, con los procesos moleculares que tienen lugar. Los primeros estudios se realizaron en córneas de gallina con operaciones de cirugía refractiva PRK. En estas, el daño se produce en el epitelio y en diferentes profundidades del estroma dependiendo de las dioptrías a corregir. Debe por tanto, regenerarse el epitelio, la unión del epitelio con el estroma y el estroma que además debe ordenarse de nuevo. Desde el punto de vista celular se produce una proliferación de las células del epitelio y de las células del estroma que a su vez aumentan de tamaño e incrementan sus orgánulos para realizar la síntesis de colágeno y PGs, esta matriz en un principio está muy desordenada. Desde el punto de vista clínico esto conlleva un haze (backscattering) y desde el punto de vista óptico a una disminución de la transmitancia que se va recuperando a medida que la cicatrización se lleva a cabo [1] Estudios realizados durante la cicatrización para ver la correlación entre la disminución de la transmisión y el “scattering”, demostraron experimentalmente, que había un incremento del “scattering” y que este estaba concentrado en ángulos pequeños.[2] Estudios posteriores se centraron en el epitelio, puesto que es el encargado de formar una superficie refractiva lisa. Durante la cicatrización tanto el epitelio como la membrana basal deben regenerarse y desarrollar sus uniones. Este proceso es largo y complicado por ello evaluamos su relación con la transmisión de la luz de forma cuantitativa. Los resultados demostraron una correlación entre la rugosidad del epitelio y la transmitancia, pero no entre el espesor de este y la transmitancia.[3]

Otros procedimientos quirúrgicos que se utilizan principalmente para el tratamiento del queratocono son los de “Cross-Linking” (CXL). Este procedimiento se realiza exponiendo a radiación UV, después de la desepitelización de la córnea e impregnación con riboflavina, con la intención de producir un entrecruzamiento del colágeno que endurezca la córnea en estas patologías. Con este procedimiento fueron intervenidos gallinas y conejos. La cicatrización en ambos casos mostró una reepitelización rápida y una muerte de los queratocitos debida, por una parte, a la desepitelización y por otra a la radiación UV; así como a una reorganización del colágeno. Se realizó un análisis cuantitativo y comparativo entre las córneas de las dos especies para estudiar la reorganización del colágeno con un microscopio de generación de segundo armónico (SHG) y se observó que el efecto de la técnica era diferente. La reorganización del colágeno dependía de la organización inicial del colágeno, así, las córneas de gallina en las que el colágeno esta inicialmente muy ordenado el efecto del CXL es mínimo mientras que en los conejos cuyas córneas tienen el colágeno inicialmente menos ordenado la

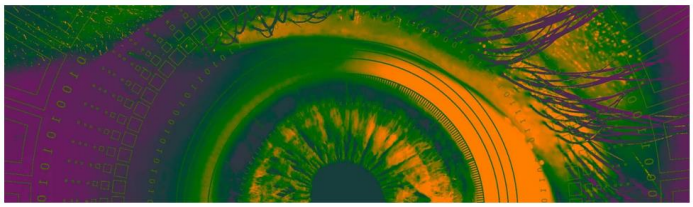

reorganización tras la intervención es mayor.[4] Dentro de estas técnicas quirúrgicas de CXL probamos a realizarlas con luz menos dañina que la radiación UV, para ello se utilizó luz verde y como fotosensibilizador el rosa bengala. La muerte de queratocitos fue menor y más superficial y la cicatrización más rápida, consiguiendo semejante efecto biomecánico.[5,6] Por otro lado, los estudios de la organización del colágeno, llevados a cabo con un SHG y utilizando el coeficiente de orden (CO) como métrica para comparar los dos tratamientos demostraron que el CO era mayor en las córneas tratadas con luz verde y rosa bengala.[7]

Daños graves se pueden producir de manera accidental en algunos puestos de trabajo como las quemaduras corneales por ácido o álcalis. El estudio de estas quemaduras supone un gran reto de reconstrucción para la córnea teniendo en cuenta los numerosos procesos que tienen lugar durante un largo plazo de cicatrización. El primer gran reto es la reepitelización, que, si bien se produce de manera rápida, estas células no se unen a la membrana basal dando lugar a úlceras recurrentes, por ello, estudiamos la síntesis de esta membrana y sus alteraciones.[8] Además, la reorganización del colágeno y las implicaciones sobre la transparencia son muy llamativas, produciéndose opacidades desde el punto de vista clínico y una disminución de la transmitancia. La diferenciación de queratocitos a fibroblastos y/o miofibroblastos, grandes células con numerosos orgánulos dedicados a la síntesis y secreción de colágeno tipo I y tipo III y PGs que dan lugar a una matriz, muy abundante y desordenada, y que se remodela a lo largo del tiempo. Esta remodelación y reorganización del colágeno fue seguida y estudiada por imágenes de SHG y cuantificadas por una herramienta matemática que suministra información sobre la orientación preferencial de las fibras (ST) e hicieron posible el estudio de los cambios estructurales a lo largo del tiempo.[9] Por otro lado, se realizó un estudio de los cambios microscópicos y moleculares que llevan a la recuperación casi total en un periodo de 6 meses.[10]

---

[1] Maria del Carmen Martinez Garcia; Jesus Manuel Merayo Lloves; Jose Tomas Blanco Mezquita; Santiago Mar Saldaña. Wound healing following refractive surgery in hens. Experimental Eye Research. 83. 2006.

[2] S. Mar; M. C. Martinez-Garcia; T. Blanco-Mezquita; R. M. Torres; J. Merayo-Lloves. Measurement of correlation between transmission and scattering during wound healing in hen corneas. Journal of Modern Optics. 56-8, 2009

[3] Pablo Perez-Merino; M. Carmen Martinez-Garcia; Santiago Mar-Sardana; Alfonso Perez-Escudero; Tomas Blanco-Mezquita; Agustin Mayo-Iscar; Jesus Merayo-Lloves. Corneal Light Transmission and Roughness After Refractive Surgery. Optometry and Vision Science. 87 - 7, pp. E469 - E474. 2010

[4] Juan M Bueno; Francisco J Ávila; M. Carmen Martinez-Garcia. Quantitative Analysis of the Corneal Collagen Distribution after In Vivo Cross-Linking with Second Harmonic Microscopy. BioMed Research International. 10, 2019.

[5] Patricia Gallego Muñoz; Lucía Ibares Frías; Elvira Lorenzo; Susana Marcos; Pablo Pérez Merino; Nandor Bekesi; Irene E Kochevar; María del Carmen Martínez García. Corneal Wound Repair After Rose Bengal and Green Light Crosslinking: Clinical and Histologic Study. Investigative Ophthalmology & Visual Science. 58-9, ARVO, 2017.

[6] Nandor Bekesi; Patricia Gallego-Muñoz; Lucía Ibares-Frías; Pablo Pérez-Merino; María del Carmen Martínez-García; Irene E Kochevar; Susana Marcos. Biomechanical Changes After In Vivo Collagen Cross-Linking With Rose Bengal-Green Light and Riboflavin-UVA. Invest Ophthalmology & Visual Science. 58 - 3, ARVO, 2017.

[7] James Germann; Eduardo Martínez-Enríquez; M. Carmen Martínez-García; Irene E Kochevar; Susana Marcos. Corneal Collagen Ordering After In Vivo Rose Bengal and Riboflavin Cross-Linking. Investigative Ophhthalmology and Visual Science. 61 - 3, 2020.

[8] Patricia Gallego Muñoz; Elvira Lorenzo Martín; Itziar Fernández; Cristina Herrero Pérez; María del Carmen Martínez García. Nidogen-2: Location and expression during corneal wound healing. Experimental Eye Research. 178-1-9, 2019

[9] Juan M. Bueno; Francisco J Ávila; Elvira Lorenzo-Martín; Patricia Gallego Muñoz; M. Carmen Martínez Gracía. Assessment of corneal collagen organization after chemical burn using second harmonic generation microscopy. Biomedical Optic Express. 12-2, 2021.

[10] Elvira Lorenzo-Martín; Patricia Gallego-Muñoz; Lucia Ibares-Frías; Susana Marcos; Pablo Pérez-Merino; Itziar Fernández; Irene E Kochevar; María Carmen Martinez-García. Rose Bengal and Green Light Versus Riboflavin-UVA Cross-Linking: Corneal Wound Repair Response. Investigative Ophthalmology & Visual Science. 59 - 12, 2018

M. Carmen Martínez *joined the Optometry School in January 1998, when she became Lecturer in Cell Biology and Histology. Nowadays, I am a teacher in biomedical engineering and Head of the Techniques Optical of Diagnostic Group multidisciplinary research group. My research is aimed at investigating the corneal wound healing process. At the beginning, I started assessing the corneal wound healing process after different refractive surgeries such as LASIK and PRK. After that, we carried out different studies of additive surgery after intracorneal segments implantation and cross-linking*

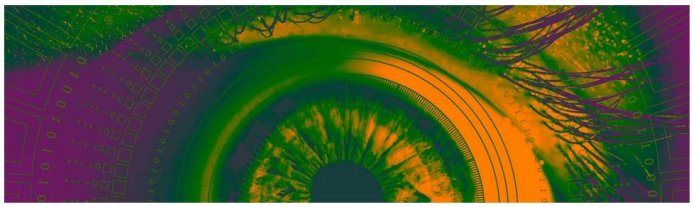

*surgeries, all of them in "in vivo" animal models. This research is underpinned by **a multidisciplinary** team of researcher ophthalmologists, biologists, physicists, and opticians, that permitted us to unravel the different aspects of the healing process. The overall aim of my research is to identify the cellular and molecular mechanisms, as well as their regulation during the healing process. With this purpose, we developed an "in vitro" model of stromal human corneal cells wound to assess the healing response after its treatment with different growth factors.*

*The cornea is a structure where collagen is organized as a network that possesses incredible optical and mechanical properties. One of the most important challenges, after an injury, is to recover transparency. We developed an "in vivo" model of alkali burn on which we studied the transmittance of the light related with the molecular expression of the ECM and by electron microscopy to reveal the collagen packing arrangements. With the same purpose, to study the recovery of transparency we are involved in collaborative projects with the University of Murcia (Dr. JM. Bueno) aimed at developing a second harmonic microscope. These **new technologies** provide information about the packing of collagen molecules and their arrangement. Three publications and several congress communications in ophthalmologist and optical physics societies demonstrate these collaborations.*

I have been supervisor of three PhD thesis with the highest distinction and Extraordinary Doctoral Award 2015-2021

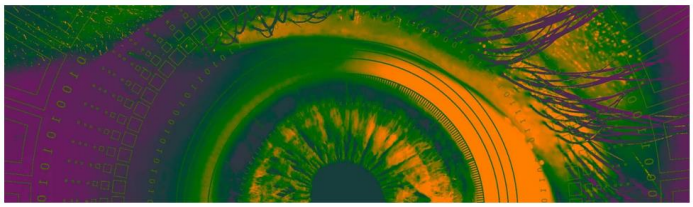

SESSION III Novel technologies for unsolved problems in Visual Optics. Minisimposium OPTICA TG Applications of Visual Science

New Intraocular lens Technologies: Ray Tracing Optimization & Bio-interfaced Pressure Sensors

Pablo Pérez-Merino

Centre for Microsystems Technology (CMST), Ghent University and imec. (Belgium)

Cataract and presbyopia affect billions of people worldwide, these ocular conditions are usually related with the natural ageing and an established solution is to replace the crystalline lens by an intraocular lens (IOL). The implantation of an IOL is the most frequently performed surgical procedure in the world, with an estimation of 20 million-cataract operations/year globally, but the recent increase in optical lens designs has not been paralleled by a further sophistication of the IOL power calculation formulas.[1] Besides, the IOL is a pure optical solution, passive in nature; so by adding more functionality with miniature electro-active components, the IOL could also act as a smart medical device inside the eye able to sense and interpret the intraocular pressure (IOP) in real-time.

1. Ray Tracing Optimization: new method for IOL power calculation

Current methods of IOL power calculation generally fail in patients with irregular corneas, such as keratoconus or after corneal refractive surgery, because they rely on assumptions about the corneal shape or estimated lens position that may lead to postoperative refractive surprises.[2,3] One reason for this shortcoming is that IOL power calculations generally aim at minimizing the residual refractive error. This study introduces IOL selection based on virtual ray tracing.[4] Custom-developed algorithms for ray tracing optimization (RTO) were used to combine the natural corneal higher-order aberrations (HOAs) with multiple sphero-cylindrical corrections in 210 higher order statistical eye models for developing keratoconus (SyntEyes KTC[5]) and 75 cataract surgery eyes with previous LASIK surgery. The magnitude of defocus and astigmatism producing the maximum Visual Strehl was considered as the optimal sphero-cylindrical target for IOL power calculation. Corneal astigmatism and the RMS HOAs ranged from − 0.64 ± 0.35D and 0.10 ± 0.04 µm (regular corneas with astigmatism) to − 3.15 ± 1.38D and 0.82 ± 0.47 µm (SyntEyes KTC at 120 months). Defocus and astigmatism target was close to neutral for eyes with low amount of HOAs, where 91.66% of eyes agreed within ± 0.50D in IOL power calculation (RTO vs. SRK/T). However, corneas with higher amounts of HOAs (>0.35 µm for a 4-mm pupil) presented greater visual improvement with an optimized target. In these eyes, only 18.05% of eyes agreed within ± 0.50D (RTO vs. SRK/T and Barrett True K). The power difference exceeded 3D in 42.2% while the cylinder required adjustments larger than 3D in 18.4% of the cases. Certain amounts of lower and HOAs may interact favourably to improve visual performance, shifting therefore the refractive target for IOL power calculation.

2. Smart IOL platform for real time IOP monitoring

The recent developments in micro-machining and implantable opto-electronic devices have enabled the integration of flexible sensors and circuits on ophthalmic platforms. Different publications demonstrated the in vivo assessment of IOP inside the eye by embedding an optical pressure sensor (Fabry–Pérot cavity-based configuration) in an IOL.[6,7] However, for IOP monitoring the implanted sensor is interrogated with an external optical system, limiting: the location of the sensor behind the iris (non-optical area) and detector automation for continuous data transfer. This work present a generalized simulation model using COMSOL Multiphysics to predict the capacitive-based pressure sensor output based on pyramid-microstructured dielectric elastomer, with various geometric and material parameters in a pressure range of 0-5 kPa, and the processing steps for the fabrication of the pyramid-microstructured parallel-plate capacitor based on silicon mould preparation and PDMS moulding (Sylgard-184) and ITO/PET electrode lamination. A 15 x15 pyramid microstructure array was

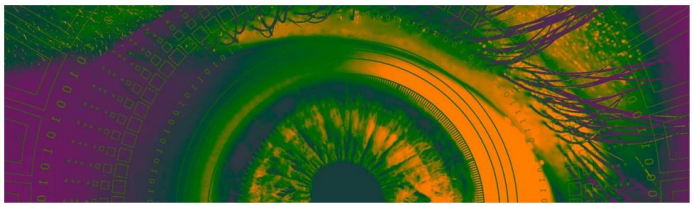

designed, where the base length of the pyramid microstructures and the spacing between them is 50 µm. Initial capacitance was 0.47 pF and the sensitivity 0.025 kPa^{-1}.

ACKNOWLEDGEMENTS: This project has received funding from the European Union's Horizon 2020 research and innovation programme under the Marie Sklodowska-Curie grant agreement No 101028137.

[1] S. Marcos et al.; *Annu Rev Biomed Eng*, **23**, 277 (2021).
[2] R. B. Melles et al.; *Ophthalmology*, **125**, 169 (2018).
[3] J. X. Kane et al.; *Ophthalmology*, **127**, 1037 (2020).
[4] P. Pérez-Merino et al.; *Sci Rep*, **13**, 4555 (2023).
[5] J. J. Rozema et al.; *Ophthalmic Physiol Opt*, **37**, 358 (2017).
[6] J. O. Lee et al.; *Microsyst Nanoeng*, **3**, 17057 (2017).
[7] J. O. Lee et al.; *IEEE Photonics Technol Lett*, **31**, 423 (2019).

Pablo Perez-Merino *completed his Ph.D. in the Visual Optics and Biophotonics group of the Institute of Optics of the Spanish National Research Council (CSIC, Spain). Currently, he is a Marie Sklodowska-Curie Fellow at the Centre for Microsystems Technology (CMST) at Ghent University and imec, where he is developing new smart optical systems and imaging technologies for ophthalmic applications. He is co-founder of a spin-off company, 2EyesVision SL.*

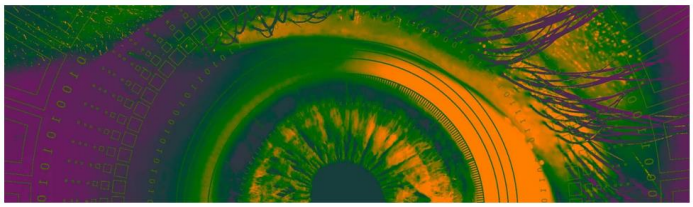

Developing multiphoton imaging of the living retina to understand the visual cycle

Zhijian Zhao and Christina Schwarz

Institute for Ophthalmic Research, Centre for Ophthalmology, University of Tübingen (Germany)

The mammalian retina is a light sensitive tissue lining the inner surface in the posterior portion of the eye. As part of the central nervous system, the retina is the most accessible tissue to study neuronal physiology. However, imaging techniques to noninvasively measure retinal function are still rare. Two-photon (2P) ophthalmoscopy has potential in quantifying retinal function via endogenous fluorophores that are involved in important physiological processes. For example, all-trans-retinol is a particularly efficient fluorophore[1,2] and a transient molecule during the regeneration of visual pigment. Via 2P absorption, it is possible to excite this fluorophore through the optical transmission window of the anterior optics of the eye with an ultrashort pulse laser at near-infrared wavelengths[3,4]. Fluorescence is then emitted in the visible wavelength range and can be captured outside the eye.

The major premise for successful application of 2P ophthalmoscopy in the living eye is light safety[5,6]. We developed a custom 2P adaptive optics scanning light ophthalmoscope (2P-AOSLO) to minimize the light levels required. The system is optimized for low dispersion due to its all-reflective design. Adaptive optics ensures spatial confinement of the excitation point spread function. Further, the 2P-AOSLO is equipped with a state-of-the-art retinal tracking system to reduce the eye-movement related image motion7. A pulse picker will be used to rapidly modulate the pulsed imaging light. Through these advanced optical techniques, we set the stage to image the retina at single cell resolution (~1 µm) and record the photoreceptor physiology during visual stimulation. In the future, the 2P-AOSLO can be used for morphological, physiological, and psychophysical studies.

ACKNOWLEDGEMENTS: ERC-StG-852220 (TrackCycle.2P)

[1] M.W. Kaplan; Experimental Eye Research, **40(5)**, 721–729 (1985).
[2] C. Chen, E. Tsina, M.C. Cornwall, R.K. Crouch, S. Vijayaraghavan & Y. Koutalos; Biophysical Journal, **88(3)**, 2278–87 (2005).
[3] R. Sharma, C. Schwarz, D.R. Williams, G. Palczewska, K. Palczewski & J.J. Hunter; Investigative Opthalmology & Visual Science, **57(2)**, 647–657 (2016).
[4] R. Sharma, D.R. Williams, G. Palczewska, K. Palczewski & J.J. Hunter; Investigative Opthalmology & Visual Science, **57(2)**, 632 (2016).
5 C. Schwarz, R. Sharma, W.S. Fischer, M. Chung, G. Palczewska, K. Palczewski, D.R. Williams & J.J. Hunter; Biomedical Optics Express, 7(12), 5148 (2016).
[6] C. Schwarz, R. Sharma, S.K. Cheong, M. Keller, D.R. Williams & J.J. Hunter; Investigative Ophthalmology & Visual Science, **59(15)**, 5973-5984 (2018).
[7] Q. Yang, J. Zhang, K. Nozato, K. Saito, D.R. Williams, A. Roorda & E.A. Rossi; Biomedical Optics Express, **5(9)**, 3174–3191 (2014).

Zhijian Zhao *did his Ph.D. in Institute of Complex Systems (Cellular Biophysics) at Research Center Jülich, (Jülich, Germany. Later, he joined Euler lab as a postdoc at the Center for Integrative Neuroscience (CIN) and Institute for Ophthalmic Research (FIA) in Tübingen, where he focused on anatomy and physiology of the retina. Currently, he is the postdoc at Christina Schwarz's lab at Institute for Ophthalmic Research, Centre for Ophthalmology. He is establishing the two-photon adaptive optics scanning light ophthalmoscope for imaging of the living retina.*

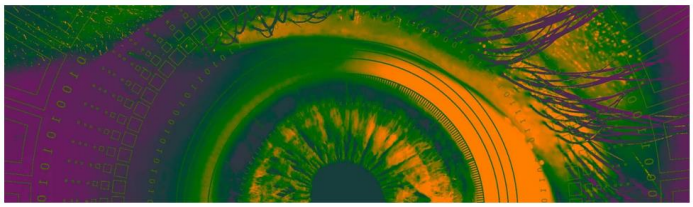

Structural and functional imaging of the retina with Spatio-Temporal Optical Coherence Tomography

Andrea Curatolo[1,2]

[1] International Centre for Translational Eye Research, Warsaw, Poland
[2] Institute of Physical Chemistry Polish Academy of Sciences, Warsaw, Poland

Imaging retinal structure and function opens the gates to a comprehensive diagnosis of the eye and vision. Several retinal diseases are currently diagnosed by their structural hallmarks and their associated alteration to a healthy retinal morphology with techniques such as optical coherence tomography (OCT)[1]. Yet, the pathological process often affects retinal function without a structural manifestation, especially in the early stages of disease. Visual acuity and psychophysical tests are the standard of care in subjective testing of retinal function and overall vision. However, having a technique that can objectively quantify both the retinal structure and its functional response to light would be very advantageous, especially to inform therapy selection and monitoring[2]. We developed a variant of full-field OCT, termed spatio-temporal optical coherence tomography (STOC-T) to capture ultrafast, 3-D, phase-sensitive OCT volumes of the retina, and deployed it in two systems for use on humans and mice[3], adding a temporally and spatially configurable visible light stimulus. With these systems, we acquired 4-D structural and functional (optoretonography) data for both human and mouse retinas and study the influence of the light stimulus on the retinal photoreceptor response. We measured the photoreceptors frequency response of three healthy human volunteers in the range from 5 Hz to 45 Hz. We compared photoreceptor frequency response results acquired from either separate measurements or a chirped frequency flicker, allowing for a faster characterization. We also demonstrate the ability to spatially map the response to a patterned stimulus with light stripes flickering at different frequencies, highlighting the prospect of characterizing the spatially-resolved, temporal-frequency response of the retina[4]. Lastly, we show the system translation required for mouse retina functional imaging and initial optoretinography results in albino mice.

ACKNOWLEDGEMENTS: Foundation for Polish Science (MAB/2019/12); The International Centre for Translational Eye Research (MAB/2019/12) project is carried out within the International Research Agendas Programme of the Foundation for Polish Science, cofinanced by the European Union under the European Regional Development Fund.

[1] M. L. Gabriele, G. Wollstein, H. Ishikawa, L. Kagemann, J. Xu, L. S. Folio, and J. S. Schuman, "Optical Coherence Tomography: History, Current Status, and Laboratory Work," Investigative Ophthalmology & Visual Science **52**, (2011).
[2] R. S. Jonnal, "Toward a clinical optoretinogram: a review of noninvasive, optical tests of retinal neural function," Annals of Translational Medicine **9**, (2021).
[3] P. Wegrzyn, S. Tomczewski, D. Borycki, W. Kulesza, M. Wielgo, K. Kordecka, A. Galińska, O. Cetinkaya, P. Ciąćka, E. Auksorius, A. Foik, R. Zawadzki, M. Wojtkowski, and A. Curatolo, *High-speed, in vivo, volumetric imaging of mouse retinal tissue with spatio-temporal optical coherence tomography (STOC-T)*, SPIE Proc. Photonics West, BiOS, Vol. PC12360 (2023)
[4] S. Tomczewski, P. Węgrzyn, D. Borycki, E. Auksorius, M. Wojtkowski, and A. Curatolo, "Light-adapted flicker optoretinograms captured with a spatio-temporal optical coherence-tomography (STOC-T) system," Biomedical Optics Express **13**, (2022).

Andrea Curatolo *is an expert in biophotonics and biomedical imaging, especially in optical coherence tomography (OCT) and derived techniques to enhance diagnostic accuracy and guide surgery, aimed at improved health outcomes, mainly in ophthalmology and oncology. Dr Curatolo holds a PhD in biophotonics from The University of Western Australia. Since 2020, Andrea works at the International Centre for Translational Eye Research (ICTER), affiliated with the Institute of Physical Chemistry of the Polish Academy of Sciences (IPC-PAS), in Warsaw, Poland, where he leads the Image-Guided Devices for Ophthalmic Care group, or IDoc in short. He is an author of more than 35 publications in Q1 peer-reviewed international journals, including three book chapters. He is also involved in the clinical translation and commercialization of biophotonics technologies; he is an inventor on several patent applications, and he is engaged in collaborations with MedTech startups.*

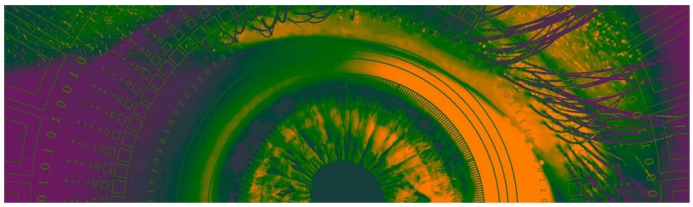

Investigating the ocular optics, biomechanics and structure using light-based technologies

Maria Viñas-Peña[1,2]

[1] Institute of Optics. Spanish National Research Council (CSIC) (Spain)
[2] Wellman Center for Photomedicine & Harvard Medical School, Massachusetts General Hospital (US)

Vision relies on a complex system, which comprises an optical camera and a neural processor, adjusting to match visual coding and environment. Light-based technologies have allowed further understanding of its limits and pave the way to the development of novel treatments. Adaptive Optics (AO) has allowed significant insights on visual science[1], from the optical properties of the eye (measure/control of the monochromatic, and very recently, chromatic aberrations[2] of the human eye, and their interactions), as well as the processes of neural adaptation behind them, and incredible achievements in the area of visual simulation. The understanding of the interactions of these aberrations and their effect upon correction is essential to explore the limits of human spatial vision, and to design and optimize new alternatives of optical corrections.

In particular the study of Myopia and possible treatments have been boosted via the development of high resolution non-invasive imaging techniques. One of the strategies under investigation is collagen cross-linking of the sclera, a procedure inspired by the fact that during ocular growth, scleral development critically determine eye size and thus the refractive status of the eye, and that strong phenomenological correlations have been found between Myopia and the morphology and tissue-structure of the eye. Therefore an intervention of the abnormal development of the sclera may provide ways to halt the excessive axial elongation. But sclera is a very challenging tissue, where mechanical and structural properties are spatially heterogeneous, varying locally and from the anterior to posterior regions. Therefore a combination of light-based technologies is needed to understand the mechanical/structural/chemical tissue changes. Optical coherence elastography (OCE) has emerged as a promising technique with high spatial resolution and high sensitivity to non-invasively quantify biomechanical properties of soft tissues[3], and has allowed very recently in vivo non-invasive quantitative measurement of the shear modulus of the human cornea and sclera, as well as in SCXL eyes[4]. But underlying structural and chemical changes in myopic eyes remain unclear. Very recently we have used Second Harmonic Generation (SHG) microscopy and Fluorescence lifetime imaging microscopy (FLIM) to investigate the structural (orientation and packaging of the collagen fiber) and chemical (number of crosslinks between the fibers) changes. Another promising strategy is the use of multifocal contact lenses (MCLs) to slow down the progression of myopia by providing the patients with adequate visual cues that could normalize the eye growth[5]. MCLs rely on the principle of simultaneous vision, where image quality of an image at far is slightly reduced in order to gain vision at near. AO based visual simulators are particularly attractive to test vision in subjects with new optical designs prior to delivering or even manufacturing a lens. Very recently, we have demonstrated that MCLs effectively expand the depth of focus using a novel simulator, SimVis based on the concept of temporal multiplexing of an optotunable lens driven at a speed above the temporal integration of the visual system, which captured the through-focus optical and visual performance of the MCL.

Moreover, in the last years AO-based visual simulators have revolutionized the management of Presbyopia, the loss of the autofocus accommodation of the human eye with age, and its treatment. AO-simulations of new corrections enable investigation of interactions between a subject's optics and a given correction, characterization of differences across corrections, and eventually selection of the correction that optimizes perceived visual quality and performance in subjects. We have shown that diverse novel refractive multifocal designs (concentric and asymmetric) as well as commercial refractive and diffractive IOLs can be simulated using different active optical elements (SLM, SimVis) integrated in an AO system, and demonstrated equivalency between the patient's vision through the simulated lenses and physical lathe-manufactured phase-plates or physical IOLs in a cuvette. Moreover, AO-based visual simulators make even possible the pre-operative simulation of post-operative multifocal vision[6,7].

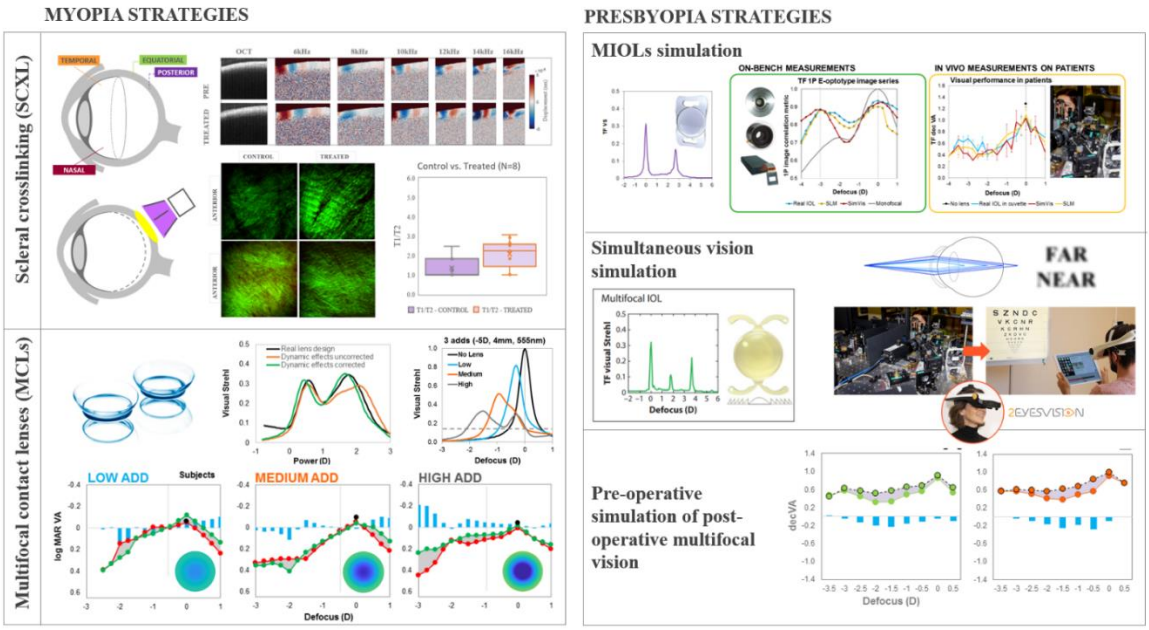

Fig 1. Applications of Light-based technologies for eye research. (1) Examples of vibrography images obtained using OCE, SHG images and T1/T2 ratios obtained from FLIM for normal and treated scleras. (2) Visual quality with real/simulated MCLs. (3) On bench and in vivo trough focus optical/visual quality with real/simulated (SLM, SIMVIS, and real IOL in a cuvette) refractive bifocal MIOL.(3) Illustrations of AO-based and clinical visual simulators. (5) Pre-operative through focus visual simulation of post-operative multifocal vision using a clinical and an AO-based visual simulators.

ACKNOWLEDGEMENTS: ViobioLab (CSIC, Spain) and YunLab (Harvard Medical School, US) research teams, as well as current funding from the European Union's Horizon 2020 Program under the Marie Sklodowska-Curie grant agreement H2020-MSCA-IF-GF-2019-MYOMICRO-893557, and the Spanish Government Ramon y Cajal program RYC2021-034218-I.

[1] S. Marcos, et al., Vision science and adaptive optics, the state of the field, Vision Res, 132, (2017).
[2] M. Vinas-Pena, et al., Understanding In Vivo Chromatic Aberrations in Pseudophakic Eyes Using on Bench and Computational Approaches, Photonics, 9(4), (2022).
[3] K. V. Larin, and D. D. Sampson, OCE - OCT at work in tissue biomechanics, Biomed Opt Express, 8(2), (2017).
[4] M. Vinas-Pena, et al., "In situ measurement of the stiffness increase in the posterior sclera after UV-riboflavin crosslinking by optical coherence elastography," Biomed Opt Express. 23;13(10), (2022)
[5] S. Vedhakrishnan, et al., "Vision with SLM simulating MCLs in an AO system," Biomed Opt Express, 12(5), (2021).
[6] M. Vinas, et al., "Pre-operative simulation of post-operative multifocal vision," Biomed Opt Express, 10(11), (2019).
[7] S. Marcos, et al., "Simulating Outcomes of Cataract Surgery: Important Advances in Ophthalmology," Annu Rev Biomed Eng, 23, (2021).

Maria Viñas-Peña *is a Ramon y Cajal scientist at the Spanish National Research Council where she investigates in the area of Visual Optics and Biophotonics. She obtained her PhD in Physics (UCM, 2016) and since then enjoyed different postdoctoral positions at the Institute of Optics, CSIC (Spain), as Marie Sklodowska Curie research fellow (2020-22) at Wellman Center for Photomedicine-Massachusets General Hospital & Research fellow at Harvard Medical School (US), and as visiting researcher at the Center for Visual Science of the University of Rochester (US). Her research focuses in the use of photonic technologies to the study of the physics of vision. Dr. Vinas has a proven track record of achievements and independent research in Visual optics & Optical engineering (>25 peer reviewed publications in Q1), as well as in competitive funding calls, and in innovation and technology transfer activities, proven by her participation in 15 competitive R&D projects in national/international calls, 16 R&D projects with international companies, and since 2015, founding partner of a start-up, 2EyesVision. She teaches in different Universities (UCM, Uva, UC3M) & Research Centers (CSIC, Wellman Center for Photomedicine), and has supervised 3 PhD students, and 4 Master students. She has received different award and fellowships (OPTICA, ARVO), as well as being named OPTICA Ambassador 2019 and, senior member (2021), and European Young Researcher Award EYRA2020 (postdoctoral category). Currently, she is the chair of the Visual Sciences committee of the Spanish Optical Society & member of the board of the OPTICA TG Applications of Visual Sciences.*

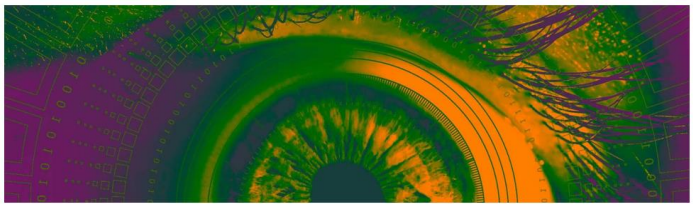

Multi-Photon Microscopy: How the microscale affects the macro-world

James A. Germann

VIOBIO, IO-CSIC (Spain)

Collagen fiber orientation and variability affects the mechanical properties of ocular tissue. For example, the anterior portion of the stroma (the thick, collagen rich layer of the cornea) has interwoven collagen fibers, while in the posterior potion of the stroma the fibers form sheets that are stacked on top of each other. This difference in interweaving between the two portions leads to differences in mechanical strength, as measured by AFM[1]. With a second harmonic generation (SHG) microscope, we can image the collagen fibers layer by layer through the entire depth of the cornea and visualize this interweaving. When the interweaving is disrupted, the cornea will suffer, as seen in keratoconus, where SHG imaging of advanced-stage keratoconic corneas can show a distinct lack of interweaving in the anterior stroma[2]. This leads to sagging of the cornea due to loss of mechanical strength. In contrast, when the corneas are treated with photo-crosslinking, a pharmaceutical treatment of keratoconus, the collagen fibers of the treated tissue appear straighter and keep their organization when removed from the ocular globe. By measuring how the organization is preserved versus depth, we have measured how effective these treatments are through the entire tissue[3].

In addition to the cornea, the sclera is also mainly composed of collagen and provides form to the ocular globe. As such, changes to the sclera affect the ocular globe as a whole, such as the thinning of the sclera and the axial elongation of the globe seen during myopia. Myopia is one of the fastest growing health crises, with the projected incidence rate projected to be 50% globally by the year 2050[4]. The refractive error associated with myopia can be corrected with a pair of spectacles, however a high refractive error will increase the risk of glaucoma[5] and retinal detachment[6]. The exact biochemical cascade that leads to myopic eye growth is still unknown, although one of the end points of scleral reformation is an increase in the expression of MMP-2[7]. To better understand the black box of myopia, we are investigating which molecules begin the myopic cascade, such as dopamine and retinoic acid[8], and the final product of the cascade, which is the reordering of the scleral microstructure[9]. We are also investigating how anti-myopia treatments, such as latanoprost and atropine, affect the microstructure of the sclera.

Thick ocular tissues can easily be measured and characterized with multi-photon confocal microscopy. Like a standard confocal microscope, the multi-photon microscope has increased axial resolution but does not require a pinhole as the probability of two photons hitting the same molecule within a femtosecond (10^{-15} s) outside of the focal volume of a high numerical aperture objective is small, even with a pulsed, coherent laser source. In our multi-photon microscopy lab, we focus on two different imaging modalities, two-photon fluorescence microscopy (2PFM) and SHG microscopy. 2PFM is identical to the one-photon case, with the molecule absorbing excitation photons and releasing fluorescence photons with slightly less energy than the absorbed photons (Stokes shift), with the difference being that two-photons are required to excite the molecule. In contrast, the SHG process is a lossless transition, so the emitted photon has all of the energy of the absorbed photons. SHG microscope does require that the measured molecules be non-centrosymmetric, as is the case in collagen. In this talk, we will be discussing our work and current trends in imaging the cornea and sclera with microscopy and an emphasis will be placed on collagen fiber organization in tissue and fluorescence in the retina. We will examine how these tools add to vision research.

[1] J. Dias and N. Ziebarth; *Exp. Eye Res.*, (2013)
[2] N Morishige et al.; *IOVS*, 48, (2007)
[3] J. Germann et al.; *IOVS*, 61, (2020)
[4] B. Holden et al.; *American Academy of Ophth.,* 123, (2016)
[5] M.Markus et al.;*American Academy of Ophth.* 118 (2011)
[6] Baba et al.; *American Academy of Ophth.*, 135, (2003)
[7] Y. Jia et al.; *IOVS*, 55 (2014)

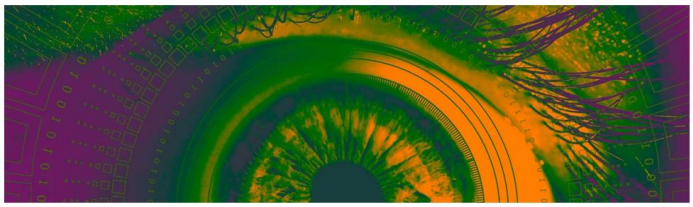

[8] I. Morgan; *Clinical and Exp. Optometry*, 86, (2003)
[9] C. Hoerig, S. McFadden, Q. Hoang, J. Mamou; *Exp. Eye Res.*, 224, (2022)

James A. Germann *is a senior postdoctoral researcher in the Visual Optics and Biophotonics group at the Institute of Optics in CSIC. He uses novel technologies to research the relationship between the microstructure of the cornea and the sclera and macroscopic properties, such as mechanical strength. He has developed different imaging devices to characterize the ocular structures at the cellular level (confocal, multiphoton, and second harmonic generation microscopy) and to study the macroscopic shape of the eye in vivo and experimental lens designs ex vivo based on Optical Coherence Tomography. For his Ph. D. project, he developed a novel four-focus microscope design for measuring and tracking single fluorescent particles in solution and measuring the 3D flow velocity of fluorescent particles.*

The societal impact of Dr. Germann's work is the study of ocular diseases, in particular myopia and keratoconus, to better understand their origin and provide an early diagnosis. Keratoconus is a blinding, ocular disease with a relatively low prevalence (15-23 cases per 100,000 people) that develops mainly in adolescents. It is caused by a change in the structural properties of the cornea and nowadays is diagnosed with the change in shape of the cornea. Myopia, also known as near-sightedness, is expected to reach epidemic proportions by 2050, with 50% of the world population myopic and some Asian countries reaching a prevalence rate of 95%. Myopia is primarily driven by the elongation of the eye that in extreme cases can compromise the structural properties of the sclera.

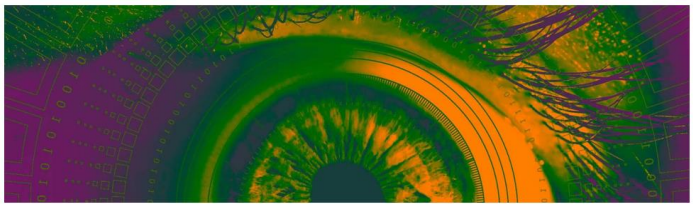

SESSION IV New horizons in refractive, cataract and eye surgery

Presbyopia-correcting intraocular lens with diffractive profile. Chromatic considerations

María S. Millán

[1] Group of Applied Optics and Image Processing, Faculty of Optics and Optometry, Universitat Politècnica de Catalunya (Spain)

In cataract surgery, an intraocular lens (IOL) replaces the natural crystalline lens. IOL power calculations of monofocal implants commonly target distinct distance vision. However, visual requirements at closer distances cannot be satisfied by monofocals and, similarly to the case of presbyopia, patients become spectacle dependent to perform their ordinary activity. Increasing patient demand for spectacle independence has been an extraordinary incentive for the development of presbyopia-correcting IOLs. The first diffractive multifocal IOLs (DMIOLs) were bifocal lenses that provided good far and near visual acuities but insufficient intermediate vision. Many current DMIOLs incorporate a third focal point to help improve intermediate vision while maintaining performance for distance and near vision. Other lenses are based on an extendeddepth-of-focus (EDOF) design to produce a long and narrow focal segment in the image domain. DMIOLs have a hybrid diffractive-refractive design that consists of a high-power refractive lens (base lens) and an additional (add) low power diffractive profile engraved on either the front or the back surface of the IOL following a sawtooth pattern of echelettes. Diffractive IOL profiles are designed to split light into a number of operative diffraction orders,[1] with optimum performance at the wavelength that corresponds to the maximum photopic efficiency of the eye (550nm). In most diffractive bifocals, the far focus corresponds to the 0th diffraction order (base power) whereas the near focus corresponds to the 1st diffraction order (near add power). However, other market-available DMIOL designs use different diffraction orders to achieve distinct properties.[2,3] In DMIOLs, the optical power and the energy efficiency depend strongly on the wavelength. This fact has a clear impact on various aspects of IOL testing such as the optical quality, chromatic aberration, halo formation and, beyond that, on the clinical postoperative visual evaluation and on the spatio-chromatic vision of implanted eyes. Theoretical analysis, numerical simulation and invitro optical bench testing have proved to be useful methods, complementary to clinical trials, to interpret these phenomena and even predict the expected postoperative visual acuity and potential risk of dysphotopsia.

Recent findings are also presented and discussed. We show the limitations of using near infrared based equipment, such as aberrometers with wavelength in the range 780 to 850 nm, for the clinical assessment of subjects implanted with DMIOLs. We also present some asymmetric alterations in the spatio-chromatic vision produced by DMIOLs, with significant changes in resolution depending on the object distance and the spectral band of illumination.

ACKNOWLEDGEMENTS: PID2020-114582RB-I00/ AEI / 10.13039/501100011033.

[1] S. Ravikumar, A. Bradley, L.N. Thibos; *J. Cataract Refract. Surg.* **40**, 1192 (2014).
[2] M.S. Millán and F. Vega; *Biomed. Opt. Express* **8**, 4294 (2017).
[3] F. Vega, M. Valentino, F. Rigato, M.S. Millán; *Biomed. Opt. Express* **12**, 3338 (2021).
[4] F. Vega, M. Faria-Ribeiro, J. Armengol, M.S. Millán; *Diagnostics* **13**, 1259 (2023).
[5] M.S. Millán, L. Clavé, A. Torrents, J. Armengol, F. Vega; *Eye and Vision* (under review, 2023).

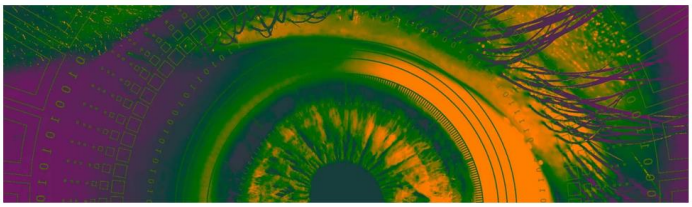

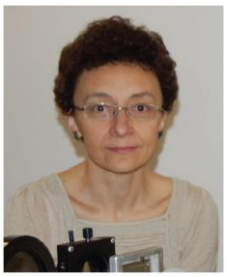

María S. Millán *is full Professor at the Universitat Politècnica de Catalunya-BarcelonaTech (UPC), Spain. Her research interests include information optics, image processing and their applications to medicine (ophthalmology), industry, and security. She leads research projects on intraocular lenses. Guest editor on the Photonics (MDPI) 2022 special issue: "Ocular imaging for eye care". She serves the optics community through several national and international societies, with particular dedication to the development of Optics in Latin-American countries. She has been representative of the Spanish ICO Territorial Committee. SPIE Fellow, EOS Fellow, OPTICA Senior and Fellow member. María S. Millán has been President of the Spanish Society of Optics. Fellow Scholar of the Colombian Academy of Mathematics, Physical and Natural Sciences.*

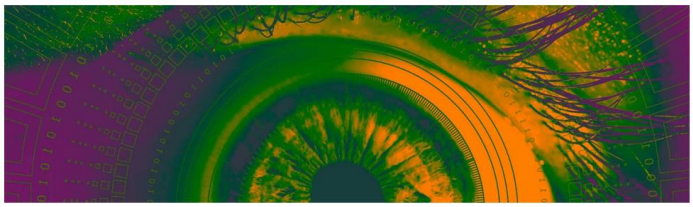

Simulation and validation of multifocal lenses with SimVis technology

Carlos Dorronsoro[1,2], Xoana Barcala[1], Irene Sisó-Fuertes[1], Eduardo Esteban[1], Amal Zaytouny[2], María Vinas[2], Alberto de Castro[2], Enrique Gambra[1], Susana Marcos[3] and Lucie Sawides[2]

[1] 2EyesVision SL, Plaza de la Encina 10, 28760, Tres Cantos, Spain
[2] Viobio Lab, Instituto de Optica, CSIC, C/ Serrano 121, 28006 Madrid, Spain
[3] Center for Visual Science, The Institute of Optics, Flaum Eye Institute, University of Rochester, NY, United States

SimVis Gekko (2EyesVision, Spain) is a novel visual simulator that allows to experience multifocal vision prior to cataract/refractive surgery or contact lens fitting. It is based on SimVis technology, which employs optoajustable lenses working under temporal multiplexing[1] to mimic the optical performance of any multifocal design (trifocal, bifocal, edof, enhanced monofocal), at all distances[2].

Different sources of information can be used for an accurate replication of the lens performance, including the actual lens design provided by the manufacturer (physical design, phase map in the pupil plane, power map…) and metrology measurements reported in the literature or obtained by external laboratories. Using this input data, the Through-Focus Visual Strehl (TFVS) corresponding to each multifocal lens is computed, and the temporal coefficients (i.e., the time that the optoadjustable lens needs to stay in each focus to mimic the lens design) are obtained[2,3,4,5]. The set of temporal coefficients corresponding to the SimVis simulation is first validated computationally by estimating its TFVS and then experimentally using a high-speed focimeter based on a high-speed camera[6].

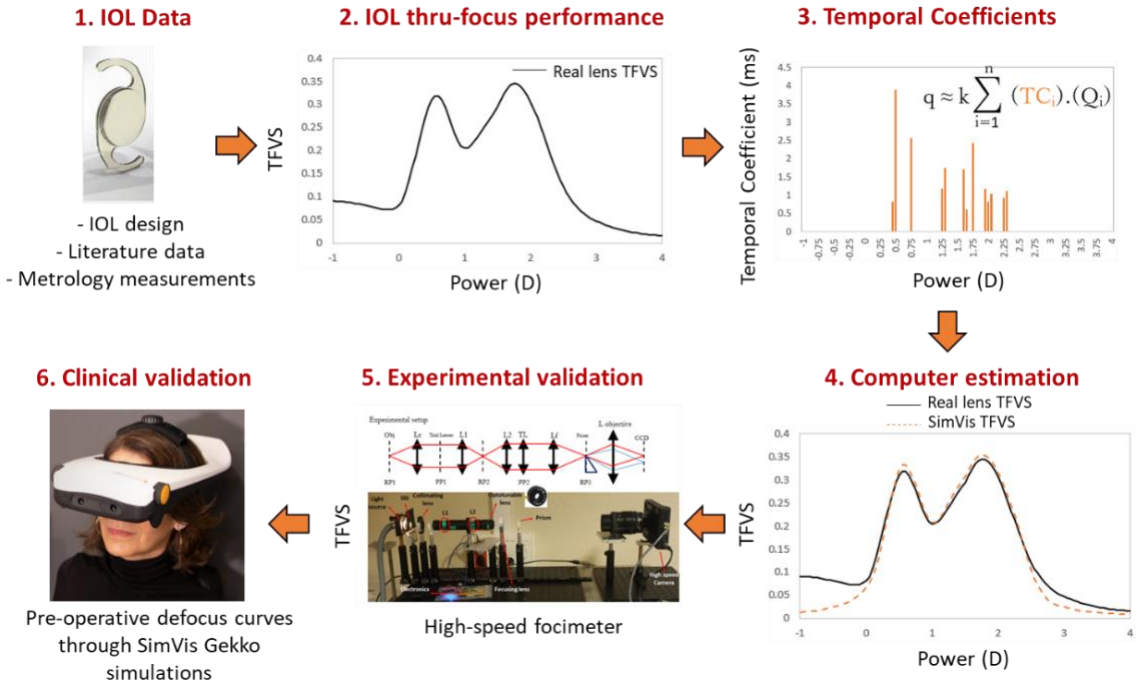

Figure 1. Validation protocol flow diagram

Finally, the simulation of the multifocal lens is validated clinically in a group of patients. For the validation of multifocal contact lenses, monocular defocus curves are obtained in the same group of subjects with both the SimVis simulation and the real multifocal contact lenses[8,9]. For the validation of multifocal intraocular lenses, bilateral defocus curves with the SimVis simulation are obtained in a group of observers, and compared with the bilateral post-operative defocus curves found in patients implanted with the corresponding real lens, as reported in scientific publications[7].

In this study we present a compendium of the different procedures used to simulate a wide variety of different multifocal lenses and the clinical validations of those SimVis simulations.

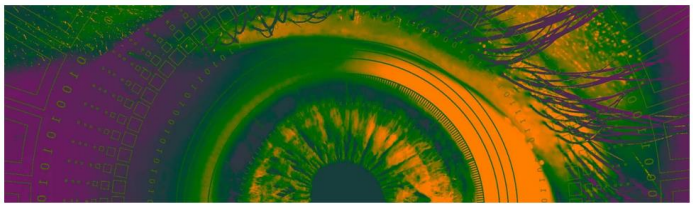

ACKNOWLEDGEMENTS: This research was supported by the Spanish Government under the Spanish Government Grant FIS2017-84753-R to SM, and ISCIII DTS16/00127 to CD; Madrid Regional Government IND2017/BMD7670 to XB and IND2017/BMD7670 to EE and AZ; and Master Clinical Research Agreement between Johnson and Johnson Vision Care (USA), 2EyesVision and IO-CSIC. This research also received funding from the SILK-EYE Ref. 833,106 Excellent Science – ERC to SM; the H2020-MSCA-IF-GF-2019-MYOMICRO-893557 to MV and National Eye Institute P30 Core Grant EY001319-46 (Center for Visual Science) and Unrestricted grant Research to Prevent Blindness (Flaum Eye Institute) to SM.

---

[1] C. Dorronsoro, A. Radhakrishnan, JR. Alonso-Sanz et al; *Optica*, **3**, 918 (2016)
[2] V. Akondi, C. Dorronsoro, E. Gambra and S. Marcos; *Biomedical Optics Express*, **8**, 3410 (2017)
[3] V. Akondi, L. Sawides, Y. Marrakchi et al; *Biomedical Optics Express*, **9**, 6302 (2018)
[4] C. Dorronsoro, E. Gambra, L. Sawides et al; *Biomedical Optics Express*, **9**, 6302 (2018)
[5] L. Sawides, A. de Castro, C. Lago et al; *Optical Design and Engineering VIII*, **11871**, 122 (2021)
[6] C. Dorronsoro, X. Barcala, E. Gambra et al; *Optics Express*, **27**, 2085 (2019)
[7] M. Vinas, C. Benedi-Garcia, S. Aissati et al; *Scientific Reports* **9**, 1539 (2019)
[8] M. Vinas, S. Aissati, AM Gonzalez-Ramos et al; *Transl Vis Sci Technol*, **9**, 20 (2020)
[9] X. Barcala, M. Vinas, S. Ruiz et al; *Contact Lens and Anterior* Eye, **45**, 101716 (2022)

Carlos Dorronsoro *(M.S. Optical Physics '96 from the University of Zaragoza, M.S. Vision Science '03 and PhD Vision Science '09 from the University of Valladolid) is Tenured Scientist at the Institute of Optics, Spanish National Research Council (CSIC, Madrid), on personal leave for Technology Transfer reasons, and currently working as a CEO of 2EyesVision (spin-off company of CSIC). He started to collaborate with the Visual Optics and Biophotonics Lab in 2001, where he performed his PhD research in the field of physical and optical implications of refractive surgery and contact lenses. He has published more than 60 research papers in the most important journals in the field of Optics and Vision Science, as well as >10 in the field of Multidisciplinary Sciences (as Plos ONE or Scientific Reports), 9 Proceedings and 5 book chapters (h=22, 1200 citations, more than 100 citations per year according to Web of Science). Carlos Dorronsoro holds 23 families of patents, 13 of them licensed to different industries. He has been principal investigator in 21 research projects. Besides ophthalmic and visual optics, Dorronsoro also has a broad industrial experience in precision optics, optical design, optical manufacturing, optical metrology & testing and camera calibration. Prior to his work for CSIC, Dorronsoro has worked for the Low-light vision laboratory of the Spanish Navy Research and Development Center (CIDA) and with various optics companies such as Leica (Switzerland), Lep (Spain) or Lenticon Laboratories (Spain). He has also been involved in management and control of international research projects and industrial collaborations, as well as in establishing research strategies in optics and photonics at a European level (WEU, now EDA). He has been Vice-President of the Visual Sciences Committee (2008-2012) of the Spanish Optical Society (Sedoptica), vice-director of the Institute of Optics (2016-2019) and promoter/co-founder of four spin-off companies (Imatrics Image Technologies SLNE, Alfa Imaging SA, Plenoptika Inc, 2Eyes Vision SL). He was visiting researcher at the University of Texas at Austin (2014-2018; Fulbright scholarship). He was regional winner of the 1st Spanish Physics Olympiad (1990), obtained a University Fellowship (1990-1996) from the Spanish Physics Society (RSEF), was awarded with a Young Investigators in Optics Award (2003, Spanish Optical Society & RSEF) and Best Patent of the Year (twice, 2010 and 2017; Madrid Reginal Government, Madri+d Foundation), Best business plan based on a doctoral Thesis (2011 University of Valladolid) and Best Thesis in Optical Imaging in Spain (years 2008 to 2010 Spanish Optical Society). In 2019 he was awarded with the Premio Física, Innovación y Tecnología 2019 (Premios de Física de la Real Sociedad Española de Física RSEF-Fundación BBVA).*

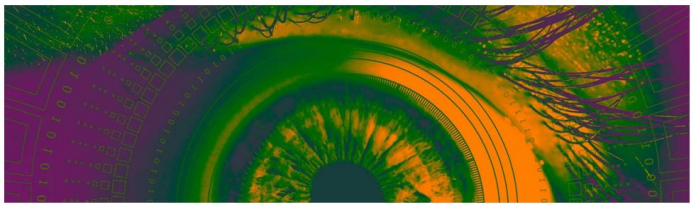

Multifocal Contact Lenses for Myopia Control

José Manuel González-Méijome

Department and Center of Physics – Optometry and Vision Science, School of Science (Portugal)

Myopia management for the young patient has changed significantly over the last two decades. Instead of compensating the refractive error, the standard of practice today moves quickly towards the prescription of active treatments that can simultaneously reduce the rate of axial elongation. This is the concept of myopia control or reduce of myopia progression. This can be achieved with specially designed spectacles (multiple lenslets, peripheral gradient), corneal reshaping (orthokeratology), soft contact lenses (bifocal or multifocal contact lenses, peripheral gradient) and/or pharmacological drugs (0.01 to 0.1% atropine) [1-4].

Soft contact lenses are the most common contact lenses prescribed and have demonstrated to have a significant impact improving the vision-related quality of life of children of and for the last 5 years, several designs have been demonstrated efficacy in myopia control including multifocal and bifocal designs for presbyopia correction and other lenses designed specifically for the young myopic eye.

The present lecture presents a summary of the main optical designs used in contact lens platforms (figure 1) for myopia management, their background science in animal models[5,6], their optical and visual performance[7-9], efficacy[10] and safety[11] outcomes (figure 2). Particular attention will be paid to new insights into the effect of treatment optics in the efficacy outcomes[12] as well as the potential effect on other potentially relevant functions such as accommodation[13], (figure 3) the electrophysiological response of the retina[14] and the structural response (figure 4) of the choroid[15].

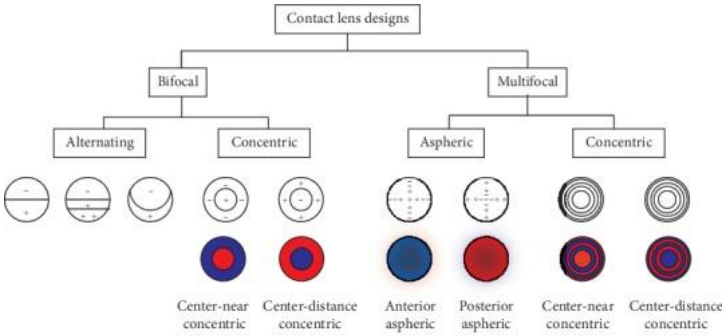

Figure 1: Optical designs used for presbyopia correction and myopia control in contact lens platforms (Remón et al., 2020).

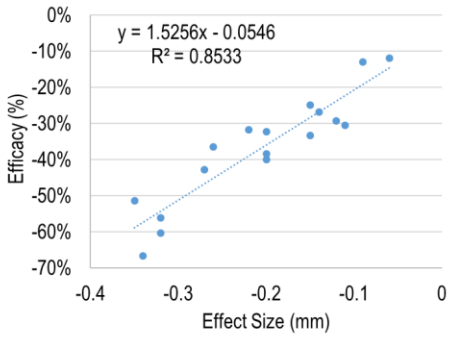

Figure 2: Correlation between the effect size and the efficacy for different myopia control methods (from the author).

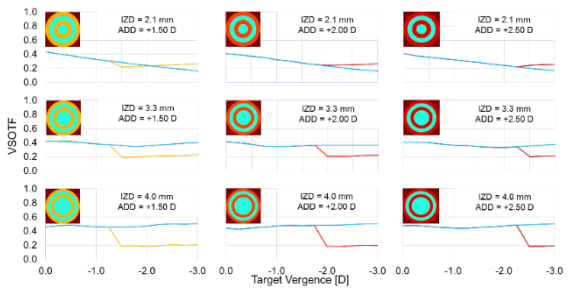

Figure 3: Changes in image quality measured with metric (VSOTF) for different target vergences, with normal accommodation (blue lines) or suppressing accommodation by the amount of plus power provided by the optics of the lens (+1.50 to +2.50D). Besides plus power, designs change their inner zone diameter (Faria-Ribeiro et al, 2018)[13].

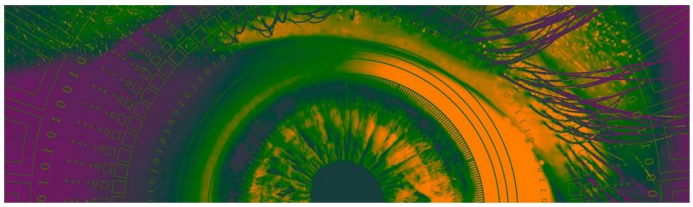

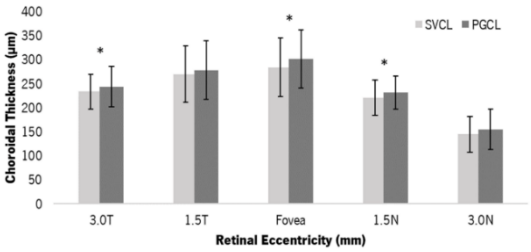

Figure 4. Average (and SD bars) of the ChT values with the SVCL and PGCL for the five eccentric choroidal zones. The ChT with the PGCL (dark grey) was thicker than the SVCL (light grey) after 30 minutes of wear. *Statistically significant differences between conditions (T-test, p-value ≤ 0.050). (Amorim-de-Sousa et al, 2023)[15]

ACKNOWLEDGEMENTS: the author acknowledges members of the Clinical and Experimental Optometry Research Lab who contributed directly or indirectly to the topics presented (A Queirós, M Faria-Ribeiro, PRB Fernandes, D Lopes-Ferreira, A. Amorim)

---

[1] Lawrenson JG, et al. Interventions for myopia control in children: a living systematic review and network meta-analysis. Cochrane Database Syst Rev.;2(2):CD014758, 2023
[2] González-Méijome JM, O'Brien M. European Council of Optometry and Optics (ECOO) position paper. Myopia Management: a comprehensive approach, 2023.
[3] Remón L, et al. Bifocal and Multifocal Contact Lenses for Presbyopia and Myopia Control. J Ophthalmol. 2020
[4] González-Méijome JM, Peixoto-de-Matos SC, Faria-Ribeiro M, et al. Strategies to Regulate Myopia Progression With Contact Lenses: A Review. Eye Contact Lens.42(1):24-34, 2016
[5] Benavente-Pérez A, et al. Axial eye growth and refractive error development can be modified by exposing the peripheral retina to relative myopic or hyperopic defocus. Invest Ophthalmol Vis Sci. 55(10), 2014
[6] Liu Y, Wildsoet C. The effect of two-zone concentric bifocal spectacle lenses on refractive error development and eye growth in young chicks. Invest Ophthalmol Vis Sci. 52(2), 2011
[7] Martins C, et al. Visual Performance and High-Order Aberrations with Different Contact Lens Prototypes with Potential for Myopia Control. Curr Eye Res. 45(1), 2020.
[8] Silva-Leite S, et al. Peripheral Refraction and Visual Function of Novel Perifocal Ophthalmic Lens for the Control of Myopia Progression. J Clin Med. 2023;12(4):1435.
[9] García-Marqués JV, et al. Short-term tear film stability, optical quality and visual performance in two dual-focus contact lenses for myopia control with different optical designs. Ophthalmic Physiol Opt. 42(5), 2022.
[10] Chamberlain P, et al. A 3-year Randomized Clinical Trial of MiSight Lenses for Myopia Control. Optom Vis Sci. 96(8), 2019.
[11] Gaume Giannoni A, et al. Ocular and Nonocular Adverse Events during 3 Years of Soft Contact Lens Wear in Children. Optom Vis Sci. 99(6), 2022.
[12] Walline JJ, et al. Effect of High Add Power, Medium Add Power, or Single-Vision Contact Lenses on Myopia Progression in Children: The BLINK Randomized Clinical Trial. JAMA. 324(6), 2020.
[13] Faria-Ribeiro M, et al. Predicted accommodative response from image quality in young eyes fitted with different dual-focus designs. Ophthalmic Physiol Opt. 38(3), 2018.
[14] Fernandes P, et al. Short-term delay in neural response with multifocal contact lens might start at the retinal level. Doc Ophthalmol. 145(1), 2022.
[15] Amorim-de-Sousa A, et al. Changes in Choroidal Thickness and Retinal Activity with a Myopia Control Contact Lens. (submitted for publication)

José Manuel González-Méijome *graduated with honors in Optometry at the University of Santiago de Compostela in 1997. After a fellowship at CCLRU, University of New South Wales in Australia, joined the Universidade do Minho in Braga, Portugal where he is currently Full Professor and Dean of the School of Sciences.*

Along with his teaching tasks in Optometry and Vision Sciences, he coordinates the line of Research in Clinical and Experimental Optometry, including the study of the retinal response to myopia control treatments, among other topics with clinical and scientific impact. He has published more than 200 articles in indexed journals (WoS h=35). He is the author or co-author of 3 books and 30 book chapters and has presented conferences in more than 30 countries. Also, it is currently: President/Dean of the Faculty of Sciences, Chief Editor of the scientific magazine "Journal of Optometry", President of the Educational Committee of the European Academy of Optometry and Optics, member of the European Qualifications Board and of the committee of evaluators of various research funding agencies in 4 countries, and Ambassador for Portugal of the Society of Ocular Surface and Contact Lenses.

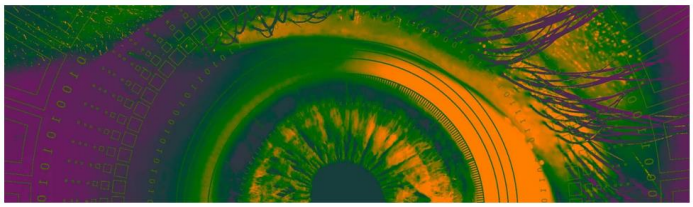

SESSION V Diagnostics tools & Visual Function

Diagnostic Tools for Keratoconus

Alejandra Consejo[1,2]

[1] Department of Applied Physics, School of Engineering and Architecture, Universidad de Zaragoza (Spain)
[2] I3A Institute for Research in Engineering, Universidad de Zaragoza (Spain)

Keratoconus is a progressive disease that affects the cornea's curvature, causing distorted vision and possible blindness if left untreated. Early diagnosis and treatment are crucial to preserving vision. Thanks to recent advances in diagnostic tools, it is now possible to detect the disease more accurately and at an earlier stage.

Scheimpflug imaging, which captures corneal topography, is considered the gold standard for diagnosing keratoconus. This technique provides detailed information about the corneal shape, thickness, and curvature, enabling more accurate diagnosis. While traditional parameters are still clinically used, new analytical methods based on machine learning are now employed to improve early detection rates. Furthermore, corneal densitometry analysis, estimated from Scheimpflug imaging, is a promising research area for early keratoconus detection.

Thanks to these diagnostic tools, earlier detection of keratoconus has led to improved patient outcomes. In this talk, we will review and discuss the latest research in early keratoconus diagnosis.

Alejandra Consejo *is a researcher specializing in Biomedical Engineering, particularly in the human eye and vision science. She is an assistant professor at the Applied Physics Department at the University of Zaragoza (Spain). She has worked in research institutions in Poland, Belgium and the UK. Her research interests range from early diagnosis of different eye diseases using the support of advanced image processing, statistics, and machine learning to the characterization of the physiology of our eyes and investigating the biocompatibility in contact lens wear. She was awarded as the best PhD graduate in Europe (EYRA, 2017), as Young Research Talent (Tercer Milenio Awards, 2021), and as leader of the best research innovation (Unita Innovation Prize 2022).*

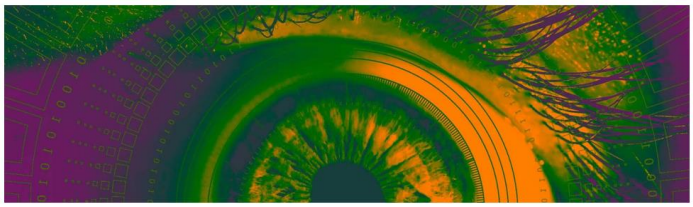

New technologies in visual refraction

Mikel Aldaba Arévalo

Centro de Desarrollo de Sensores, Instrumentación y Sistemas, Universitat Politècnica de Catalunya (Spain)

The ocular refractive status refers to the locus within the eye conjugate with optical infinity during minimal accommodation, and depending on it, eyes can be classified as emmetropic or ametropic (myopic, hyperopic or astigmatic refractive error). Refraction is the term applied to the technique to determine the refractive status, in order to arrive at the dioptric lens combination that results in maximum visual acuity with minimal accommodation. Uncorrected refractive error is the main cause of visual impairment worldwide, mainly in developing regions because of the lack of eye care professionals, and it is expected to increase further due to the "myopia boom". Automated technology capable of performing accurate refractions could help reduce this problem; moreover, it would also be beneficial in developed countries where cost-effective methods based on new technologies are demanded. To date, none has completely succeeded, mainly for two reasons: (i) the lack of control of accommodation during refraction and (ii) the fact that objective methods do not consider the patient's psychophysical response.

This talk will start introducing the role that refraction plays on research and industry and addressing the question of "Why refractive error is important?". After that, the presentation will follow with a review of basic concepts of ocular refraction such as its definition and measurement, including the state-of-the-art of subjective, objective and automated refraction methods and ophthalmic devices. Finally, some of the new lines of research that have recently shown up will be presented.

Mikel Aldaba *received a BSc in Optics and Optometry in 2003 from the University of Valladolid, Spain, and a BSc in Optometry and Vision Science in 2005 from the University of Minho in Braga, Portugal. Subsequently, he enrolled in the PhD programme in Optical Engineering from the Polytechnic University of Catalonia (UPC), obtaining his degree in 2012 with a thesis on the eye's accommodative response measurement by means of a double-pass system. He has authored 22 peer-reviewed articles, has presented communications in 54 conferences, has published two book chapters and holds three patents. His research is primarily focused in visual optics, where, in the last 15 years, he has been working on different topics such as accommodation, refraction, aberrations, optical quality, intraocular lenses, dry eye, instrumentation and colour vision. Currently he is Tenure Track Lecturer at UPC as Serra Hunter fellow and member of the Spanish Optical Society's Vision comitte board.*

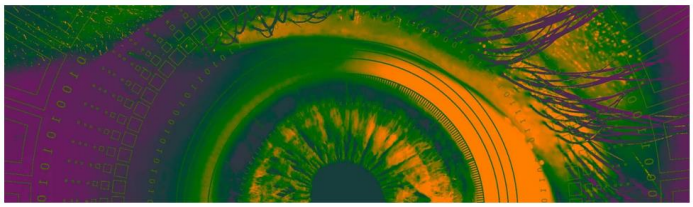

Clinical applications of a visible and near-infrared multispectral camera for reflectance evaluation of eye fundus structures

Meritxell Vilaseca

Centre for Sensors, Instruments and Systems Development (CD6), Universitat Politècnica de Catalunya (UPC) (Spain)

Optical imaging systems for noninvasive fundus diagnosis are crucial to assist ophthalmologists in their daily practice. In particular, high-resolution color fundus cameras are widely used in the clinical setting. However, since they provide RGB images, some retinal structures and substances with different spectral signatures associated with specific ocular diseases may remain undetected due to metamerism or limited spectral range.

In the last years, there have been some attempts to include MultiSpectral Imaging (MSI) technology in fundus cameras, thus combining spectroscopy with imaging technology to provide both spectral and spatial information of retinal landmarks. MSI fundus cameras are expected to improve the capability of identifying the absorption properties of the retina in-vivo, which may be relevant to advance the diagnosis and treatment of many diseases. For instance, they can spotlight degenerated tissue, vascular hemorrhages, drusen, etc., and also build oxygenation maps of the retinal vasculature. Furthermore, if the spectral sensitivity of MSI cameras is not limited to the visible range, they are able to provide information from layers that are commonly hidden in color images. In particular, the use of wavelengths beyond 900 nm, in which radiation can penetrate deeper into the biological tissue, allows the choroid to be observed.

Nevertheless, most of the recently developed fundus cameras that include MSI technology consist of traditional fundus cameras with the original illumination or detection systems replaced, which have low spatial resolution and require spatial scanning, or exhibit slow spectral sampling owing to the use of tunable filters or light-emitting diodes (LEDs). Consequently, the relatively long acquisition time leads to artifacts in the images due to eye movements; to avoid this, they only include few spectral bands. Snapshot MSI posed a solution to this problem, but at the expense of spatial resolution and computational cost. Moreover, most of these systems operate only in the visible range.

In this talk, we will review the results obtained with a newly developed benchtop MSI fundus camera that performs fast imaging of the eye fundus in the VIS and NIR regions (400 to 1300 nm) with high spectral (15 bands) and spatial resolutions, overcoming all the limitations described above[1]. The device is based on CCD and InGaAs sensors, and narrow-band LEDs. Fundus images (Fig. 1) and reflectance curves of structures of healthy and pathological eyes will be shown[2], especially those reflecting in the relatively unexplored range beyond 900 nm, which can potentially be useful for improving the medical diagnosis of certain diseases affecting deeper fundus layers.

Additionally, we are currently working on the development of a portable MSI fundus camera based on a smartphone and the first results obtained will also be discussed.

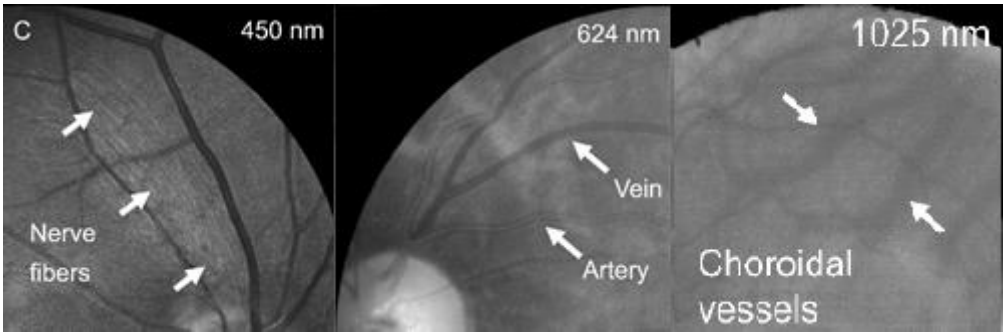

Figure 1: Spectral images of some fundus structures taken at different wavelengths.

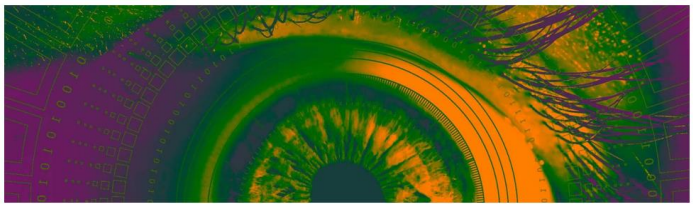

ACKNOWLEDGEMENTS: This publication is part of the project PID2020-112527RBI00, funded by MCIN/AEI/10.13039/501100011033.

[1] T. Alterini, F. Díaz-Doutón, F. J. Burgos-Fernández, L. González, C. Mateo, and M. Vilaseca. Fast visible and extended near-infrared multispectral fundus camera. Journal of Biomedical Optics, 24(9), 096007 (2019).
[2] F. J. Burgos-Fernández, T. Alterini, F. Díaz-Doutón, L. González, C. Mateo, C. Mestre, J. Pujol, J. and M. Vilaseca. Reflectance evaluation of eye fundus structures with a visible and near-infrared multispectral camera. Biomedical Optics Express, 13(6), 3504-3519 (2022).

Meritxell Vilaseca *is a full professor at the Universitat Politècnica de Catalunya (UPC). BSc in Optics and Optometry (UPC, 1996), BSc in Physics (Universitat Autònoma de Barcelona, 2000), and PhD in Optical Engineering (UPC, 2005). She leads the VIsual Optics and SPECtral Imaging Group (VISPEC) of the Center for Sensors, instruments and Systems Development (CD6), a research center at UPC that operates in the field of optics and photonics engineering. Her research focuses on visual optics, eye tracking, biophotonics, color and hyperspectral imaging. She has participated in 53 competitive research projects (in 20 as PI), and in 31 contracts with companies (in 6 as PI). The most relevant projects in the last 5 years are: Ministerio de Ciencia e Innovación-Agencia Estatal de Investigación (Refs: TED2021-130409B-C5, PID2020-112527RB-I00, DPI2017-89414-R, EIN2019-103116), Generalitat de Catalunya-ACCIÓ/AGAUR (Refs: TECSPR16-1-0085, INNOTECRD19-1-0020, 2019 PROD 00013 / IU68-016991), Ministerio de industria y Turismo (MINETUR) (Refs: AEI-010500-2021-21, AEI-010500-2018-83), EU European Commission (Innovative Training Networks [ITN] call H2020-MSCA-ITN-2015) (Ref: 675512). She has authored 63 publications in peer-reviewed journals (17 in the first quartile) (WOS h=17), 6 publications in non-indexed journals, 5 book chapters, and holds 9 patents and 1 utility model (4 of them licensed to companies). She has participated in international (111 communications, 9 of them invited) and national (58 communications) conferences. She has also authored more than 250 technical reports for companies in the framework of technology transfer services. She has supervised 9 PhD theses and is currently supervising 3 pre-doctoral students in the Optical Engineering Doctoral Program.*

At present, she is the scientific director of the CD6 (since 2019), a member of the TC8-07 Technical Committee of the 8th Division of the CIE (International Commission on Illumination) "Multispectral Imaging", of the European Optical Society (EOS), the Optical Society of America (Optica) and the Spanish Society of Optics (SEDOPTICA).

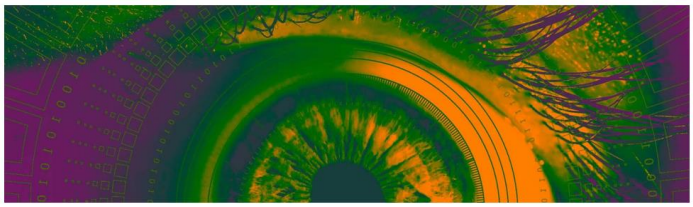

Alcohol, driving, and visual performance

Miriam Casares López[1], José J. Castro Torres[1], Francesco Martino[1], Sonia Ortiz-Peregrina[1], Pilar Granados-Delgado[1] and Rosario G. Anera[1].

[1] Department of Optics, Faculty of Sciences, University of Granada (Spain)

Introduction: Vision is perhaps the most important perceptual function influencing driving and, thus, visual impairment may alter driving performance[1]. It is known that some psychoactive substances, such as alcohol, have a negative effect on vision. Specifically, driving under the influence of alcohol, a behavior frequently adopted by drivers, is one of the leading causes of road accidents[2,3]. Speed management is an important indicator of how participants adapt their driving speed to compensate for a complex situation[4]. Therefore, the aim of this study was to assess the influence of vision and other factors on speed management under the influence of alcohol.

Methods: a total of 31 volunteers (16 females) were enrolled in the study. All participants completed three experimental sessions: a session with no alcohol consumption (baseline), a session after the intake of 300 ml of red wine (Alcohol 1), and a session after 450 ml red wine (Alcohol 2). The Breath alcohol concentration (BrAC) was measured in each session. In the three experimental sessions, vision was assessed by means of the contrast sensitivity and the retinal Straylight (log(S)). Driving performance was evaluated using a fixed-base driving simulator. The speed adaptation was calculated in each scenario as the difference between the driving speed and the speed limit.

Results: Monocular and binocular contrast sensitivity was reduced following alcohol consumption (χ^2=26.50; p<0.001 and χ^2=21.87; p<0.001, respectively). The straylight increased under the influence of alcohol (χ^2=30.06; p<0.001). Such differences were significant when comparing Alcohol 1 and Alcohol 2 conditions. Regarding driving performance, in average, participants drove above the speed limit in the three experimental conditions. Participants drove faster in Alcohol 1 condition compared to baseline. However, in Alcohol 2 condition, participants slower than in baseline conditions (Table 1). The speed management varied in the different scenarios. Factors other than the experimental condition, such as road complexity, driving experience, and the subjective perception of the influence of alcohol on driving performance, influenced speed management. Also, contrast sensitivity showed a significant influence on speed management (t=2.322; p=0.021).

	Baseline	Alcohol 1	Alcohol 2	p-value
BrAC (mg/l)	--	0.18 ± 0.08	0.29 ± 0.11	--
Monocular CS (log)	125.26 ± 18.20	108.80 ± 19.09	102.16 ± 18.87	B-A1: 0.003* B-A2: <0.001** A1-A2: 0.162
Binocular CS (log)	153.42 ± 11.87	140.46 ± 20.83	137.51 ± 21.63	B-A1: 0.013* B-A2: <0.001** A1-A2: 0.547
log(S)	0.87 ± 0.10	0.93 ± 0.14	0.98 ± 0.14	B-A1: 0.005* B-A2: <0.001** A1-A2: 0.229
Speed Adaptation (km/h)	8.80 ± 14.54	9.59 ± 14.44	7.17 ± 14.08	B-A1: 1.000 B-A2: 0.082 A1-A2: 0.007*

Table 1: Mean values ± SD of the BrAC, the speed adaptation in the general route, and the visual variables in the three experimental conditions: baseline (B), Alcohol 1 (A1), and Alcohol 2 (A2). The p-value resulting from the pairwise comparisons are also included.

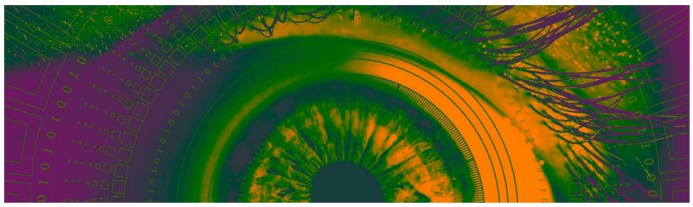

Conclusions: Visual performance deteriorated following alcohol consumption, particularly for high alcohol dosages. Speed management was also influenced by alcohol use, in such a way that participants speeded more for low alcohol concentrations, and slowed more for higher alcohol concentrations. Different factors determined the speed selected by drivers, including contrast sensitivity. This indicated that participants with better contrast felt more confident when driving under the influence of alcohol.

ACKNOWLEDGEMENTS: We thank Local Police of Granada City (Granada, Spain) and Dräger Iberia (Madrid, Spain) for lending us the breath analyzer, and Pago de Almaraes wineries for providing us with the wine used in the studio. Financial support: Grants PID2020-115184RB-I00, funded by MCIN/AEI/10.13039/501100011033, and A-FQM-532-UGR20, funded by FEDER/Junta de Andalucía-Consejería de Transformación Económica, Industria, Conocimiento y Universidades. Agencia Estatal de Investigación (PID2019-105684RB-I00/AEI/10.13039/501100011033).

---

[1] C. Owsley and G. Jr. McGwin. Vision and driving; *Vision Res*., **50**(23), 2348 (2010).
[2] Observatorio Nacional de Seguridad Vial; *Dirección General de Tráfico. Siniestralidad relacionada con el consumo de alcohol y drogas*, (2016–2017).
[3] Z. L. Li, X. W., X. H. Zhao and Q. Z. Zhang. Effects of different alcohol dosages on steering behavior in curve driving. *Hum Factors*, **61**, 139 (2029).
[4] O. Oviedo-Trespalacios, M. M. Haque, M. King and S. Washington. Self-regulation of driving speed among distracted drivers: An application of driver behavioral adaptation theory; *Traffic Inj Prev*, **18**(6), 599 (2017).

Miriam Casares López *holds a bachelor degree in Optics and Optometry and MSc in Advanced Optics and Optometry from the University of Granada. PhD in Physics and Space Science from the University of Granada since May 2021 (Cum Laude). With more than 1500 hours of teaching experience in the Bachelor degree in Optics and Optometry as Substitute Professor (since 2016) and Assistant Professor (since February 2023) at the Department of Optics (University of Granada). A total of 18 research papers indexed in JCR (21 contributions in Scopus) and 18 conference contributions in the research line of visual quality and its influence on driving performance under different experimental conditions, particularly under the influence of psychoactive substances.*

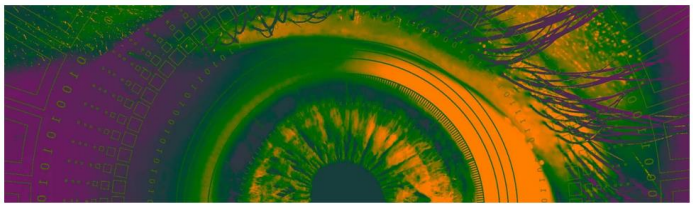

YOUNG RESEARCHERS SESSION: PAPERS

T1	**Aina Turull-Mallofré**	Prediction of the spherical subjective refraction using accommodation data in machine learning models
T2	**Rosa Vila-Andrés**	In-line characterization of toric contact lens permanent marks using a lensless microscope
T3	**Eduardo Esteban-Ibañez**	Clinical validation of daily soft multifocal contact lens simulations using SimVis Gekko based on in-vitro measurements
T4	**André Amorim**	Age and gender contribution to refraction and keratometry based axial length estimates derived using a support vector regression algorithm
T5	**Alba M. Paniagua-Díaz**	Straylight and Optical Memory Effect characterization of ex-vivo cataractous crystalline lenses
T6	**Alejandro Martínez Jiménez**	Dual Ultrahigh Speed Swept-Source & Time Domain Optical Coherence Tomography system using a time-stretch laser and a KTN deflector

Prediction of the spherical subjective refraction using accommodation data in machine learning models

Aina Turull-Mallofré[1], Mikel Aldaba[1], Meritxell Vilaseca[1], Jaume Pujol[1], Carlos E. García-Guerra[1]

[1] Centre for Sensors, Instruments and Systems Development (CD6), Universitat Politècnica de Catalunya, (Rambla Sant Nebridi 10, 08222, Terrassa, Spain)

Contact: aina.turull@upc.edu

With the uncorrected refraction as the first cause of visual impairment[1], especially in developing countries, there is a rising interest in the development of novel automated and objective systems and methodology to perform accurate estimations of the refractive error. Nowadays, subjective refraction (SR) is considered the gold standard technique to determine refraction as it considers the psychophysical response of the patient as well as is able to maintain a proper control of the accommodation, which is a key factor to not over/underestimating refraction. Moreover, during the past few years, some studies have used machine learning (ML) for predicting the subjective refraction.[2–5] However, none of them considered data about accommodation in their works. The purpose of this work was to assess the performance of machine learning regression models in the prediction of the spherical component of the subjective refraction (M_{SR}) by using information about the accommodative response.

First, the objective refraction of the participants was measured with the commercial autorefractor Grand Seiko WAM-5500 (Grand Seiko Co. Ltd., Hiroshima, Japan). Then, the accommodative response was measured as changes in the spherical equivalent (M) during a sweep of lenses with gradual decreasing powers from +1.00 D to -1.00 D in steps of 0.25 D relative to the objective refraction. With this sweep of lenses, a curve of accommodation from a relaxed state with positive lenses (fogging lenses) to the activation of accommodation was obtained. The set-up used for measuring the accommodative response was a custom-developed Hartmann-Shack aberrometer coupled to a phoropter working as an open field instrument[6]. Additionally, the SR was measured following the conventional procedure[7] to obtain the real value of M_{SR}.

Three ML models were trained and tested for M_{SR}: Normal Equation (NE), Gradient Descent (GD) and Extreme Gradient Boosting (XGB). These models were trained in a set of 132 eyes and tested in a set of 44 eyes randomly chosen. Input variables were the measured M with each lens of the sweep, the spherical component of the objective refraction (OR), and the age. The performance and agreement between the real and predicted values of M_{SR} and between the M_{SR} and OR values were analysed with the Mean Absolute Error (MAE), Root Mean Square Error (RMSE), the percentages of agreement for thresholds of 0.25 D and 0.50 D and the Bland-Altmann analysis.

Participants' mean age ± standard deviation (SD) was 32.60 ± 15.25 years in a range from 19 to 73 years and the mean spherical equivalent error ± SD was -0.86 ± 1.67 D ranging from -5.38 D to +2.75 D. When comparing the results of the OR to M_{SR}, the MAE and RMSE were 0.34 D and 0.44 D, respectively. The percentage of agreement obtained for thresholds of 0.25 D and 0.50 D were 56.82% and 78.98%, respectively. The mean difference ± SD of the differences between methods and 95% limits of agreement (LOA) were -0.160 ± 0.413 (-0.97, 0.65) D.

Regarding the results achieved with the different models, the comparison has been done between the predicted M_{SR} obtained for the 44 eyes in the test set and the real value of M_{SR} of these subjects. Actual M_{SR} values of the test set ranged from -5.38 D to +1.50 D. In table 1, the values of MAE,

RMSE, minimum and maximum predicted value, percentage of agreement for the 0.25 D and 0.50 D thresholds and the 95% LOA are shown.

Model	MAE	RMSE	Min	Max	Agreement (%)		Bland-Altman (D)	
					0.25 D	0.50 D	Mean Difference ± SD	95% LOA
NE	0.21	0.29	-5.35	+1.00	70.45	93.18	-0.103 ± 0.269	-0.42, +0.63
GD	0.20	0.28	-5.35	+0.98	70.45	93.18	-0.098 ± 0.264	-0.42, +0.62
XGB	0.24	0.35	-4.93	+1.03	65.90	90.90	+0.089 ± 0.342	-0.58, +0.76

Table 1: Summary of the agreement between real and predicted values of M_{SR}.

The three models improved the prediction of the subjective refraction in comparison to the use of the OR as an estimator of SR. The performance of NE and GD were similar and reduced the values of MAE and RMSE a 38% and 36%, respectively, compared to OR. Meanwhile, the XGB model did not perform as well as NE and GD but still reduced MAE and RMSE a 30% and 20% respectively, in comparison to OR. Regarding the percentage of agreement for the two thresholds, the three models performed significantly better than the OR and the percentage of agreement in the threshold of 0.50 D increased from a 78.98% to a 93.18% with NE and GD and to a 90.90% with XGB. The 95% LOA were also improved by all three models with respect to OR, with slightly limited results with the XGB model compared to NE and GD.

In conclusion, ML models that considered accommodation data provided better results for the estimation of the M_{SR} than the OR, with similar performances in the NE and GD models and lightly weaker results with XGB. Nonetheless, further work should be carried out to improve the current results. In this sense, the data sets used for training and testing in the present study are significantly small in comparison to other studies that use ML for the prediction of the SR, for which the size of the data set should be increased. Furthermore, considering new input variables and algorithms in future approaches may also be interesting.

ACKNOWLEDGEMENTS: This publication is part of the project PID2020-112527RB-I00, funded by MCIN/AEI/10.13039/501100011033; The first author gratefully acknowledges the Universitat Politècnica de Catalunya and Banco Santander for the financial support of her predoctoral grant FPI-UPC; The author Mikel Aldaba is a Serra Húnter Fellow.

[1] Alswailmi FK.; Global prevalence and causes of visual impairment with special reference to the general population of Saudi Arabia; *Pak. J. Med. Sci.* **34**(3), 751 (2018).
[2] R. Rampat, G. Debellemanière, J. Malet, and D. Gatinel; Using Artificial Intelligence and Novel Polynomials to Predict Subjective Refraction, *Sci. Rep.* **10**(1), 1 (2020).
[3] J. Chun, Y. Kim, K.Y. Shin, S.H. Han, S.Y. Oh, T.Y. Chung, K.A. Park, and D.H. Lim, Deep learning-based prediction of refractive error using photorefraction images captured by a smartphone: Model development and validation study, *JMIR Med. Inform.* **8**(5), 1 (2020).
[4] C.S. Hernández, A. Gil, I. Casares, J. Poderoso, A. Wehse, S.R. Dave, D. Lim, M. Sánchez-Montañés, and E. Lage; Prediction of manifest refraction using machine learning ensemble models on wavefront aberrometry data, *Artif. Intell. Data Sci. E-Health Vis. Res. Clin. Act.* **15**, S22 (2022).
[5] J. Espinosa, J. Pérez, and A. Villanueva; Prediction of Subjective Refraction From Anterior Corneal Surface, Eye Lengths, and Age Using Machine Learning Algorithms, *Transl. Vis. Sci. Technol.* **11**(4), 1 (2022).
[6] C.E. García-Guerra, J. Martínez-Roda, J.C. Ondategui Parra, A. Turull-Mallofré, M. Aldaba, and M. Vilaseca, System for objective assessment of the accommodation response during subjective refraction, *Transl. Vis. Sci. Technol.* (to pe published)
[7] W.J. Benjamin; *Borish's Clinical Refraction*, 2nd ed. (Elsevier, 2006).

In-line characterization of toric contact lens permanent marks using a lensless microscope

Rosa Vila-Andrés, Vicente Micó and José J. Esteve-Taboada

Departamento de Óptica y Optometría y Ciencias de la Visión. Universitat de València. Carrer del Dr. Moliner, 50, 46100, Burjassot, Valencia

Contact: Rosa.Vila@uv.es

Introduction: In-line holography, proposed in 1949 by Gabor[1], provides an effective technique for the characterization of objects of interest in terms of amplitude and phase data. As every interference process, in-line holography is based on the interference, over a photographic plate in the Gabor implementation but using digital sensors in modern realizations, of a reference and an object beam. The first one, comes from the non-diffracted light emanating from a coherent source while the second one, is created by the diffracted light coming from the sample illuminated with the reference beam. In ophthalmic optics, a wide variety of objects can be found available for their observation with an in-line holographic configuration, provided their weak diffractive character, which is one of the Gabor's requirements. A good example of samples would be the engraved permanent marks present in progressive addition lenses, where the holography was demonstrated to be a very efficient way to examinate them[2,3]. On the other hand, contact lenses are one of the most popular ways to compensate the refractive errors of the population with a spherocylindrical compensation over the cornea. These lenses, include also different types of permanent marking to indicate the information about their manufacturing process and ensure a correct position and orientation on the eye. The functionality of these marks, requires a proper shape, with depth value in the micron range and a high transparency to ensure an acceptable esthetical aspect and the comfort of users. These aspects may difficult the observation of the marks without a proper magnification. In this study, we present preliminary results of a lensless microscope based on digital in-line Gabor's holography for the characterization of the engraved marks of three commercial soft toric contact lenses: Miru 1-Month (Menicon), Soflens (Bausch & Lomb) and MyDay Toric (Cooper).

Methods: The sample preparation was carried out placing each soft contact lens inside a cuvette filled with saline solution to minimize the effect of the curvature and dioptric power of the lenses. The microscope, consisting of a laser source of 450 nm, a variable neutral density filter adjusting the optical power illuminating the sample and a digital sensor (Basler A312f, 782 x 582 pixels, 8.3 µm pixel size), was assembled in a vertical configuration ensuring a horizontal positioning of the lens to prevent its displacement by gravity. The device was firstly calibrated with a USAF1951 resolution target placed at the measuring distance. Once the holograms were recorded, back propagation from the CCD plane (the hologram) to the image one (the plane where the lens is placed), was done by numerical implementation of the angular spectrum method. This process was followed by the application of a phase retrieval algorithm and zero padding to remove the twin image contribution to the final image and to improve image quality and visibility. All measures were performed with a lateral magnification close to one.

Results: In perfect concordance with the theoretical resolution limit obtained from the sampling criteria based on the pixel size (ρ_{teo}=16.01 µm), the smallest resolved element on the USAF was G6-

E1 (64 lp/mm or ρ_{exp} = 15.6 µm), as it is shown in Figure 1. The configuration and the image processing algorithms applied to the USAF and the samples, allowed a proper characterization of the engraved marks in terms of amplitude and phase data, that can provide a good reconstruction of their depth and shape, providing the direct relationship between phase values and optical path differences. An example is available in Figure 2 were two of the marks' shapes are characterized in terms of its phase values.

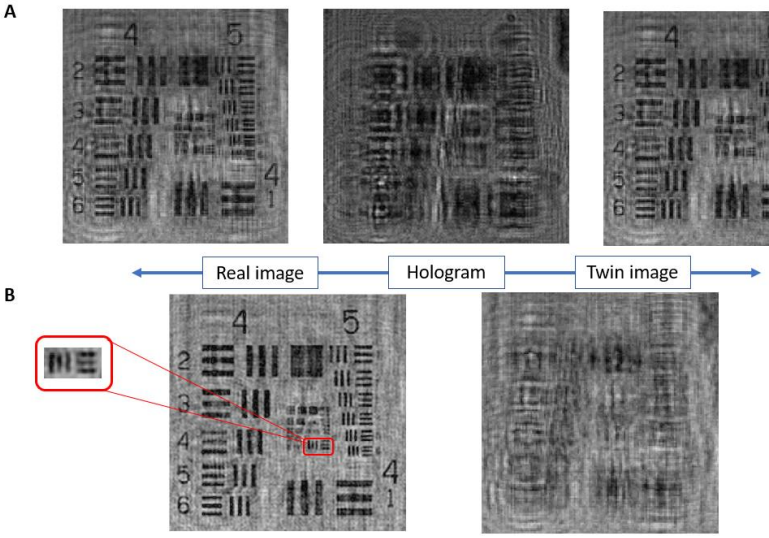

Figure 1: A) Presence of symmetrical twin images after back and front propagation of the hologram. B) Twin image removal after the application of a phase retrieval algorithm to the hologram.

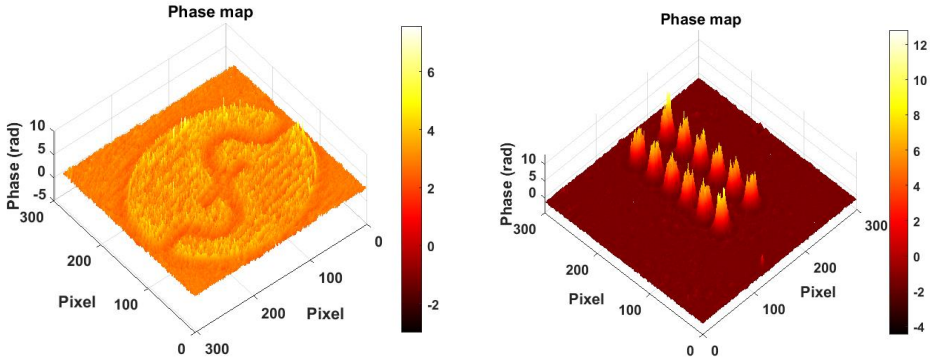

Figure 2: Phase maps in radians related to the engraved marks of one of the examined soft contact lens.

Conclusion: This study provides preliminary results of a holographic microscope and its applicability to visualize and characterize the engraved marks of contact lens, that have been proved to be a good sample to apply Gabor's in-line holography. The developing and application of iterative phase-retrieval algorithms to the obtained results, has helped to enrich the image quality in this process.

ACKNOWLEDGEMENTS: This research has been granted by the Grant PID2020-120056GB-C21 funded by MCIN/AEI/10.13039/501100011033 and by the Spanish Ministerio de Universidades FPU21/05151.

References

[1] D. Gabor; *Nature*, **Vol.161**, 777 (1949).
[2] B. Perucho and V. Micó; *Journal of biomedical optics,* **Vol.19**, 16017 (2014).
[3] B. Perucho, J. A. Picazo-Bueno, C. Ferreira & V. Micó. *Optometry and Vision Science*, **Vol. 93**, 534 (2016).

Clinical validation of daily soft multifocal contact lens simulations using SimVis Gekko based on *in-vitro* measurements

Eduardo Esteban-Ibañez[1,2], Diego Montagud-Martínez [3,4], Lucie Sawides [1,2], Amal Zaytouny [1], Alberto de Castro [1], Irene Sisó-Fuertes[2], Xoana Barcala [2], David P. Piñero [5], Walter D. Furlan [4], Carlos Dorronsoro [1,2] and Enrique Gambra [2].

[1] Instituto de Óptica "Daza de Valdés", Consejo Superior de Investigaciones Científicas, IO-CSIC (C/Serrano, 28003, Madrid, Spain)

[2] 2EyesVision SL (Plaza de la Encina, 10, núcleo 3, planta 4ª, 28760, Tres Cantos (Madrid), Spain)

[3] Centro de Tecnologías Físicas, Universitat Politècnica de València (Camí de Vera, s/n, 46022, Valencia, Spain)

[4] Departamento de Óptica y Optometría y Ciencias de la Visión, Universitat de València, (Carrer del Dr. Moliner, 50, 46100, Burjassot (Valencia), Spain)

[5]Departamento de Óptica, Farmacología y Anatomía, Universidad de Alicante (Carr. de San Vicente del Raspeig, s/n, 03690 San Vicente del Raspeig (Alicante), Spain)

Contact: eesteban@2eyesvision.com

Nowadays, there are various options available to correct presbyopia including eyeglasses, intraocular lenses and contact lenses, among others. Despite a large number of contact lens users worldwide, this number decreases as patients age and start experiencing presbyopia symptoms. A contact lens dropout has reported to reach 41% in presbyopic patients aged 65-70 years[1]. This decline occurs despite the availability of numerous bifocal or multifocal contact lens designs. Possible reasons for this use decrease include issues such as age-related dryness of the eyes, lack of awareness about these designs, poor visual performance or the complex and lengthy adaptation process.

For this reason, visual simulators such as SimVis Gekko (2EyesVision SL, Spain)[2-5] could play a crucial role in improving the adaptation process. The objective of this study was to validate clinically SimVis Gekko simulations of daily soft multifocal contact lens (MCL) designs from three different manufacturers: Dailies Total1 (Alcon), MyDay (CooperVision) and Biotrue ONEday (Bausch+Lomb). The input data used to calculate these SimVis Gekko simulations, for different additions, was obtained from *in-vitro* measurements using NIMO TR-1504 and a subsequent computational processing[6].

The clinical validation measurements included Through Focus - Visual Acuity (TF-VA) curves using negative lenses and VA at three real distances (4 m, 0.66 m and 0.40 m), with real MCLs and SimVis Gekko simulations monocularly, in eight presbyopic patients. The patients were distributed in two groups (n = 4) according to their near addition: low addition (from +0.75 D to +1.25 D) and high addition (from +1.75 D to +2.50 D). Results obtained with SimVis Gekko simulations for different MCL designs and additions had good agreement with the ones obtained with real MCLs. All MCL designs showed a partial correlation ($r_{xy,z}$)[7] and Root Mean Square Error (RMSE) ranging from 0.905 to 0.978 and 0.033 logMAR to 0.062 logMAR, respectively, when comparing the TF-VA of SimVis Gekko simulations and Real MCLs across subjects. The mean VA differences at real distances between real MCLs and SimVis Gekko simulations were lower than 0.06 logMAR (three letters of

optotypes) considering manufacturer, addition and distance.

The clinical measurements conducted in the current study demonstrate the highly accurate validation of the SimVis Gekko MCL simulations when compared to Real MCLs. Finally, the implementation of these simulations binocularly in the fitting process of MCLs has the potential to speed up this fitting process, save chair-time and enable testing of several designs in a single session.

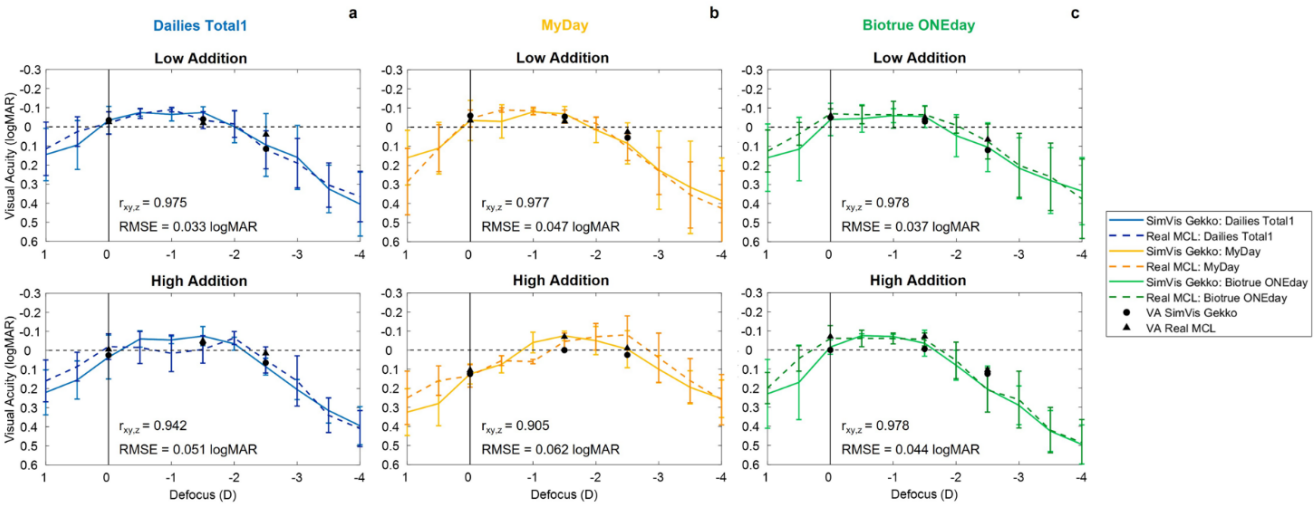

Figure 1. Clinical validation of simulated MCLs using SimVis Gekko for each addition group. TF-VA curves and real distances VA measurements with both the three families of real MCLs and the respective MCLs simulations using SimVis Gekko: (a) Dailies Total1 (blue color) (b) MyDay (yellow color) and (c) Biotrue ONEday (green color); for low (upper row) and high addition (bottom row).

ACKNOWLEDGEMENTS: This work was supported by multiple funding sources, including the Madrid Regional Government under the Industrial Doctorate Grant (IND2020/BMD-17442) to E.E-I. and A.Z., the Ministerio de Universidades, Spain (funded by the European Union Next Generation EU) under the Margarita Salas Grant to D.M.-M. and the Ministerio de Ciencia e Innovación, Spain, under Ayudas a proyectos de colaboración publico-privada (CPP2021-008388) to A.d.C. and C.D., Torres Quevedo Grant (PTQ2021-011963) to I.S.-F. and Ramon y Cajal Grant (RYC2021-033355-I) to L.S.

[1] SA. Naroo, M. Nagra and N.Retallic; Contact Lens Anterior Eye, **45**, 101599 (2022).
[2] C. Dorronsoro, A. Radhakrishnan, JR. Alonso-Sanz et al; Optica, **3**, 918 (2016).
[3] V. Akondi, C. Dorronsoro, E. Gambra and S. Marcos; Biomedical Optics Express, **8**, 3410 (2017).
[4] V. Akondi, L. Sawides, Y. Marrakchi et al; Biomedical Optics Express, **9**, 6302 (2018).
[5] X. Barcala, M. Vinas, S. Ruiz et al; Contact Lens and Anterior Eye, **45**, 101716 (2022).
[6] M. Vinas, S. Aissati, AM Gonzalez-Ramos et al, Transl Vis Sci Technol, **9**, 20 (2020)
[7] BL. Brown and SB. Hendrix. Partial Correlation Coefficients. Wiley Stats Ref Online, 1–8 (2014).

Age and gender contribution to refraction and keratometry based axial length estimates derived using a support vector regression algorithm

André Amorim[1], António Queirós, Nuno Castro and José M. González-Méijome

[1] Department and Center of Physics – Optometry and Vision Science, School of Science (4710-057, Braga, Portugal)

Contact: (amorim.andre.89@gmail.com)

Reliable accurate estimations of the axial length (AL) of the eye from refraction and keratometric data are clinically relevant and might provide valuable information in the absence of an ocular biometer.

Previous studies have attempted to do this based on regression models. Morgan et al.[1] used a linear mixed regression model that used the reciprocal of the mean anterior corneal radius of curvature and spherical equivalent refractive error in 1046 subjects, obtaining 95 % limits of agreement for the two measures of ± 0.73 mm. More recently, Queirós et al.[2] developed a model that estimated the axial length of the eye with a 95% confidence interval (CI) of approximately +/- 1.00 mm, based on 1783 children subjects. In the same study, the authors observed that 1-year changes in axial length could be estimated within +/-0.25 mm 95% CI. Using machine learning (ML) tools, Tang et al.[3] were able to predict axial length from k-mean, spherical equivalent cycloplegic refraction, central corneal thickness and white-to-white distance, along with data of age and gender [3]. A robust linear regression model provided a coefficient of determination (R^2) value of 0.87 and relatively minimal averaged errors between the predicted AL and true AL.

In this study we used data from 1098 eyes of subjects from 6 to 25 years of age. The input variables were average keratometry, non-cycloplegic refraction, sphere J_0, J_{45}, age and gender. A support vector regression algorithm was used to estimate the axial length. The data was divided in 66% for training and 33% for testing. Various models were considered, involving linear, RBF and polynomial kernels, and varying its hyperparameters. Five-fold cross-validation was used to help selecting the best parameter set, using a grid search method. Furthermore, feature selection was performed by including different sets of predictors in the model, and the one with best performance was selected. Model comparison was based on the R^2 metric, while for final evaluation, the root mean squared error (RMSE) between the actual value measured and the estimated value was also considered.

Results showed that the best model used all non-correlated features (average keratometry, non-cycloplegic refraction, sphere, J_0, J_{45}, age and gender), while the best hyperparameters set was a RBF kernel with a gamma of 0.01, an epsilon of 0.1 and a regularization factor C of 10. An R^2 value of 0.79 and a RMSE of 0.43mm were obtained. Residual analysis showed that the error distribution was approximately normally distributed (Figure 1), with a mean of zero, with a standard deviation equal of 0.43. When comparing the true and predicted values, our results seem slightly better than Queirós et al.[2] in a similar sample, but inferior to the what was obtained by Morgan et al.[1] Tang et al.[3]. We also found that including gender and age in the model slightly improved the RMSE, demonstrating they are relevant predictors for axial length.

In conclusion, axial length estimation using machine learning tools presented a high correlation and moderate-to-low bias against actual axial length in the test subset, performing better than a previous estimate on a similar sample. This was possible even in the absence of cycloplegic refraction which is a clear advantage over previous methods. This exploratory study shows potential for improving ML tools to accurately estimate the axial length based on routine optometric parameters, including non-cycloplegic refraction and adding information on astigmatic refraction, age and gender. Future research will involve exploring the addition of feature transformations and mixed terms to the model, and using larger datasets might provide additional prevision in the estimated.

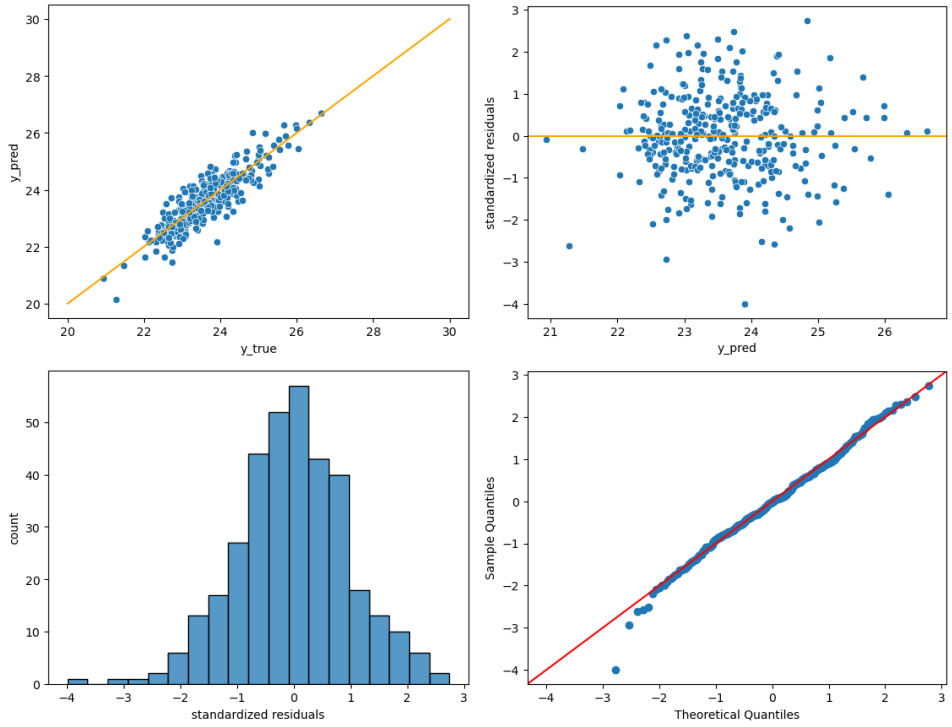

Figure 1: Residual plots computed using from the predictions obtained from the best model.

---

1. Queirós A, Amorim-de-Sousa A, Fernandes P, Ribeiro-Queirós MS, Villa-Collar C, González-Méijome JM. Mathematical Estimation of Axial Length Increment in the Control of Myopia Progression. J Clin Med. 2022;11(20):6200. Published 2022 Oct 20. doi:10.3390/jcm11206200

2. Morgan PB, McCullough SJ, Saunders KJ. Estimation of ocular axial length from conventional optometric measures [published correction appears in Cont Lens Anterior Eye. 2020 Aug;43(4):413]. Cont Lens Anterior Eye. 2020;43(1):18-20. doi:10.1016/j.clae.2019.11.005

3. Tang T, Yu Z, Xu Q, et al. A machine learning-based algorithm used to estimate the physiological elongation of ocular axial length in myopic children. Eye Vis (Lond). 2020;7:50. Published 2020 Oct 22. doi:10.1186/s40662-020-00214-2

Straylight and Optical Memory Effect characterization of ex-vivo cataractous crystalline lenses

Alba M. Paniagua-Díaz[1], Dulce Simón[1], Carmen Martínez[1], Elena Moreno[1], Inés Yago[2], José María Marín[2] and Pablo Artal[1]

[1]Laboratorio de Óptica, Universidad de Murcia, Campus de Espinardo, 30100 Murcia, Spain

[2] Oftalmología, Hospital Universitario "Virgen de La Arrixaca", El Palmar, Murcia, Spain

Contact: a.paniagua-diaz@um.es

Cataracts increase the amount of intraocular light scattering in the crystalline lens causing vision impairment by blurring and reducing the contrast in the retinal images. Wavefront shaping techniques in combination with the Optical Memory Effect have been suggested for the optical (non-surgical) correction of scattering in cataractous lenses[1]. In this context, we aim to characterize the scattering properties of excised human lenses by measuring their OME.

Methods. The Optical Memory Effect (OME) is an intrinsic correlation of scattering media that provides the isoplanatic patch of a cataract's correction imaging technique, determining how the transmitted speckle pattern changes with a tilt/shift of the incident beam[2]. We measured this using a 594-nm laser incident on different cataractous lenses by recording the transmitted speckle pattern for different values of tilt/shift of the lens and comparing them via a cross-correlation (Fig. 1a). For each cataract stage, we also characterized scattering using the straylight parameter, measured with the Optical Integration Method[3], we took dark field images (Fig.2a-d) of the lenses and measured the Michelson Contrast of the transmitted images (Fig. 2e-f). A total of 34 lenses of donors aged between 29 and 67 were measured.

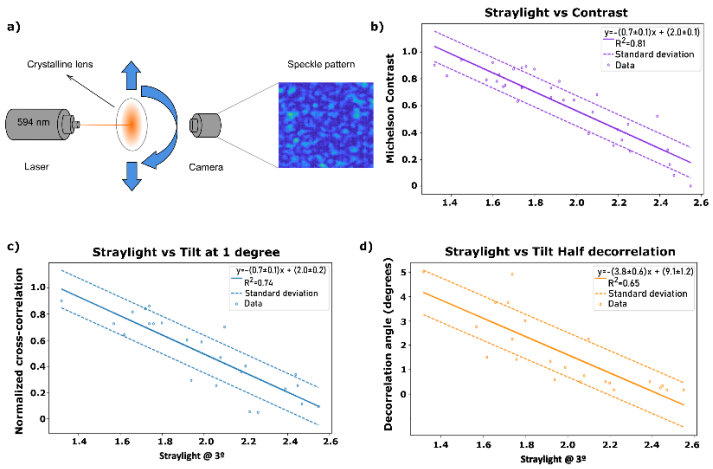

Figure 1: a) Schematic of the OME measuring experimental set-up and a recorded speckle pattern. b) Graph showing the relationship between the Michelson contrast of the transmitted images and the straylight parameter at 3 degrees. c) Representation of the normalized cross-correlation for a tilt of 1 degree vs the straylight parameter at 3 degrees of the different lenses. d) In this graph we represent the angles at which the transmitted speckle patterns are decorrelated by half as a function of the straylight of the cataractous lenses, which provides the isoplanatic patch of the media.

Results. There is a linear relationship between the straylight parameter, image contrast and OME decorrelation (Fig.1b-e), providing a new tool for the prediction of the OME range when only quantitative scattering measurements are taken. In severe cataracts (straylight parameter Log10[s]>2), the OME provides an isoplanatic patch of about 1 degree in tilt and 400 µm in shift, a range that is linearly increased as the optical opacity of the cataract decreases.

Conclusions. The OME of cataractous excised human lenses has been measured for the first time and is found to be non-negligible for cataracts, being strongly dependent on the scattering strength. This work paves the way to approaches for the non-invasive and real-time correction of cataracts using wearable devices.

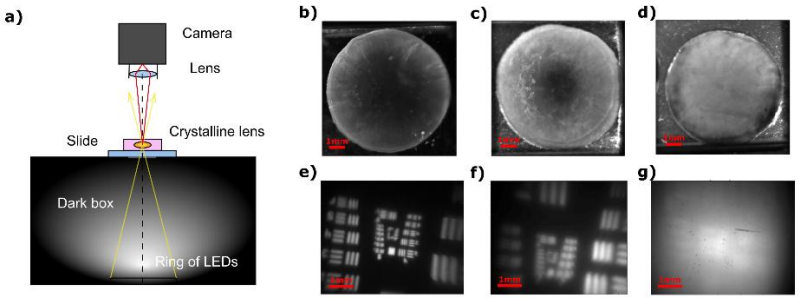

Figure 2: a) Setup for the dark field imaging. Only the scattered light is captured by the camera. b-d) Dark Field Images of a crystalline lens with cataract of different maturity stages, with straylight parameters at 3º of 1.76, 1.99 and 2.47 respectively. c) USAF-target image through the lenses shown in in the same column with Michelson Contrasts of 0.89, 0.64 and 0.08, respectively.

---

[1]Paniagua-Díaz, A. M. *et al*. *Optics Express*, **29**(25), 42208 (2021).
[2]Osnabrugge, G. *et al*. Optica, **4**(8), 886 (2017).
[3]Ginis, H. *et al*. J. Vis. **12**(3), 20 (2012).

Dual Ultrahigh Speed Swept-Source & Time Domain Optical Coherence Tomography system using a time-stretch laser and a KTN deflector

Alejandro Martínez Jiménez[1], Sacha Grelet[2], Patrick Bowen Montague[2], Adrian Bradu[1] and Adrian Podoleanu[1]

[1] School of Physical Sciences, University of Kent, CT2 7NZ, Canterbury, United Kingdom
[2] NKT Photonics, Blokken 34, Birkerød, Denmark

Contact: a.martinez-jimenez@kent.ac.uk

1. INTRODUCTION

Optical coherence tomography (OCT) is an imaging technology that allows non-destructive 3D imaging. Recently, an increased interest manifest for higher acquisition speed to overcome the distortions in the images, due to sample movements[1]. Several high-speed swept source concepts have been developed for the telecommunication wavelengths[2] due to the availability of high-speed detectors at this band. However, numerous challenges are raised when performing sweeping at shorter wavelengths, such as 1060 nm which would be essential for eye and skin imaging. To overcome this issue, we used a recently developed 40 MHz swept source[3], paired with a KTN crystal, which together allows a 400 Hz OCT volume production rate[4].

2. METHODS

The experimental set-up is presented in Fig.1. The swept source consists of a time-stretched laser that sweeps at 40 MHz. This is obtained by using a femtosecond laser in which the pulses are coupled into a photonic crystal fiber (PCF), supercontinuum generation by coherent mechanism is produced with 200 nm bandwidth at -10 dB. After the PCF, the light is passed through a 2.7 km single mode fiber that stretch each wavelength into a different time. Then the light is amplified to be used with a suitable power for OCT.

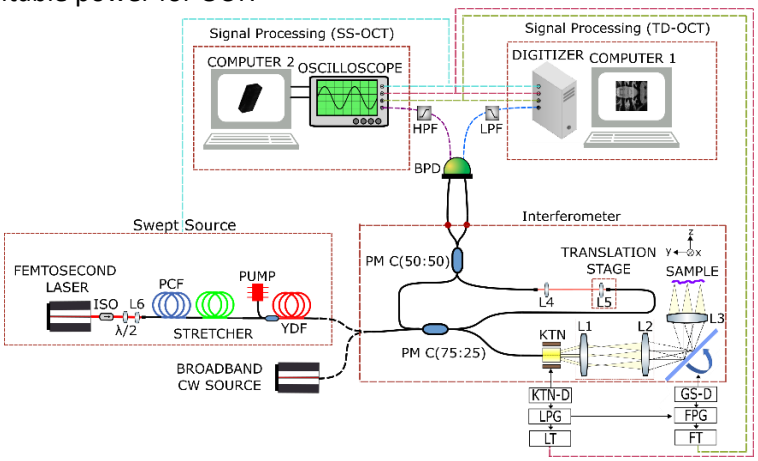

Fig.1: *Experimental set-up*, SS: swept-source; TD: Time domain, Interferometer (KTN: beam deflector using a KTN crystal, GS: galvanometer scanner, PM C: polarization maintaining couplers); Signal processing block (BPD: balanced photodetector, HPF: High pass filter, LPF: Low pass filter); Triggers (LT: line, FT: frame); Pulse generators (LPG: line, FPG: frame); Drivers (KTN-D: KTN, GS-D: galvanometer scanner). Lenses: L1, L2, L3, L4, L5 and L6 of focal lengths 3 cm, 7.5 cm, 4.5 cm, 1.5 cm, 1.5 cm and 4.51 mm respectively.

Due to data transfer-speed and processing speed limitations, real-time SS-OCT processing is not possible. For that reason, a time-domain system is used to guide the position of the sample, hence

reference here to a dual imaging system. As scanners, we pair a KTN crystal with a galvanometer scanner. The KTN crystal is able to scan at 100 kHz when a 200 V sinusoidal signal is applied, and -240 V DC bias. The deflection angle is determined by the high voltage applied onto the crystal. At 200 V, the lateral scanning along X is 2.95 mm, whilst using the galvo at 2.5 V along Y, the lateral scanning is 6.6 mm. The interferometric signal from the SS is then captured by a 23 GHz balanced photodetector and digitized using a 20 GHz oscilloscope, which is connected to a computer for data transfer and processing.

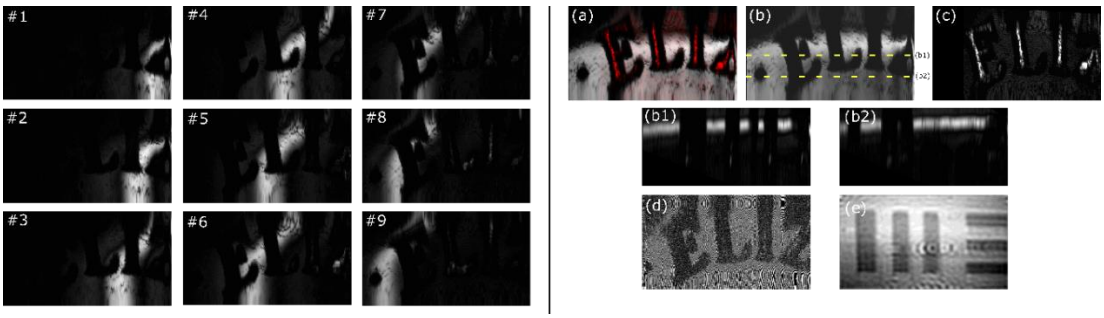

Fig.2: *En-face* OCT images of a tilted coin in which the coherence gate is seen bright #1-9. (a) Corrected en-face image for tilt of the coin, bottom surface coin in grey and top surface coin in red. (b) Corrected *en-face* image for tilt of the coin, showing the bottom surface coin with (b1,b2) B-scans at the yellow positions. (c) Corrected *en-face* image for tilt of the coin, showing the top surface coin. (d) Time domain OCT image using broadband continuous wave source. (e) USAF Target *en-face* image using time domain OCT.

3. RESULTS & CONCLUSIONS

A coin is used as a sample to perform OCT topography. The coin is slightly tilted and therefore the narrow coherence gate led to fragmented *en-face* OCT images Fig.2 (#1-9). The bright patch in the *en-face* OCT images represents a projection of the coherence gate on the sample. Two such cuts are shown, corresponding to the *z* position of the coin base Fig.2 (b) and corresponding to the *z* position of the top of the letters Fig.2 (c). B-scans on the yellow positions are shown in Fig.2 (b1-b2), and time domain images from the alignment of the coin Fig.2 (d), and lateral resolution measured using a USAF Target Fig.2 (e).

In this abstract, an ultrahigh speed OCT system with a volume rate of 400 Hz is presented. This is based on a 40 MHz swept source paired with a fast KTN scanner. A time domain subsystem enables proper adjustment of the sample, before imaging with the high-speed SS-OCT system. Due to the high-frequency of the photodetected signal, high-speed electronics is needed which complicates the acquisition and therefore, the real-time visualization. With such large speeds, there is a need for methods that allow real-time display of the SS-OCT images.

ACKNOWLEDGEMENTS:
The authors thank the European Commission for the Innovative Training Networks "NExt generation of Tunable LASers for optical coherence tomography" (ITN-NETLAS) program of the Marie Sklowdowska-Curie actions (H2020-EU.1.3.1., grant agreement No. 860807)

[1]A. de Castro, E. Martínez-Enríquez, and S. Marcos; ***14**, 2138, Biomed. Opt. Express* (2023).
[2]T. Klein and R. Huber; *Biomed. Opt. Express* **8**, 828 (2017).
[3]S. Grelet, A. Martínez Jiménez, R. D. Engelsholm, P. B. Montangue, A. Bradu and A. Podoleanu; *IEEE Photonics Journal*, **14**, 1 (2022).
[4]A. Martínez Jiménez, S. Grelet, V. Tsatourian, P. B. Montangue, A. Bradu and A. Podoleanu; *IEEE Photonics Technology Letters*, **34**, 1277 (2022).

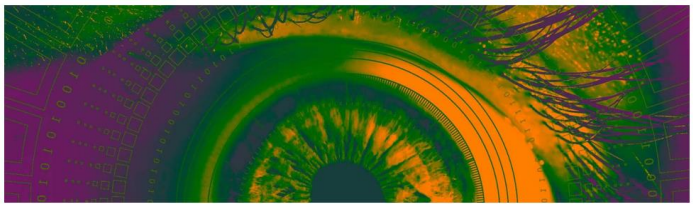

YOUNG RESEARCHERS SESSION: POSTERS

P1	**Ebrahim Safarian Baloujeh**	Effect of small angle misalignments on ocular wavefront Zernike coefficients
P2	**Francesco Martino**	Do interocular differences affect binocular visual performance after inducing forward scattering?
P3	**Joan Goset**	Eye movements inPost-COVID-19 condition patients
P4	**PaulaGarcía**	Colorimetric screen characterization based on a non-primary constancy colour model
P5	**Diana Gargallo**	Using a clinical OCT to characterize the edge shape of Contact Lenses (CL)
P6	**Pilar Casado**	Exploring the relationship between axial length and disability glare vision
P7	**Lourdes Camblor**	Caracterización del color percibido en visión con luz infrarroja pulsada
P8	**Danielle Viviana Ochoa**	Effects of optical irradiation with laser and LED light sources on cell cultures of leukemia
P9	**João M.M Linhares**	A Color Vision Test – comparing results between computer screens
P10	**José A.R. Monteiro**	A Color Vision Test Assessed by Neural Networks
P11	**Laura Clavé**	Colour vision change after multifocal diffractive IOL implantation
P12	**Victor Rodriguez-Lopez**	Direct Subjective Refraction: a new approach for refractive error measurements and the impact of accommodation
P13	**Sara F.Lima**	Impact of refractive error compensation methods on a webcam eyetracking system
P14	**Alba Herrero-Gracia**	Comparison of the Farnsworth Munsell 100 Hue and MUC tests in the over 50s
P15	**Anabel Martínez-Espert**	Assessment of the optical performance of presbyopic intraocular lenses by measuring of the Through the Focus Point Spread Function
P16	Withdrawn	
P17	**IñakiBlanco-Martínez**	Contribution of the anterior corneal topography to off-axis wavefront aberration: a pilot study
P18	**Inas Baoud Ould Haddi**	Effect of aberrometry in intraocular lenses on visual quality
P19	**Raquel Salvador-Roger**	Calibration of a tunable Lens for optometric applications

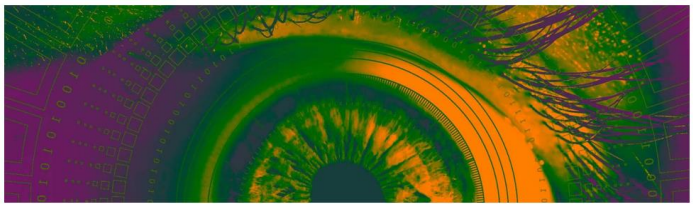

P20	**Sara Ferrer-Altabás**	Low-cost manually tunable lens for astigmatic compensation in optical instruments
P21	**Fátima Cuéllar**	Optical imaging quality and expected range of vision of two presbyopia-correcting intraocular lens designs
P22	**Marina Bou**	Development of a portable and low-cost multispectral fundus camera
P23	**María Mechó-García**	Repeatability in wavefront measurement at different pupil sizes in Young subjects
P24	**Santiago Sager**	A compact binocular adaptive optics visual simulator for clinical use in highly aberrated patients
P25	**Sara Silva-Leite**	Visual Function of Myopic Young Adult swith a Novel Ophthalmic Lens for the Control of Myopia Progression
P26	**Jessica Gomes**	Dynamic accommodation from wavefront aberrometry in symptomatic and asymptomatic subjects
P27	**XinyuWang**	Adaptive Optics vision simulator for 2-photon vision
P28	**ErikM.Barrios**	Restoration of retinal images using dictionary learning-based methodology
P29	**María Pilar Urizar**	Towards a low-cost optical biometer: development of a low-cost optical delay line for axial scans and a whole-eye beam scanner for fixation checks
P30	**Elena Moreno**	Wavefront shaping and optical memory effect of ex-vivo cataractous crystalline lenses
P31	**Pilar Granados-Delgado**	Eye dominance and visual quality
P32	**Amal Zaytouny**	Clinical validations of the SimVis binocular visual simulator

Effect of small angle misalignments on ocular wavefront Zernike coefficients

Ebrahim Safarian Baloujeh[1], José M. González-Méijome[2]

[1] INMA, Consejo Superior de Investigaciones Científicas & Universidad de Zaragoza (5009, Zaragoza, Spain)
[2] Department and Center of Physics – Optometry and Vision Science, School of Science (4710-057, Braga, Portugal)

Contact: esafarian@unizar.es

Aberrometry is an objective technique to measure the wavefront aberration of the eye, commonly reporting the results as Zernike polynomials. Ensuring that the wavefront sensor and the eye are continuously aligned is crucial when measuring changes over time. Simulating lens decentration due to accommodation proved to affect higher order aberrations [1]. Another study showed decentered contact lens induced third-order aberrations [2]. Decentration and tilt of intraocular lenses also showed increase in wavefront aberrations and a deterioration in optical performance [3]. Precise fixation, proper alignment of instruments and accurately determining the position of the pupil center are considered essential for measurement variability and obtaining accurate high order wavefront error measurements [4].

The use of extended objects as fixation targets raises the likelihood of misalignment when performing repeated measurements. The purpose of this study was to evaluate the impact of sustained reading on temporal changes of the wavefront error, and the potential impact of small changes in fixation on wavefront measurements as potential limitation to detect small temporal differences in wavefront error.

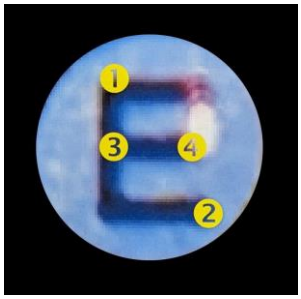

Figure 1: Fixation target used in IRX3 aberrometer (Imagine Eyes, Orsay, France).

Two experiments were conducted. In the first experiment, 13 volunteers who were in good health and aged between 44 and 57 years were recruited for the study. They were instructed to engage in a near vision reading task under two different lighting conditions. In the first condition, the ambient light was set to its maximum level (255.81 lux) and the brightness of the reading device was adjusted to the highest value. This was determined by measuring the luminance of a white circle (362.54 cd/m^2) and a black circle (2.23 cd/m^2) using a luminance meter. The Michelson contrast for this condition was calculated to be 0.987. In the second condition, the ambient light was dimmed to 0.97 lux and the brightness of the device was set to the lowest value. The luminance of the white and black circles in this condition were measured as 5.46 cd/m^2 and 0.02 cd/m^2, respectively, resulting in a Michelson contrast of 0.992.

For the reading task, a Microsoft Surface Book 2 laptop with a screen size of 3000 x 2000 pixels was utilized. Before starting the reading task, baseline aberrometry measurements were

conducted by the same observer. Participants positioned their chin and forehead on a head movement stability tool at a distance ranging from 20 cm to 45 cm from the reading device. This distance was carefully chosen to induce maximum accommodation effort, causing the text to start to become blurred. The participants were then asked to read a text for a duration of 20 minutes under both high and low lighting conditions.
Aberrometry measurements were performed using an IRX3 Shack-Hartmann aberrometer from Imagine Eyes (Orsay, France) at several time points: before the reading activity, immediately after the activity, as well as 5 and 10 minutes after completing the task. Each measurement was conducted three times, and the results were averaged for subsequent analysis. The aberrometric data obtained for each eye was rescaled based on the smallest value of the maximum round pupil recorded during each measurement.
The measurements reveal that immediately after engaging in visual tasks, there is an increase in defocus aberration (C_2^0 coefficient), but this value returns to the baseline level in 48% of the eyes during subsequent measurements. As for the C_4^0 coefficient, which represents primary spherical aberration, it initially decreases immediately following the task and then increases in 36% of the eyes. Regarding vertical coma (C_3^{-1} coefficient), a pattern of increase followed by a decrease is observed in 58% of the eyes. This phenomenon can potentially be explained by the downward drop of the crystalline lens during accommodation caused by gravity, leading to changes in higher order aberrations.

The second study group consisted of 10 volunteers with ages ranging from 24 to 49 years who were asked to look at different points of fixation E-letter. The wavefront aberrations of their eyes were recorded three times and their average for analysis. Defocus was compensated with help of the Badal system of the aberrometer, so subjects could observe the fixation E-letter clearly without wearing vision aids and without accommodating.
Analysis of these results showed that the C_4^0 coefficient increased in 50% of eyes when subjects changed their fixation gaze from point 1 to 2 in the figure 1. Moreover, the C_3^{-1} coefficient indicated a decreasing trend in 55% of eyes under the same conditions. The changes resulted from altering the fixation gaze are in the range of changes observed after a near vision task in the first experiment and might be a confounder when trying to detect such small changes in the wavefront error.
According to the results, it was found that after a sustained visual task under different lighting conditions small changes in Zernike coefficients can be detected, demonstrating some predominant patterns. However, considering that the fixation target uses an extended object (E-letter equivalent to 0.5 decimal acuity/0.3 logMAR/10 arcmin from top to bottom), misalignments might contribute to the random changes, which could make it difficult to detect minor anatomical or physiological changes in the human eye over time. Instead of letters to ensure focus and fixation, or other recognition fixation patterns, it is suggested to use non-recognition targets such as the Maltese cross to consistently make patients to look at a very specific point in the center of the target, while still having to focus to see the target as clear as possible. It is expected that this approach removes part of the random variations of the wavefront measurements.

Acknowledgements:
Funded by the European Union's Horizon 2020 research and innovation programme under the Marie Skłodowska-Curie grant agreement No 956720.

[1] L. He, RA. Applegate; *J Cataract Refract Surg*, **37(7)**, 1313 (2011).
[2] C. A. Fedtke, k. Ehrmann, V. Thomas, RC. Bakaraju; *Clin Optom,* **8**, 57 (2016).
[3] T. Lawu, K. Mukai, H. Matsushima, T. Senoo; *J Cataract Refract Surg*, **45(5)**, 662 (2019).
[4] DE. Koenig, RA. Applegate, JD. Marsack, EJ. Sarver, LC. Nguyen; *Clin Exp Optom*. **92(3)**, 246 (2009).

Do interocular differences affect binocular visual performance after inducing forward scattering?

Francesco Martino[1], José Juan Castro-Torres[1], Miriam Casares-López[1], Sonia Ortiz-Peregrina[1] and José Ramón Jiménez[1]

[1] Laboratory of Vision Sciences and Applications, Department of Optics, Faculty of Sciences, University of Granada (Prof. Adolfo Rancaño, s/n 18071, Granada, Spain)

francesco@ugr.es

Introduction: Assessing binocular visual performance is an important aspect of a visual examination. To evaluate binocular vision, the different visual functions and stereopsis are taken into account. The latter is defined as the capacity of the visual system to see in-depth the surrounding environment. In addition, interocular differences represent an important factor to consider in visual performance. Indeed, they are induced in ocular disease affecting one eye, such as cataract[1], in ocular disorders such as amblyopia[2] or following refractive surgery[3]. A further phenomenon to consider with regard to interocular differences is intraocular light scattering (forward scattering). This phenomenon produces a veiling luminance on the retina causing a deterioration in retinal image quality[4]. As a result, many visual functions are impaired, such as contrast sensitivity and visual discrimination capacity at night (perception of halos)[5]. To our knowledge, there is a lack of studies examining different degrees of interocular differences on binocular visual performance.

Purpose: To assess binocular visual performance by means of stereopsis and various binocular visual functions after inducing monocular forward scattering by filters, and in addition, to study the influence of interocular differences on stereopsis.

Methods: Seven young healthy subjects were enrolled. Four Bangerter foils and one fog filter (BPM2) were used to induce different levels of monocular forward scattering, causing different levels of interocular differences. In order to analyze the impact of the forward scattering, several visual functions were measured binocularly in terms of visual acuity, contrast sensitivity, visual discrimination capacity and distance stereoacuity. The filter was placed on the dominant eye. Additionally, interocular differences were calculated for four ocular parameters: the Objective Scatter Index (OSI), Strehl ratio (SR), modulation transfer function cut-off (MTF cut off) and straylight (log[s]).

Results: A statistically significant deterioration in visual acuity, contrast sensitivity and stereoacuity was observed for all of the filter conditions with respect to the natural state (baseline). Under these conditions, the most significant degradation was found for the Bangerter foils. Similarly, the interocular difference for the three retinal image quality parameters (OSI, SR and MTF cut-off) and log(s) also increased significantly for the Bangerter foil condition, but not for the BPM2 filter (except log(s)). A statistically significant correlation was found between the interocular differences and the stereopsis, such as the greater the interocular differences, the greater the distance stereoacuity and in consequence, the poorer the binocular visual performance.

Conclusion: Increased forward scattering in the dominant eye resulted in interocular differences, which significantly reduced the overall binocular visual performance, including several important visual functions (visual acuity, contrast sensitivity and visual discrimination capacity) and distance stereoacuity. The results suggest that marked interocular differences in ocular parameters should be taken into account in cases of ocular pathology (cataract), amblyopia, refractive surgery or emmetropization technique such as monovision to correct presbyopia.

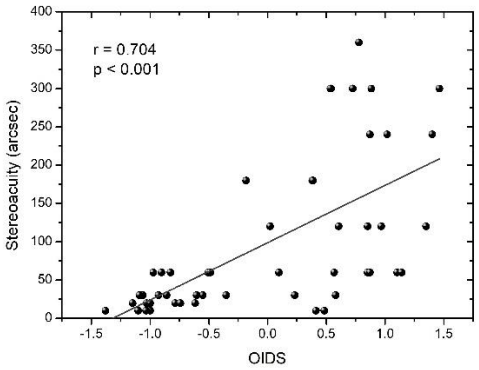

Figure 1: The overall interocular difference score (OIDS) of the ocular parameters analyzed as a function of distance stereoacuity (arc sec)

		VA	CSF	Stereoacuity (arcsec)	VDI
Baseline	(no filter)	1.3 ± 0.1	166 ± 4	20 ± 8	0.13 ± 0.04
Bangerter foils	BF_0.8	1.1 ± 0.1	139 ± 14	83 ± 90	0.18 ± 0.09
	BF_0.6	1.1 ± 0.1	137 ± 17	104 ± 64	0.23 ± 0.12
	BF_0.4	1.1 ± 0.2	127 ± 17	180 ± 98	0.26 ± 0.13
	BF_0.3	0.9 ± 0.2	134 ± 24	231 ± 122	0.19 ± 0.09
Fog filter	BPM2	1.2 ± 0.2	146 ± 14	36 ± 24	0.15 ± 0.08

Table 1: Mean values of the binocular visual functions: Decimal visual acuity (VA), averaged contrast sensitivity function (CSF), distance stereoacuity and visual disturbance index (VDI) for the different Bangerter foils and fog filter used

		Interocular differences			
		SR	MTF cutoff	OSI	log(s)
Baseline	(no filter)	0.08 ± 0.05	10.9 ± 5.9	0.21 ± 0.20	0.06 ± 0.04
Bangerter foils	BF_0.8	0.15 ± 0.07	29.4 ± 10.2	3.41 ± 0.46	0.37 ± 0.16
	BF_0.6	0.14 ± 0.06	28.2 ± 8.5	4.77 ± 1.22	0.54 ± 0.05
	BF_0.4	0.16 ± 0.07	31.4 ± 8.2	5.66 ± 1.14	0.72 ± 0.06
	BF_0.3	0.17 ± 0.07	33.2 ± 9.1	7.35 ± 1.04	0.69 ± 0.10
Fog filter	BPM2	0.04 ± 0.04	4.1 ± 4.2	0.27 ± 0.21	0.29 ± 0.08

Table 2: Mean (standard deviations) interocular differences for the ocular parameters analyzed: Strehl ratio (SR), modulation transfer function cut-off (MTF cut-off), objective scatter index (OSI) and straylight (log(s)) under the various experimental conditions (baseline and wearing each of the Bangerter foils and fog filter)

ACKNOWLEDGEMENTS: Grants PID2020-115184RB-I00, funded by MCIN/ AEI/10.13039/501100011033, and A-FQM-532-UGR20, funded by FEDER/Junta de Andalucía-CTEICU.

[1] Olson RJ, Braga-Mele R, et al; *Ophthalmology*, **124,** 119 (2017).
[2] Holmes JM and Clarke MP; *Lancet*, **367**, 1343 (2006).
[3] Anera RG, Castro JJ et al; *J Refract Surg,* **27**, 597 (2011).
[4] Castro JJ, Jimenez JR et al; *J Mod Opt*, **57**, 103 (2010).
[5] Cinta Puell M and Palomo-Alvarez C; *Optom Vis Sci*, **94**, 505 (2017).

Eye movements in Post-COVID-19 condition patients

Joan Goset[1], Valldeflors Vinuela-Navarro[1], Clara Mestre[1], Meritxell Vilaseca[1] and Mikel Aldaba[1]

[1] Center for Sensors, Instruments and Systems Development, Universitat Politècnica de Catalunya, Rambla Sant Nebridi 10, Terrassa 08222 (Barcelona), Spain

Contact: joan.goset@upc.edu

Once the main urgency of the COVID-19 pandemic has finished, the concern about the long-term impact of this disease has raised. In fact, Post-COVID-19 condition (PCC) patients report a broad spectrum of symptoms, including affectation of the central nervous system and cognitive impairment. In general, neurodegenerative and neurological disorders are known to have an adverse impact on the oculomotor system[1,2], and so this has led to speculation about whether PCC may also have a similar effect[3,4]. However, the exact nature and extent of any potential influence remains unknown and further research is still needed.

Recently, eye movements have been identified as a potential biomarker for the assessment of neurological impairment at early stages thanks to eye tracking technology[5], which makes it possible to collect precise, accurate and sophisticated data about the eye positions and movements non-invasively. In addition, eye tracking systems are becoming easier to use, and they are expected to be an excellent tool in clinical environments in the next years.

Accordingly, the objective of this study was to evaluate and compare the oculomotor function by means of eye tracking technology in healthy and PCC. To do so, we conducted a study at the Hospital de Terrassa on 16 healthy control participants (10 females and 6 males), 38 COVID-19 patients with mild symptoms who recovered at home (34 females and 4 males), and 19 COVID-19 patients with severe symptoms who were hospitalized (10 females and 9 males), both with PCC.

During the study, participants performed a battery of visual tasks that elicited voluntary saccades (using gap, overlap and posner paradigms), smooth pursuits (rectilinear and sinusoidal) and fixations (with and without peripheral distractors) while the eye tracker EyeLink 1000 Plus (SR Research) recorded their eye movements. The raw data collected were analysed, and several parameters were calculated, including the number of saccades and micro-saccades, latency, Root Mean Square error (RMS) and Bivariate Contour Ellipse Area (BCEA) during the fixation test, among others.

Prosaccadic and antisaccadic movements had a longer latency in the mild COVID group in comparison to controls. Also, saccades during horizontal smooth pursuit were significantly larger in severe and mild COVID participants. Figure 1 shows a comparison between two representative participants of the control and severe COVID groups in the smooth pursuit task. The fixation stability was poorer in mild COVID participants, who showed higher BCEA and RMS. Figure 2 depicts the eye-tracking data during the fixation task for two of these cases: a control and a mild COVID participant.

These results unveil differences in the oculomotor function of controls and PCC individuals. The abnormal parameters and the characteristics of the individuals might be useful to differentiate pathophysiologic mechanisms of PCC.

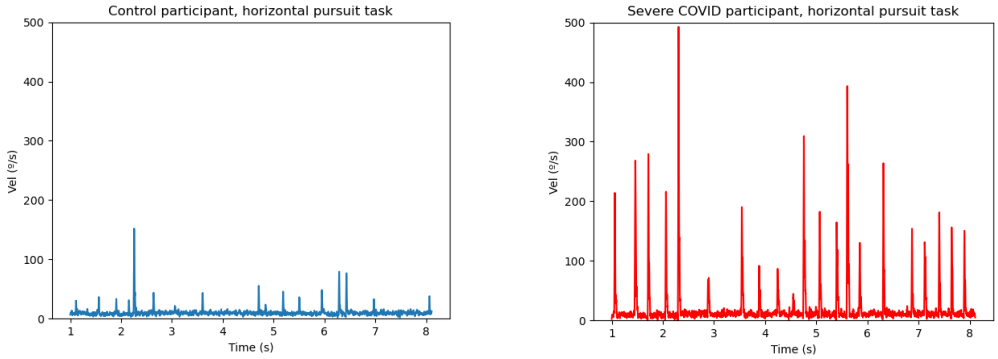

Figure 1: Velocity of the saccades in the horizontal pursuit task of two representative examples: a control participant (left) and a severe COVID participant (right). The latter shows a higher saccade velocity, indicating larger amplitude of saccades compared to the control participant.

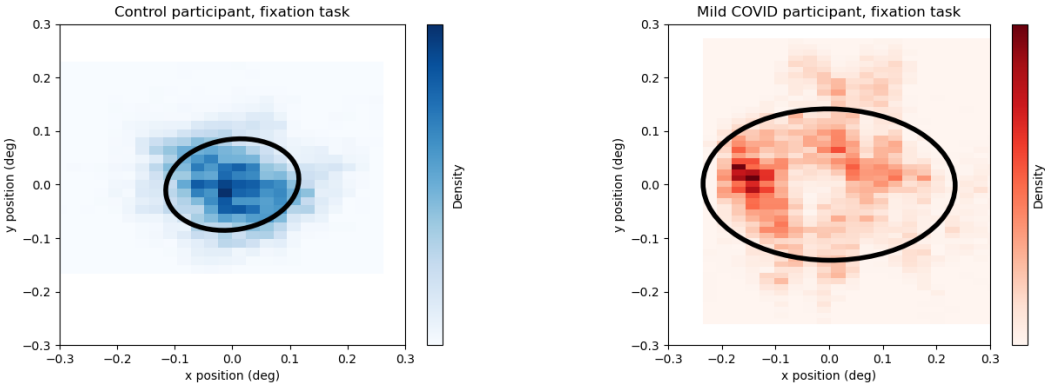

Figure 2: 2D histogram of gaze positions in the fixation task of a control participant (left) and a mild COVID participant (right). The BCEA contour is depicted in black, which takes the 68% of points[6] and represents the dispersion of the data for both cases. The control's gaze positions are less spread.

ACKNOWLEDGEMENTS: This publication is part of the project PID2020-112527RBI00, funded by MCIN/AEI/10.13039/501100011033. J.G. thanks the Spanish Government for the predoctoral FPI grant he received.

---

1. Opwonya, J. *et al.* Saccadic Eye Movement in Mild Cognitive Impairment and Alzheimer's Disease: A Systematic Review and Meta-Analysis. *Neuropsychol Rev* **32**, 193–227 (2022).
2. Tao, L. *et al.* Eye tracking metrics to screen and assess cognitive impairment in patients with neurological disorders. *Neurol Sci* **41**, 1697–1704 (2020).
3. García Cena, C. *et al.* Eye Movement Alterations in Post-COVID-19 Condition: A Proof-of-Concept Study. *Sensors* **22**, 1481 (2022).
4. Carbone, F. *et al.* Cognitive dysfunction 1 year after COVID -19: evidence from eye tracking. *Ann Clin Transl Neurol* **9**, 1826–1831 (2022).
5. Beltrán, J., García-Vázquez, M. S., Benois-Pineau, J., Gutierrez-Robledo, L. M. & Dartigues, J.-F. Computational Techniques for Eye Movements Analysis towards Supporting Early Diagnosis of Alzheimer's Disease: A Review. *Computational and Mathematical Methods in Medicine* **2018**, 1–13 (2018).
6. Crossland, M. D. & Rubin, A. G. S. The Use of an Infrared Eyetracker to Measure Fixation Stability: *Optometry and Vision Science* **79**, 735–739 (2002).

Colorimetric screen characterization based on a non-primary constancy colour model

Paula García, Mª Josefa Luque and Mª del Carmen García

Optics and Optometry and Vision Sciences, Physics Faculty, University of Valencia, Carrer del Dr. Moliner (46100, Burjassot, Valencia)

Contact: paugarba@alumni.uv.es

Aim: Electronic displays are a powerful tool for stimulus visualization for psychophysical experiments[1]. Controlling the colour of the stimuli being represented on the screen is essential in isolating the response of particular visual mechanisms and to allow clinicians to obtain more precise results and conclusions about visual perception[1,2]. To this end, displays must be colorimetrically characterized. In this work, we analyse if a particular LED backlight screen can be characterized by a model assuming constancy of primaries.

Experimental Method: The video display device used for this study was a Lenovo MT 81HN laptop with LED backlight (Lenovo Group, Beijing, China) and measurements were taken with the ColorCAL MKII Colorimeter (Cambridge Research Systems, UK). Laptop settings 'energy save mode', 'night mode' and 'automatic brightness' were turned off and the device was always plugged into the electricity. Measurements were taken in a dark room with the colorimeter placed in the centre of the screen. Functions based on the Colorlab toolbox[2,3] for MATLAB (MathWorks, Massachusetts, USA) were used for display characterization and colorimetric operations. Statistical Package for the Social Sciences (SPSS, IBM, USA) was used for statistical analysis.

First of all, a characterization measurement based on three independent channels was conducted. Stimuli filled the whole screen and the colorimeter was centred in the middle, with the aid of crosshairs shown at the beginning of the measurements. The chromaticity and luminance of each primary and of the monitor achromatic stimuli were measured at 26 linearly spaced digital levels, transformed into CIE1931 tristimulus values, labelled as experimental data and stored. In order to compare different characterization models, 100 random colours were generated and measured. The corresponding RGB values were saved in a file for further processing.

Model 1 assumes primary constancy and additivity. This premise states that the tristimulus values of a colour reproduced with the mixture of the three primaries can be calculated by applying Grassman's laws (Equation 1). To substantiate this model, we used the minimum square fitting method to determine the monitor's ICC Profile (International Color Consortium, Virginia, USA), that is, the chromaticity coordinates of each primary colour ($x_{i,p}$, $y_{i,p}$, $z_{i,p}$), the luminance of primaries ($Y_i(n_{i,p})$) and the background colour (B-L) for each digital level (n_i) from the data experimentally measured[2].

$$\begin{pmatrix} X(C) \\ Y(C) \\ Z(C) \end{pmatrix} = \left[\begin{pmatrix} x_{R,P}/y_{R,P} & x_{G,P}/y_{G,P} & x_{B,P}/y_{B,P} \\ 1 & 1 & 1 \\ z_{R,P}/y_{R,P} & z_{G,P}/y_{PG} & z_{B,P}/y_{B,P} \end{pmatrix} \begin{pmatrix} Y_R(n_{R,P}) \\ Y_G(n_{G,P}) \\ Y_B(n_{B,P}) \end{pmatrix} \right] + \begin{bmatrix} X_{B-L} \\ Y_{B-L} \\ Z_{B-L} \end{bmatrix}$$

Equation 1

Model 2 does not assume primary constancy but still requires additivity. This supposition maintains that the chromaticity of the primary colours can vary and affect accuracy of colour reproduction. For this model, Equation 1 was also used but with some changes: background is not considered and the primary coordinates of each primary are dependent on the digital values and are obtained by interpolation.

Once the parameters for each model are obtained, the same calculation procedure is conducted. With the equation for each case, theoretical tristimulus values are calculated for the experimental

RGB colours and a reference white of the video display (RGB=[1 1 1]) and CIELAB descriptors are computed from these tristimulus values.

Once LAB values are obtained, a comparison on how different the colour experimentally measured was from the model predictions (theoretical) was conducted. Colour reproductions errors (ΔE) were calculated with the CIEDE2000 formula[4] shown in Equation 2, which contemplates lightness, chroma and hue. This contrast was carried out twice (once for each model) and it is based on the difference between two colours in a perceptually uniform colour space: the lower the ΔE, the smaller the difference between the two colours is. Moreover and, according to the average values described by Yang et al[4]., these colour differences can be classified in terms of perception and how difficult it is to differentiate two colours: hardly, slight, noticeable, appreciable, much, very much and strongly.

$$\Delta E = \sqrt{\left(\frac{\Delta L'}{K_L S_L}\right)^2 + \left(\frac{\Delta C'}{K_C S_C}\right)^2 + \left(\frac{\Delta H'}{K_H S_H}\right)^2 + R_T\left(\frac{\Delta C'}{K_C S_C}\right)\left(\frac{\Delta H'}{K_H S_H}\right)}.$$

Equation 2

Results: Results showed statistically significant differences between the median of the colour reproduction errors from both models (Z= 7,692, p< .05) as calculated by Wilcoxon signed-rank test. Mean difference for *Model 1* was 3,81 and 2,30 for *Model 2*. As it is shown in Figure 1, results for *Model 2* are less disperse than in *Model 1.* Additional statistical descriptive data is shown below.

Discussion: Choosing the appropriate screen characterization model is a critical step in any psychophysical measurement as it can significantly affect the accuracy and reliability of the projected colour. Results obtained with CIEDE2000 formula showed that *Model 2* had lower colour differences from the experimental data, indicating a better colour reproduction. Furthermore, these differences are denoted as perceptually noticeable[4] whereas for *Model 1* are appreciable[4]. For that reason, a model based in additivity but not requiring primary constancy is more effective for characterizing colour reproduction on this particular video display.

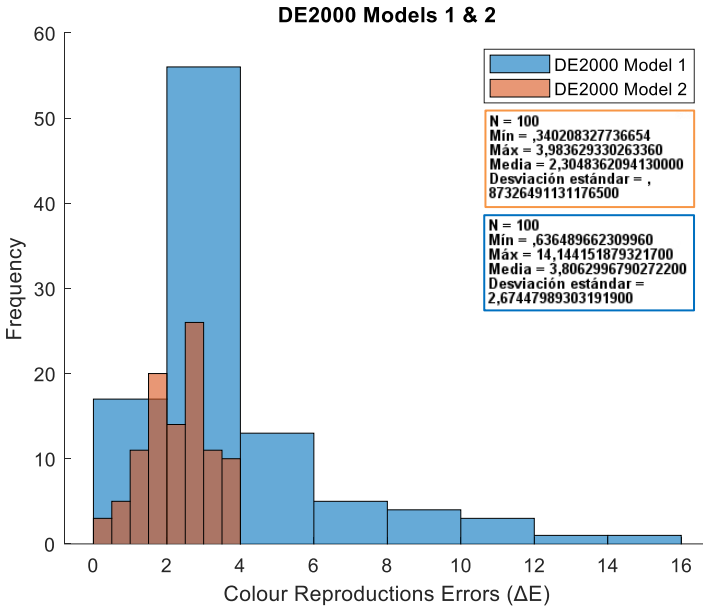

Figure 1: Histogram of colour reproduction errors for both *Model 1* and *2*

[1]To, L., Woods, R. L., Goldstein, R. B., & Peli, E; *Vision research, 90*, 15-24, (2013).
[2]García-Domene, M. C., Luque, M. J., & de Fez, D.; *Optik*, *198*, 163252, (2019).
[3]J. Malo and M.J. Luque. "COLORLAB: a color processing toolbox for Matlab"
[4]Yang, Y., Ming, J., & Yu, N; *Advances in Multimedia*, 11-11. (2012).

Using a clinical OCT to characterize the edge shape of Contact Lenses (CL).

Diana Gargallo[1], Nerea Tolón[1], Jorge Ares[1] and Sofía Otín[1]

[1] Applied physics, Science faculty, University of Zaragoza (C. de Menéndez Pelayo, 24, 50009, Zaragoza, Spain)

Contact: dgargallo@unizar.es

Optical Coherence Tomography (OCT)[1] devices are widely used in optometry and ophthalmology clinics to diagnose and study the integrity of ocular health, and/or to observe and evaluate the adaptation of contact lenses (CLs)[2]. Additionally, some researchers are also taking advantage of the high-precision interferometric capabilities of OCT to measure the mechanical properties of contact lenses in vivo or the geometrical shape of the ocular surface. Some researchers have successfully demonstrated the application of specific spectral-domain OCT-embedded devices to measure the topographic surface and central thickness of rigid and/or soft contact lenses in vitro[3,4,5].

CLs must not only provide good visual quality but also minimal interference with the physiological processes of surrounding tissues and be comfortable to wear. To achieve this condition, it is necessary to find the geometry of the posterior surface of the lens that achieves a correct support relationship with the ocular surface of the individual wearing it.

The technology proposed in this study could help CL professionals to monitor and control the geometry of the edges of the CLs they fit to their patients, which is difficult to evaluate without non-destructive techniques[6]. Unfortunately, OCT devices marketed for in vivo ocular examination cannot be easily applied to measure CLs in vitro because they are not designed to correctly position the lenses for precise measurement. Therefore, in this work, a specific opto-mechanical adapter was developed to measure the edges of Rigid Gas Permeable CLs and Soft CLs with a commercially available OCT device for clinical application from B-scan data provided by this clinical OCT.

The edges of a sample of 4 soft CLs and 4 rigid gas-permeable CLs (corneal and scleral) were successfully characterized using the following devices: 1) A spectral-domain clinical OCT (3D OCT-1000, Topcon Co.) with a central wavelength of 840 nm and a full-width at half-maximum bandwidth of 50 nm. This device can acquire B-scans with a lateral scanning range of 6 mm and an axial range of 2 mm in anterior segment scanning mode. 2) An optomechanical adapter for OCT edge measurement of contact lenses designed using Inventor® software (AutoDesk Inc., USA) and fabricated using polylactic acid via a commercial 3D modeling deposition-fused printer. The adapter includes a movable holder for placing an inclined-surface mirror to redirect the probe beam towards the surface of the contact lenses and collect and redirect the backscattered beam towards the OCT pupil entry.

The measurement procedure consisted of the following steps: first, placing the CL in a stabilised horizontal position with the concave side facing up on the OCT CL adaptor; second, transversely aligning the CL with the OCT optical axis; third, adjusting the axial OCT position to position the image profile within the reference axial interval displayed on the B-scan live video display; and finally, acquiring 6-mm-wide horizontal B-scan images in anterior chamber measurement mode and exporting them as portable network graphics image files.

In Figure 3, the results of the 24-bit color B-scan images (454x170 pixels) of the edges of the 8 CLs are shown. The images demonstrate the ability to distinguish between different edge geometries (gas-permeable rigid CLs edges in blue, soft CLs edges in red). The same crop size and scale (see scale bar in Figure 3(f)) were used for all sub-images. Optical distortion caused by different curves and refractive indices or by the distortion of the OCT cross-scan was not corrected since the edge B-scan images were only for qualitative observation.

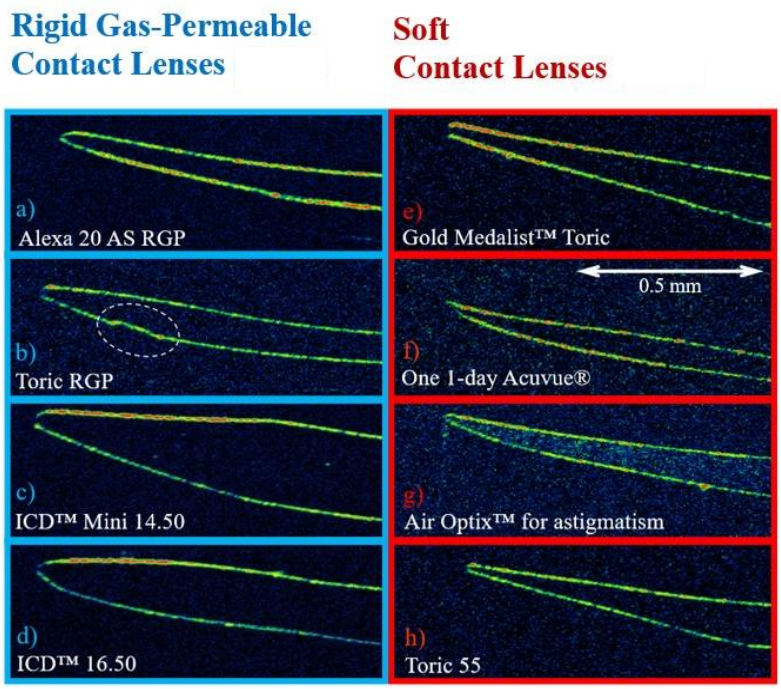

Figure 1: In vitro original B-scan images cropped from different edges of gas-permeable rigid contact lenses and commercial soft contact lenses. (a) Spherical RGP lens "Alexa 20 Aspherica" (Tiedra), (b) Toric RGP lens "Torica GP Polycon II" (Lenticon), (c) Rigid scleral lens "ICD™, (d) Rigid scleral lens "ICD™ (Paragon), (e) Toric SCL "Gold Medalist™ Toric" (Bausch & Lomb), (f) Spherical SCL "Acuvue® 1-Day" (Johnson & Jonhson), (g) Toric SCL "Air Optix™ for Astigmatism" (CIBA Vision), and (h) Toric SLC "Toric 55" (Aspect Vision Care). The scale size shown in subFigure (f) is the same for all sub-images. In subfigure (b), the toric mark is surrounded by a discontinuous white circle.

---

[1] AF. Fercher, W. Drexler et al. Optical coherence tomography: principles and applications; *Reports on Progress in Physics,* **66**, 239 (2003).

[2] M. Shen, L. Cui et al. Characterization of soft contact lens edge fitting using ultra-high resolution and ultra-long scan depth optical coherence tomography. *Investigative Ophthalmology & Visual Science*; **9**;52 (2011).

[3] K. Karnowski, I. Grulkowski et al. Quantitative optical inspection of contact lenses immersed in wet cell using swept source OCT; *Optics Letters*, **39**, 4727 (2014).

[4] I. Verrier, C. Veillas and T. Lépine. Low coherence interferometry for central thickness measurement of rigid and soft contact lenses; *Optics Express,* **17**, 9157 (2009).

[5] M. Shen, MR. Wang et al. Entire contact lens imaged in vivo and in vitro with spectral domain optical coherence tomography; *Eye Contact Lens*, **36**, 73 (2010).

[6] P. Tankam, J. Won et al. Optical Assessment of Soft Contact Lens Edge-Thickness; *Optometry and Vision Science*, **93**, 987 (2016).

Exploring the relationship between axial length and disability glare vision

Pilar Casado[1], Victoria Collados and Jorge Ares

[1] Departamento de Física Aplicada, Facultad de Ciencias, Universidad de Zaragoza, 50009 Zaragoza, Spain

Contact: pilarcasado@unizar.es

When the eye is exposed to intense light sources, a veil of light is formed on the retina. This phenomenon is known as intraocular straylight. This veil is superimposed on the retinal image, leading to a reduction in contrast, and a decrease in object visibility. In extreme cases, where the veil of light is too intense, object perception may be completely lost, resulting in *total disability glare.*

The sources of intraocular straylight are corneal and crystalline lens scattering, fundus reflectance, and translucency of the ocular wall and iris. Although age and pigmentation are the main factors[1], recent studies have shown that refractive error and some biometric parameters, such as axial length, also influence intraocular straylight[2].

The aim of this study was to evaluate the impact of disability glare on the visibility of an object, in relation to the axial length of the eye. This evaluation was carried out using a system specifically designed for the study of disability glare vision[3]. The system consists of two channels, one for the visualization of the stimulus and the other for the presentation of the glare source. Participants were divided into two groups according to their axial length: 15 subjects in the high axial length group (24.87 ± 0.58 mm) and 15 subjects in the low axial length group (23.24 ± 0.46 mm). Sinusoidal stimuli of minimum perceptible contrast and of different spatial frequencies (0.2, 0.3, 0.6, 0.9, 1.2, and 1.8 c/°) were used in this study. The intensity of the glare source was progressively increased until the visibility of the stimulus was completely lost. At that point, the illuminance at the corneal plane that had caused total disability glare was measured using a lux meter.

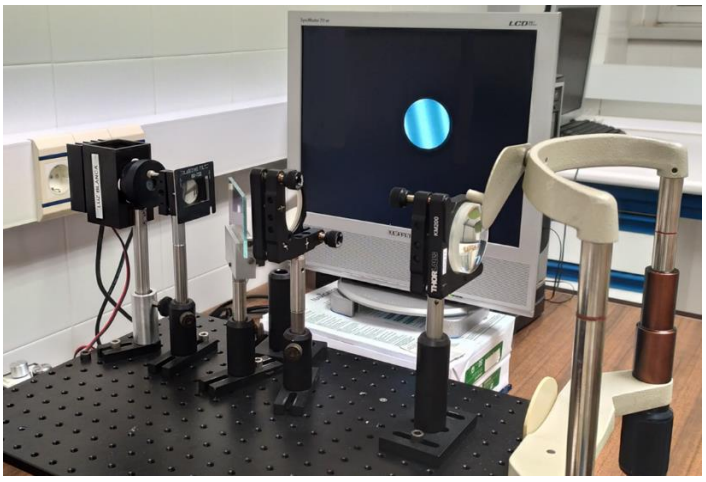

Figure 1: Experimental system used in the study

For all measured spatial frequencies, the high axial length group showed a lower value of illuminance in the corneal plane causing total disability glare. This suggests that people with high axial length allow less light before being dazzled. The results obtained are consistent with previous literature[2], which has shown increased straylight in eyes with longer axial lengths.

Besides requiring correction for their refractive error, myopic eyes have several disadvantages compared to emmetropic eyes. Due to their longer axial length, myopic eyes are more prone to developing retinal pathologies. Moreover, it has been demonstrated that their recovery time from photostress is more prolonged[4], and, as suggested by our results and those of other previous studies, they have greater intraocular straylight.

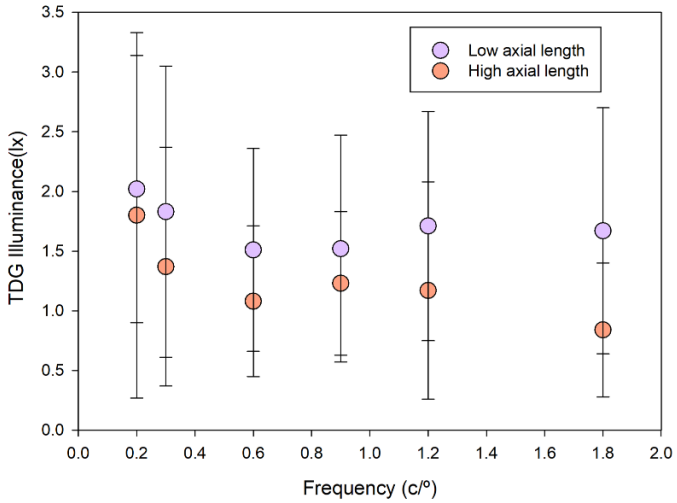

Figure 2: Mean and error bars of total disability glare illuminance as a function of spatial frequency for the two groups of subjects: low axial length(purple) and high axial length (orange).

ACKNOWLEDGEMENTS: Authors thanks the funding grant to Department of Industry and Innovation (Government of Aragon) (research group E44_23R).

---

[1]TJTP. Van den Berg, L. Franssen, B. Kruijt and JE. Coppens. History of ocular straylight measurement: A review. *Z Med Phys*. **23**, 6–20 (2013).
[2]D. Christaras, J.J. Rozema and H. Ginis, Ocular axial length and straylight. *Ophthalmic and Physiological Optics,* **40**, 316–322 (2020).
[3]P. Casado, F.J. Ávila, M.V. Collados and J.Ares. A study on disability glare vision in young adult subjects. *Sci Rep* **13**, (2023).
[4]F.J. Ávila, P. Casado and J. Ares, Photostress Recovery Time after Flash-Lighting Is Increased in Myopic Eyes. *Photonics* **10**, (2023).

Caracterización del color percibido en visión con luz infrarroja pulsada

Lourdes Camblor[1,2], Pedro Gil[1,2], Juan Tabernero[1,2], Silvestre Manzanera[1,2], Christina Schwarz[3], Pablo Artal[2]

[1]Laboratorio de Óptica, Universidad de Murcia, Murcia, España

[2]Departamento de Electromagnetismo y Electrónica, Universidad de Murcia, Murcia, España

[3]Institute for Ophthalmic Research, University of Tübingen, Tübingen, Alemania

Contacto: lourdes.camblorn@um.es

El ojo humano puede percibir luz pulsada en el infrarrojo cercano como si fuera luz visible con aproximadamente la mitad de la longitud de onda original debido a un proceso conocido como absorción en dos fotones (2P)[1,2]. A pesar de que este fenómeno se conoce desde hace décadas, todavía no se ha realizado una caracterización cuantitativa y completa de la visión 2P en función de los parámetros de la fuente de luz y de su longitud de onda. El objetivo de este estudio es determinar cómo se percibe el color cuando se estimula la visión mediante el mecanismo 2P con diferentes longitudes de onda de luz infrarroja pulsada.

Para ello, hemos llevado a cabo un experimento de ajuste de color en el que utilizamos un láser supercontinuo y una fuente visible para proyectar dos estímulos (2P y visible). Para estudiar la dependencia de la percepción del color en 2P con la longitud de onda, seleccionamos mediante filtros siete longitudes de onda en el infrarrojo cercano: 880, 900, 920, 950, 1000, 1050 y 1100 nm. Trabajamos con una potencia de 30 μW en el plano de pupila, la cual hemos comprobado que se encuentra dentro de los límites de seguridad[2], una frecuencia de repetición de 15 KHz y un pulso de 1 ns. El color del estímulo visible puede ser modificado por el sujeto con el fin de igualarlo con el color percibido en visión 2P. Tras esto, medimos el color de la fuente visible utilizando un espectrómetro.

La figura 1 muestra la caracterización de cada longitud de onda infrarroja en sus coordenadas de color percibidas para un sujeto. Es posible apreciar cómo varía el tono percibido según aumenta la longitud de onda infrarroja emitida, pasando desde tonos rojizos, a azulados y verde-amarillos.

La figura 2 muestra la longitud de onda dominante en cada color frente a la longitud de onda del láser infrarrojo. Como referencia, se muestra la recta Y=X/2 que representaría el efecto “puro” de 2P. Se observa que para las longitudes de onda más cortas los datos tienden a diferir de la recta, mientras que para longitudes de onda más larga el ajuste lineal es mejor.

El efecto visual en longitudes de onda cortas es una percepción rojo-azulada que se correspondería con una combinación de absorción lineal de las colas visibles del espectro IR (percepción roja) y del efecto 2P a esas longitudes de onda (percepción azul).

En resumen, el experimento realizado permite caracterizar el color percibido en 2P y modelizar el efecto 2P en función de la longitud de onda definida del láser. Entender los parámetros que activan el efecto de la visión en 2P es crucial para su posible aplicación a nuevos test de diagnóstico de problemas visuales relacionados con la retina.

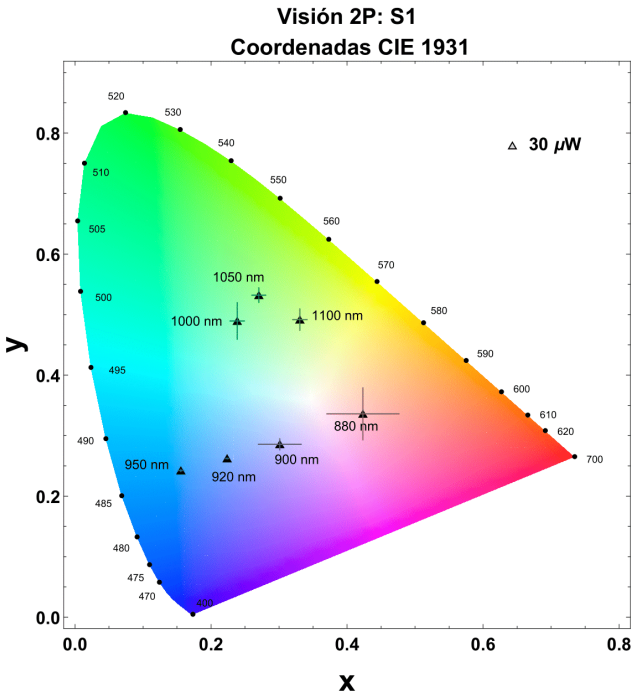

Figura 1: Coordenadas CIE 1931 de los colores percibidos por uno de los sujetos.

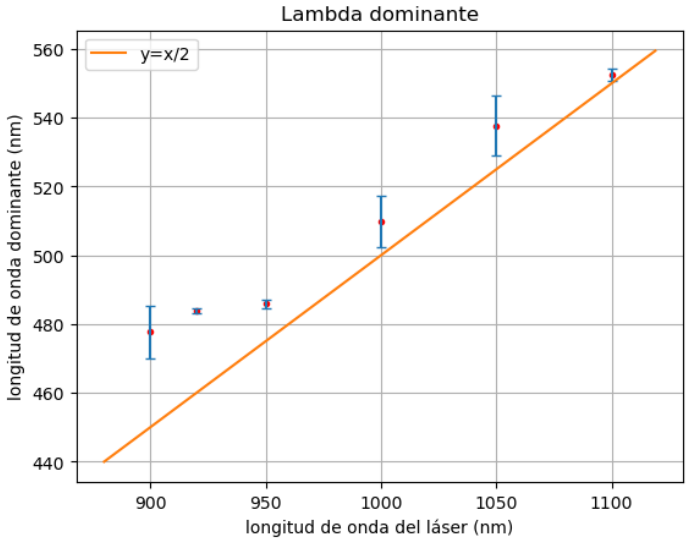

Figura 2: Longitud de onda dominante por cada sujeto frente la longitud de onda del láser.

---

[1]Palczewska, G., et al. Human infrared vision is triggered by two-photon chromophore isomerization. *Proceedings of the National Academy of Sciences*, *111*(50), E5445-E5454. (2014).

[2] Manzanera, S., Sola, D., Khalifa, N., & Artal, P. Vision with pulsed infrared light is mediated by nonlinear optical processes. *Biomedical Optics Express*, *11*(10), Article 10. (2020).

[3] Delori, F. The ANSI 2014 Standard for Safe Use of Lasers. *Frontiers in Optics 2014 (2014), Paper FW1F.2*, FW1F.2. (2014).

Effects of optical irradiation with laser and LED light sources on cell cultures of leukemia

[1,2]Danielle Viviana Ochoa, [1]Jose Oscar Gutiérrez y [2]Efraín Solarte

[1] Grupo de Investigación de Farmacología Univalle, Facultad de Salud, Universidad del Valle sede San Fernando, Calle 4b # 36-00, San Fernando, 760042 Cali, Valle del Cauca, Colombia.
[2] Grupo de Investigación de Óptica Cuántica, Facultad de Ciencias Naturales y Exactas, Universidad del Valle, Calle 13 # 100-00, 760042, El Ingenio, Cali, Valle del Cauca, Colombia

Contact: danielle.ochoa@correounivalle.edu.co

The study of childhood cancer in Colombia has become a priority for the health system, since: There is detection in advanced stages, late attention, secondary and adverse effects after conventional treatment.
This causes a great socioeconomic impact and a high mortality rate in childhood, since cancer is one of the leading causes of mortality and this phenomenon is recognized worldwide[1].
One of the main reasons is that its treatment is not selective and children who have suffered from it experience recurrence of the disease after conventional treatment by chemotherapy, radiotherapy or surgery, in addition to secondary and adverse effects, given that these treatments not only eliminate cancer cells but normal ones; that is, there is no selectivity for leukemic cells.
The motivation of this research project is to design, build and launch an experimental setup that allows the implementation of a new technology that targets and treats leukemia cells without harming the surrounding environment (normal cells), called optical therapy[2].
This technology is the subject of research around the world (it has not only allowed biomedical advances, but also at an industrial, technological and engineering level).
The application of light energy in biological tissues, it can give rise to different applications in both biological sciences and health sciences[3].
Therefore, experiments will be carried out that allow studying the light-matter interaction, through optical therapy with laser and led sources that promise a new revolution in the research field, since they have good space-time resolution, which it makes it selective according to its wavelength and specific according to its directionality.

Keywords: Biophotonics, Irradiation, LASER, LED, Leukemia.

ACKNOWLEDGEMENTS:
- Laboratorio de Farmacología, Escuela de Ciencas Básicas, Facultad de Salud, Universidad del Valle sede San Fernando.
- Laboratorio Óptica Cuántica, Escuela de Física, Facultad de Ciencias Naturales y Exactas, Universidad del Valle.

[1] Chen, S. H., et. Al. Journal of Experimental and Clinical Medicine, **6 (1),** 1–9 (2014).
[2]Banavath, H. N., et.al. Journal of Photochemistry and Photobiology. **35-40,** 1357 (2018).
[3]Hopkins, S. L., et.al. Photochem. Photobiol. Sci. **15,** 644 (2016).

A Color Vision Test – comparing results between computer screens

João M.M Linhares[1], Andreia Gomes[1], Paulo Jorge Alves[1], José A.R. Monteiro[1] and Sérgio M.C. Nascimento[1]

[1] Physics Center of Minho and Porto Universities (CF-UM-UP), University of Minho, Gualtar Campus, 4710-057 Braga, PT

Contact: jlinhares@fisica.uminho.pt

Computerized color vision tests are typically available on dedicated hardware. A color vision test was developed to run on a web browser, without the need for specific hardware: CVTwithNN. This color vision test can estimate an observer's color vision thresholds, response times, and eye movements with a webcam.

The purpose of this work was to compare the chromatic thresholds obtained for normal color vision observers when estimated on a calibrated and an uncalibrated screen.

Four squares with random background luminance noise were presented on a general computer screen with a uniform grey background. One of the squares was randomly selected to present a test color with a particular hue and saturation. The size of the stimuli was adjusted in size to be the same across participants and computer screens. Twenty-six hues were tested, on or near the dichromatic confusion lines. Initial hue saturation was randomly selected, from an optimized saturation value, close to the normal color vision chromatic threshold.

Chromatic thresholds for each hue were estimated after a staircase procedure that was tested 10 times with only the last 8 responses being considered for the estimation of the observers' chromatic threshold. Chromatic thresholds were estimated by computing the color difference between the observers' color perception and the reference white of the computer screen in use.

The observers' task was to point and select the colored square with the computer mouse.

Two conditions were considered: the condition where the computer screen of the participants' laptop was used and uncalibrated (Laptop), and the condition of using one computer screen calibrated in color and luminance (Display). The viewing setup in the Display condition was always the same across participants, ensuring the stimulus size and color, the observers' distance to the screen, and the dark environment, as the experiment was always executed at the Colour Science Laboratory (https://sites.google.com/view/csl-uminho/). The viewing setup of the Laptop condition was uncontrolled, but participants were guided towards providing information about the pixel size, turning all environment lights off, disabling any night light mode on the screen, using a laptop screen, and ensuring that the computer screen brightness and zoom were at adequate levels.

46 normal color vision observers performed the CVTwithNN on the Display screen, while a subset of 42 observers repeated the CVTwithNN using the Laptop. Chromatic thresholds were averaged across observers.

Figure 1 represents in a black line the average chromatic threshold estimated across observers for the Display condition. The magenta line represents the average chromatic threshold estimated across observers for the Laptop condition. Chromatic thresholds were represented in the CIE1976UCS(u',v') color space. For reference, vertical lines represent the dichromatic confusion lines. Error bars represent the standard deviation associated with the estimation of the average. Hue 0 degrees was considered to be at 3 hours, progressing counterclockwise. The 26 hues considered were around the confusion lines, as represented in Figure 1.

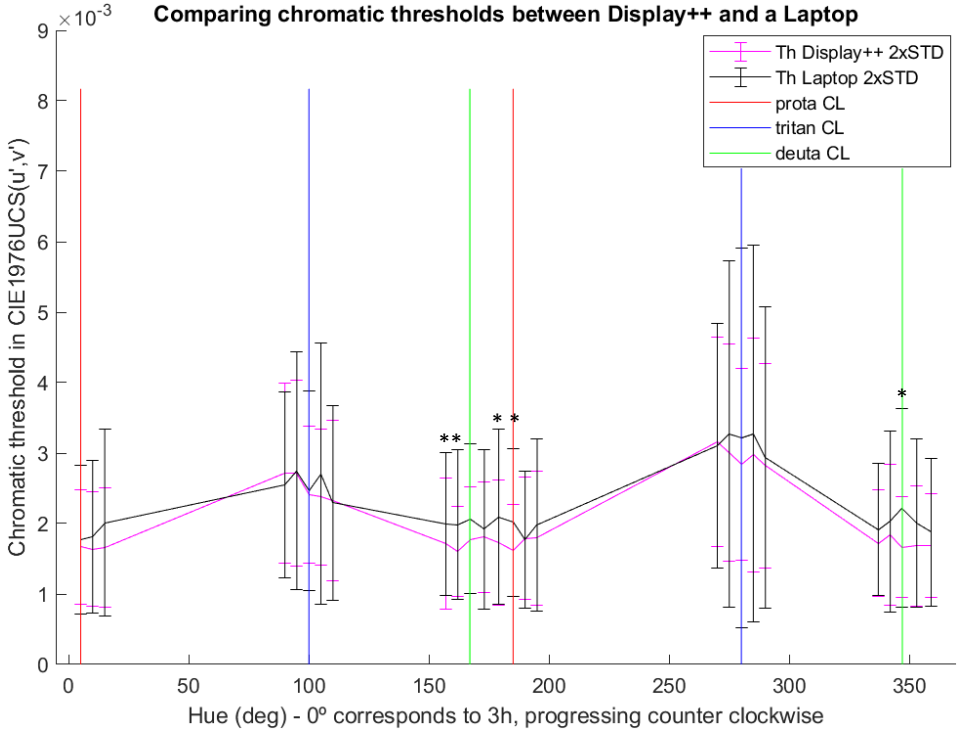

Figure 1: Average thresholds estimated across observers for 26 hues for the Display condition (magenta line) and the Laptop condition (black line). Vertical lines represent the dichromatic confusion lines. Error bars represent the standard deviation associated with the average. Thresholds differences with statistical significance are highlighted with * (*p<0.05*).

It was found that the chromatic thresholds found for normal observers can be correlated with traditional color vision tests, and as represented in Figure 1, chromatic thresholds are comparable across different computer screens. The average difference between the thresholds estimated for the Laptop and the Display conditions was found to be about 12%±8% of the threshold obtained for the Display condition across all hues. It was also found that hues at degrees 157º, 162º, 179º, 185º, and 347º had statistical differences with *p<0.05*, after estimating the significance of the differences using the nonparametric Kruskal Wallis test. These hues are signaled in Figure 1 with an *.

These results seem to indicate that the assumptions made to run the color vision test on unknown computer screens with the instructions given to the participants, may be sufficient to obtain chromatic thresholds comparable to traditional color vision tests, even if the test was done in non-controlled conditions.

ACKNOWLEDGMENTS:
"This work was supported by the Portuguese Foundation for Science and Technology (FCT) in the framework of the Strategic Funding UIDB/04650/2020 and the research project EXPL/FIS-OUT/0398/2021."

A Color Vision Test Assessed by Neural Networks

José A.R. Monteiro[1], Paulo Jorge Alves[1], Andreia Gomes[1], Sérgio M.C. Nascimento[1], and João M.M Linhares[1]

[1] Physics Center of Minho and Porto Universities (CF-UM-UP), University of Minho, Campus of Gualtar Rua da Universidade, 4710 - 057 Braga, Portugal

Contact: alexmonteiro1995@gmail.com; id9887@alunos.uminho.pt

Traditional computerized color vision tests resort to the magnitude of measured chromatic thresholds to ascertain the color vision of an observer[1–3]. The limits of perceived colors are tested against a background that will be conspicuous to normal color vision observers, but inconspicuous to color vision deficient (CVD) observers.

The purpose of this work was to devise a Neural Network capable of performing independent and automatic classification of the color vision of an observer, using as inputs the sRGB chromaticity coordinates, response times, and eye movements obtained using a color vision test on a computer screen calibrated in color and luminance (Display++).

Chromatic discrimination limits were estimated using a staircase procedure that tested color vision close to the dichromatic confusion lines. Only the last 8 responses (out of 10) were considered in the analysis.

58 normal color vision observers and 8 CVD observers performed the test on Display++. CVD participants were diagnosed using the results of the anomaloscope and the CAD color vision tests.

A *Sequential* Neural Network was implemented with a dense structure of (256-128-64-16-1 nodes), with *relu* and *sigmoid* activation functions, *dropout* commands to prevent overfitting of the neural network, the *Adam* optimizer, and the *binary crossentropy* loss function[4,5]. The performance of the neural network was estimated by computing its accuracy, by using ***Eq.1***, where variables are related to the results obtained after training the Neural Network and inspecting the test results.

$$\boldsymbol{Eq.1} \qquad Accuracy = \frac{True\ Positive + True\ Negative}{True\ Positive + False\ Positive + False\ Negative + True\ Negative}$$

The database was divided into a training set and a testing set following different splitting strategies: ***T1*** observers' responses considering sRGB chromaticity coordinates, response times, and eye movements. ***T2*** observers' responses considering only sRGB chromaticity coordinates.

Table 1 shows the averages and standard deviations of the estimated accuracy for five consecutive trials with a random division between training/test for conditions ***T1*** and **T2**.

It was found that the implemented neural network had an accuracy of more than 90% across all conditions.

The accuracies found across conditions considered seem to indicate that the implemented Neural Network can analyze and classify the color vision of human observers, with an accuracy greater than 90% of success. Nevertheless, more data is needed to increase the accuracy and the classification of the neural network.

Table 1: Average of the accuracy found for each testing condition (± standard deviation). The average was estimated across 5 consecutive trials with the database randomly divided into training and testing set for conditions ***T1*** to ***T2***.

Test condition	**Accuracy (%)** **Average across 5 trials (± STD)**
T1	91.43±7.00
T2	92.85±4.52

References[1]

1. Hardy LH, Rand G, Rittler MC. Tests for the Detection and Analysis of Color-Blindness I The Ishihara Test: An Evaluation. *J Opt Soc Am*. 1945;35(4):268. doi:10.1364/JOSA.35.000268

2. Vision NRC (US) C on. COLOR VISION TESTS. In: *Procedures for Testing Color Vision: Report of Working Group 41*. National Academies Press (US); 1981. Accessed April 29, 2023. https://www.ncbi.nlm.nih.gov/books/NBK217823/

3. Seshadri J, Christensen J, Lakshminarayanan V, Bassi CJ. Evaluation of the New Web-Based "Colour Assessment and Diagnosis" Test. *Optom Vis Sci*. 2005;82(10):882-885. doi:10.1097/01.opx.0000182211.48498.4e

4. Brownlee J. *Deep Learning With Python: Develop Deep Learning Models on Theano and TensorFlow Using Keras*. Machine Learning Mastery; 2016.

5. Denoyer L, Gallinari P. Deep Sequential Neural Network. Published online October 2, 2014. Accessed April 29, 2023. http://arxiv.org/abs/1410.0510

ACKNOWLEDGEMENTS:
"This work was supported by the Portuguese Foundation for Science and Technology (FCT) in the framework of the Strategic Funding UIDB/04650/2020 and the research project EXPL/FIS-OUT/0398/2021.

Colour vision change after multifocal diffractive IOL implantation

Laura Clavé[1,2], Jesús Armengol[2], Fidel Vega[2], Aurora Torrents[2] and María S. Millán[2]

1 Hospital de Mataró, Servicio de Oftalmología, Consorci Sanitari del Maresme, 08304 Mataró, España

2 Grupo de Óptica Aplicada y Procesado de Imagen, Departamento de Óptica y Optometría, Universitat Politècnica de Catalunya-BARCELONA**TECH**, Terrassa, España

Contact: laura.clave@upc.edu

Trifocal diffractive presbyopia-correcting intraocular lenses (IOLs), allow vision for far, intermediate, and near distance. The spectral on-bench analysis of these IOLs shows differences between the three foci not only in terms of chromatic difference of power but also related to the energy efficiency (EE). The diffraction orders involved in their design may contribute also to mitigate the longitudinal chromatic aberration (LCA) produced by the dispersive nature of the lens material and the ocular media.[1,2] The EE is an optical quality indicator that strongly depends on the wavelength. In the visible spectrum, the largest differences are found between red and blue illuminations. These effects have been observed already in vitro,[1-3] but scarcely studied in vivo.[4]

The aim of this work is to show the impact of the spectral dependence of diffractive multifocal IOLs on the spatial and chromatic vision of pseudophakic eyes. To this purpose, we assessed the visual acuity (VA) of 40 pseudophakic subjects implanted with trifocal diffractive lenses of two different designs, FineVision (PhysIOL S.A., Liège, Belgium) and AT LISA tri 839 MP (Carl Zeiss Meditec AG, Jena, Germany), at two fixed distances – far (0.0 D) and near (-3.0 D) – under successive White (W), Red (R), Green (G), and Blue (B) illumination, with constant luminance of the optotype chart. Figure 1 shows the results for the two groups of patients.[5]

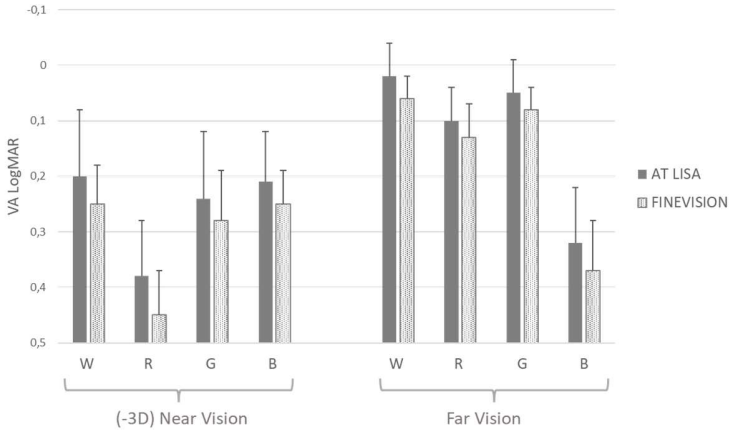

Figure 1: Mean VA (logMAR) values reached by two groups of pseudophakic patients at far and near vision under W, R, G, and B illumination. Error bars represent the standard deviation.

In general, the mean VA values are better in far than in near vision for all the illumination conditions (Figure 1), except for the B light, which reaches better VA at near vision. It is also worth mentioning further asymmetry for the R light. The good VA achieved at far under R light drops off dramatically to the worst at near, even below the poor VA outcomes obtained at far under B light.

Figures 2(a,b) show the through-focus red and blue EE curves obtained for these lenses in a model eye on optical bench; figures 2(c,d) show the logMAR VA mean values measured under red and blue illuminations at far and near vision. The two IOLs present an unbalanced distribution of EE with illuminations R and B in the far and near foci. This fact give rise to changes in the VA depending on either the R or B illumination and on the far or near viewing distance.

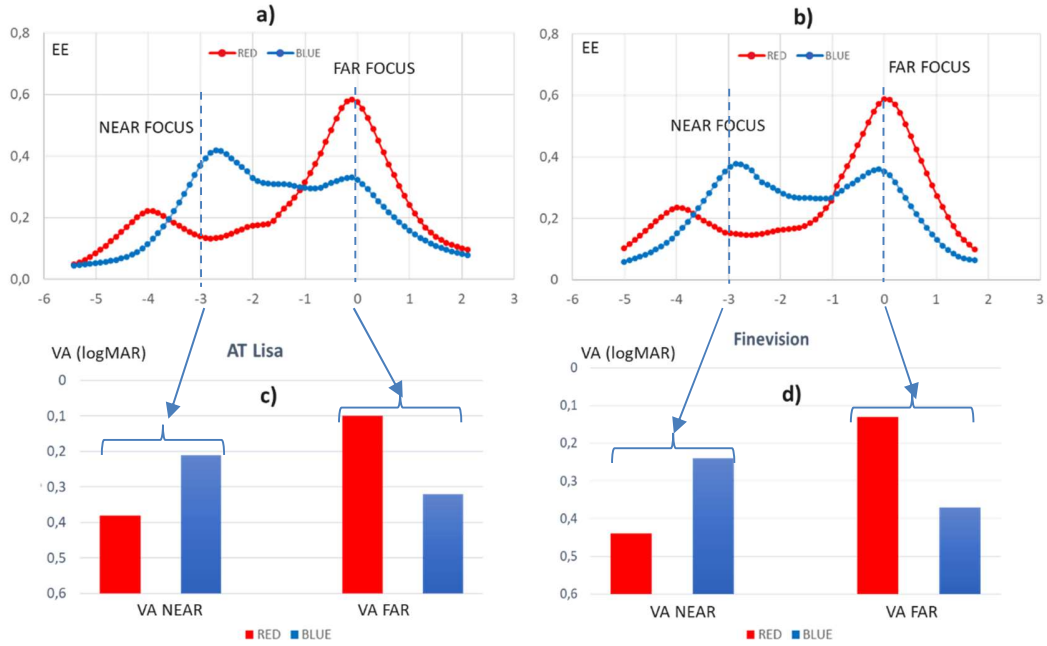

Figure 2: Through-Focus red and blue EE curves for the AT LISA (a) and FineVision (b); red and blue logMAR VA mean values obtained with subjects implanted with the AT LISA (c) and the FineVision (d).

Both groups of pseudophakic patients (AT LISA and FineVision) obtained similar results: VA outcomes were fairly unbalanced for the R and B illumination. In all cases, R illumination allowed subjects to reach better VA at far vision than B light. The opposite happened at near vision, for which the best VA values were obtained with B illumination. These clinical VA results are fully consistent with the experimental R, G, B through-focus EE curves obtained with the trifocal IOLs in the model eye on optical bench.

ACKNOWLEDGEMENTS: PID2020-114582RB-I00/ AEI / 10.13039/501100011033.

References

[1] Millán, M. S., Vega, F. & Ríos-López, *Investig. Ophthalmol. Vis. Sci.* 57 (2016).
[2] Millán, M. S. & Vega, F. *Biomed. Opt. Express* 8 (2017).
[3] Armengol, J. *et al. Biomed. Opt. Express,* 11 (2020).
[4] Vinas-Pena M. *et al*. *Photonics*. 9 (2022).
[5] Millán M. S. *et al*. *Eye and Vision* (2023).

Direct Subjective Refraction: a new approach for refractive error measurements and the impact of accommodation

Victor Rodriguez-Lopez[1], Carlos Dorronsoro[1]

[1] Instituto de Óptica Daza de Valdes, CSIC, (Serrano 121, 28006, Madrid, Spain)

Contact: victor.rl@io.cfmac.csic.es

The traditional method for evaluating refractive errors is called subjective refraction and has barely evolved in the last 200 years. In this method, the patient must identify letters through different lenses, until a letter of small size on an eye chart is identified[1]. Although the gold standard, the traditional method is affected by fatigue, consumes a great amount of time (6min), has high variability (0.27D), and is highly influenced by the accommodation[2].

We have developed a new method that uses a tunable lens conjugated with the pupil of the eye via a 4f optical system to induce defocus variations without inducing displacements or magnification differences. This new method, called Direct Subjective Refraction (DSR), takes advantage of the induction of fast and periodic changes in defocus (temporal defocus wave) and a stimulus composed of blue and red components that, in combination with the longitudinal chromatic aberration of the eye, produces a chromatic flicker perception. When the defocus change temporal defocus wave happens in the myopic side of the retina, the blue components of the image are perceived to flicker more. When the defocus change happens in the hyperopic side of the retina, the red components flicker more. When the defocus change is centered with the retinal plane, flicker is minimum and similar in both colors. The task in this method is to minimize the flicker, and the direction of focus is guided by the flicker in the red or blue components.

In this study, 25 subjects (29.9±7.3 years) participated with a refractive error distribution of 3 hyperopes, 8 emmetropes, and 14 myopes (average refractive error -1.62±2.32D). For the DSR, subjects looked at the stimulus through the optical system that induced temporal defocus waves of 15Hz of frequency and 0.25D of amplitude, and the task was to minimize the flicker. Subjects also performed, in the same setup and conditions, an unsupervised version of the traditional subjective refraction (UTSR), where we used a black-and-white version of the stimulus, and the task was to focus the target (with no defocus wave). Subjects performed adjustment staircases with 10 different myopic and hyperopic starting points (ranging from -1.00 to +1.00 D) around their current prescription. The average across repetitions provided the residual spherical equivalent and the standard deviation the repeatability. Subjects were able to change the optical power in coarse and fine steps of 0.25 and 0.10 D, respectively. The experimenter explained the tasks subjects (minimize flicker and minimize blur), and they performed them autonomously.

The DSR method provided high convergence of the staircases (Figure 1 for an example), with a low standard deviation across repetitions (±0.17 D on average) compared to the UTSR (±0.47 D on average). Hyperopic and myopic starting points provided the same results for the DSR ($p>0.05$) but not for the UTSR ($p<0.05$), suggesting that accommodation does not influence the result of the DSR method (see Figure 1). In terms of time per repetition, the UTSR method took 21 seconds on average and the DSR method 39 seconds, compared with the 6 minutes of the traditional subjective

refraction.

The Direct Subjective Refraction using temporal defocus waves is a repeatable (±0.17 D), fast (<1min), and easy task for the subject, which is barely affected by the accommodation, that stays relaxed while performing the evaluation. It has high potential for clinical measurements of the refractive error.

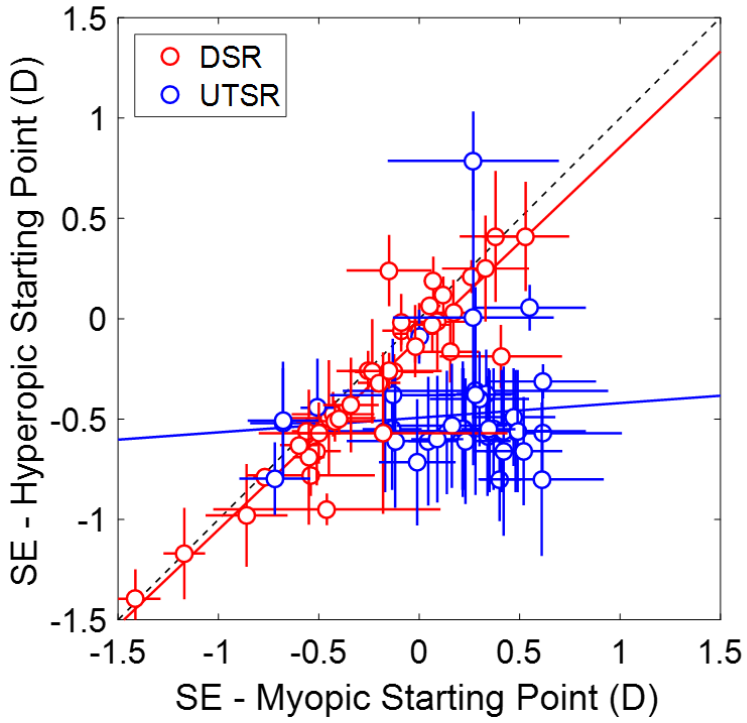

Figure 1. Effect of accommodation in flicker-minimization and blur-minimization tasks. Analysis of myopic and hyperopic starting points. Residual refraction obtained from the average of all hyperopic starting points versus the residual refraction obtained from the average of all myopic starting points for the Direct Subjective Refraction (DSR, red) and Unsupervised Traditional Subjective Refraction (UTSR, blue) tasks. The error bars indicate the standard deviation across repetitions.

References

1. D. B. Elliott, "Clinical Procedures in Primary Eye Care, 3rd edition," Clin. Exp. Optom. 91, 496–497 (2008).
2. V. Rodriguez-Lopez and C. Dorronsoro, "Beyond traditional subjective refraction," Curr. Opin. Ophthalmol. Publish Ah, 228–234 (2022).

Impact of refractive error compensation methods on a webcam eye tracking system

Sara F. Lima[1], Paulo J. Alves[1], José A.R. Monteiro[1], Andreia Gomes[1], Madalena Lira[1] and João M.M. Linhares[1]

[1]Physics Center of Minho and Porto Universities (CF-UM-UP), University of Minho, Campus of Gualtar Rua da Universidade, 4710 - 057 Braga, Portugal

Contact: sarafernlima@gmail.com; pg42757@alunos.uminho.pt

The aim of this work was to assess the impact of different refractive error compensation methods in the data acquired with an eye tracking system that used a webcam and ran on a webpage.

Webgazer[1], a webcam eye tracking system that ran on a webpage was used to track the participants eye position. A vision test was devised to force the movement of the participants' eyes through the screen, while performing a perception task followed by a selection task.

Four grey squares were placed in the centre of a computer screen (Display++, Cambridge Research Systems, Rochester, UK), as represented in Figure 1. As the stimulus appeared on the screen, one of the squares started reducing its luminance, progressively, as represented in Figure 1, on the left by the red arrow. For each trial, the square that changed luminance was selected randomly. The observers' task was to click over the square that was changing luminance using the computer mouse. To force the movement of the participants' eyes through the screen, the selection had to be made on the outermost corner of each square, on a reduced area, as highlighted by the red circles in Figure 1, on the left. The outermost corners were selected to maximize the possible influence of using frames while performing the experiment, and to prevent focus over the central area of the stimulus resulting in limited eye movement. The four squares had a combined size of about 5.3 cm, subtending about 6º of visual angle.

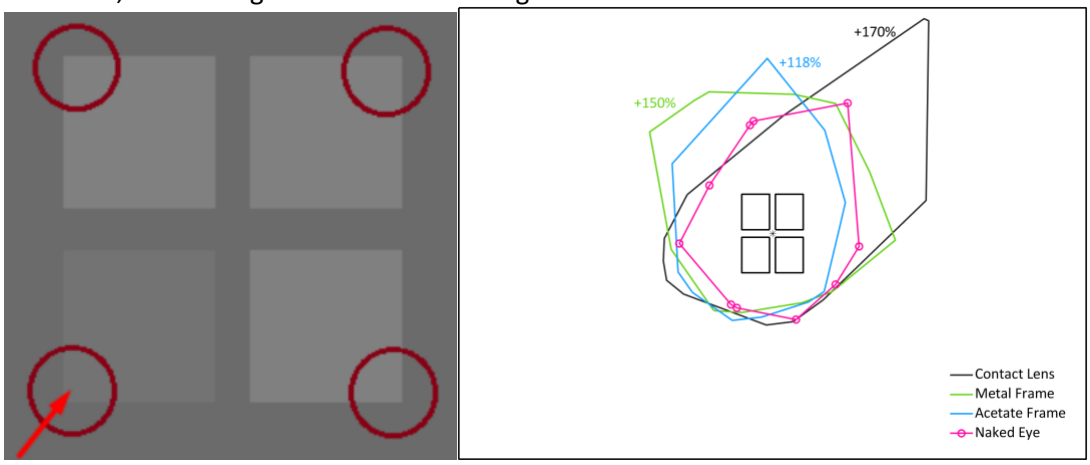

Figure 1: Left - Stimuli setup, representing the four squares, with the red arrow identifying the square that was different and expected to be selected. The selection with the computer mouse had to be made in the extreme corner of the squares, as represented by the red circles. Right – Maximum gamut of the eye fixations, enclosing all eye fixations of all observers for the naked eye condition (magenta lines and circles), Contact lens condition (black line) and Acetate and Metal frames conditions (blue and green lines respectively).

Eye movements were recorded with a webcam (Spedal HD Pro Webcam C926, running at 1080P and 60fps), place just below the line of sight towards the central area of the computer

screen.

Observers seated with eyes level towards the central area of the screen, without environmental light, at about 50 cm from the screen.

Thirty emmetrope observers repeated the experiment under four different viewing conditions, in a randomized order and had to select the darker square 101 times in each condition. The conditions were: Naked Eye – The test was performed with no obstruction of the visual field and was assumed to be the condition to compare others with; Contact Lenses – The test was performed using contact lenses (verofilcon A, Alcon, -0.5D); Acetate and Metal Frames – The test was performed using thick acetate and thin metal frames with neutral clear lenses (Lenses EssilorLuxottica Portugal).

Condition	**Average response Time±STD (ms)**	**Average Eye movement distance±STD (pixel)**	**Gamut area of eye movement (pixel (variation in %))**
Naked eye	1557±228	297±55	197422
Contact lenses	1556±248	295±60	335000 (+170%)
Metal frame	1563±222	303±43	296133 (+150%)
Acetate frame	1562±265	334±68	233571 (+118%)

Table 1: Average and standard deviation across observers and trials of the time and eye movement for each condition. Maximum area of eye movement distance for each condition.

Table 1 summarizes the averages (and standard deviations) across the 30 observers for the response time, the screen distance between consecutive eye fixations (in pixels), and the area of the screen that enclosed all eye fixations used during the eye movements (gamut area), as represented on Figure 1, on the right side for the naked eye condition (magenta lines and circles), Contact lens condition (black line) and Acetate and Metal frames conditions (blue and green lines, respectively).

It was found that the response time observers took was similar across all the conditions. The average eye movement distance was found to be statistically different only for the Acetate Frame (*p-value*=0.020 - ANOVA for repeated measures), with an increase when compared with the Naked Eye condition. When comparing the gamut areas, it was found that all conditions with compensation methods had a higher gamut than the Naked Eye condition.

Despite the differences observed, the results seem to suggest using contact lenses or frames while recording the eye movements with a webcam and the Webgazer system did not impair the visual field of observation, the number of eye fixation points and the distance the eyes travelled during their movement.

ACKNOWLEDGEMENTS: "This work was supported by the Portuguese Foundation for Science and Technology (FCT) in the framework of the Strategic Funding UIDB/04650/2020 and the research project EXPL/FIS-OUT/0398/2021. A special Thank You to EssilorLuxottica for the support during the experimental process.

References:

1. Papoutsaki, A. *et al.* WebGazer: Scalable webcam eye tracking using user interactions. *IJCAI International Joint Conference on Artificial Intelligence* 2016-Janua, 3839–3845 (2016).

Comparison of the Farnsworth Munsell 100 Hue and MUC tests in the over 50s

Alba Herrero-Gracia[1], MA Díez-Ajenjo[1], RM Hernández-Andrés[1] and MJ Luque-Cobija[1]

[1] Department of Optics and Optometry and Vision Sciences, Faculty of Physics, University of Valencia, C/ Doctor Moliner, 50. 46100 Burjassot-Valencia.

Contact: alhegra@alumni.uv.es

Purpose: To compare the Farnsworth Munsell (FM) Hue 100 and Measurement of Chromatic Thresholds (MUC) tests in people over 50 years of age to determine if results between them are consistent.

Methods: A descriptive, observational, prospective and cross-sectional study was conducted. Patient inclusion criteria were: 50 years or older, no history of surgery or ocular or systemic pathologies affecting vision, no medication with side effects on vision and no chromatic anomalies. All participants signed an Informed Consent form. The study followed the ethical principles for medical research in humans established by the Declaration of Helsinki.

All participants underwent anamnesis, trial frame refraction and visual acuity with the ETDRS test to ensure that they met the inclusion criteria. All wore the optimal correction that provided the highest visual acuity to ensure that refractive errors did not influence the results. They were finally tested with the FM 100 Hue and MUC tests[1].

The variables analysed with IBM SPSS Statistics 28.0.1.1 were *age*, *gender*, total error score (*TES*), partial total error score for the blue-yellow and the red-green axes (*PTESBY* and *PTESRG*)[2], colour index $(\sqrt{PTESBY} - \sqrt{PTESRG})^2$, *PTESRG/TES*[3] value of the FM 100 Hue test and the value of the major (*a*) and minor (*b*) semiaxis, orientation (ϑ) and the *area* of the best-fit ellipse of the colour discrimination threshold provided by the MUC test[1].

Patients performed the tests seated in a chair at a table in a darkened room. FM Hue 100 test was administered under illumination by a GretagMacbeth Sol-Source lamp (230 Volt, 60 Hz) simulating the D65 illuminant and providing 470 Lux illumination, controlled with the Konica Minolta Chroma Meter CL-200 luxometer with integrating sphere sensor. An observation distance of 40 cm was maintained. The MUC test was presented on a colorimetrically characterized HP PROBOOK 450G7 computer (resolution 1920*1080 pixels, screen size 34.5*19.5 cm), at 100% brightness and contrast, connected to the mains. A viewing distance of 80 cm was maintained. Both tests were performed monocularly. The dominant eye of each participant was selected using the red filter sensory dominance test. To identify patients with colour vision abnormalities, Kinnear's normative values for the FM 100 Hue test were used[4].

In the statistics, a descriptive analysis of centrality and dispersion was performed, as well as the analysis of the normality of the variables (Kolmogorov-Smirnov test). Spearman's Rho test was used to analyse the correlation among the different variables. To determine the dependence between the different variables and *age* and *gender*, a multivariate linear model was used. Statistical comparison between groups was performed using the multiple comparison test with the Tukey-Kramer criterion. Differences were considered statistically significant when p-value <0.05.

Results: 94 subjects were recruited. Twelve of them were excluded for being outside the normative values of Kinnear[4]. Of the remaining 82, 45 were females (61±7 years) and 37 males (63±7 years). Only age, $\sqrt{PTESBY} - \sqrt{PTESRG}$ and *PTESRG/TES* value followed a normal distribution, but the rest of the variables did not follow a normal distribution (Table 1). A positive significant correlation was found between *TES* and *a*, *PTESRG* and *a*, *PTESBY* and *a*, $\sqrt{PTESBY} - \sqrt{PTESRG}$ and ϑ,

PTESRG/TES and *ϑ*, *TES* and *area*, *PTESRG* and *area*, *PTESBY* and *area*, *PTESRG/TES* and *area*. A negative significant correlation was found between *PTESRG* and *ϑ* and *PTESRG/TES* and *ϑ*. A lineal incremental dependence of the variables was found with *age* only for *b*, *TES*, *PTESRG* and *PTESBY* (Figure 1 shows an example). *Gender* had no significant influence on any variable. Participants were grouped by *age* (Group 1, 50-59 years, 28 subjects; Group 2, 60-69, 40; Group 3, 70-79, 14). A statistically significant difference was found between Groups 1 and 2 and between Groups 1 and 3 for *TES*, *PTESRG* and *PTESBY*, with lower values in Group 1 than Groups 2 and 3. In the case of the test MUC no significative differences were found in *a*, *b*, *ϑ* and *area* between age groups.

Conclusion: It was expected to find a correlation between *area* and *TES*, between *a* and *PTESBY* and between *b* and *PTESRG*, because the major axis of the ellipse (*a*) was expected to be correlated with the blue-yellow axis (*PTESBY*) which is the most affected with age[4], but it was also found a correlation between *a* and the red-green axis (*PTESRG*). Comparing with Kinnear[4], a lineal incremental dependence of the variables of test FM 100 Hue with *age* was also found for the same age groups. Comparing with García-Domene[3], *PTESRG/TES* is also not age-dependent. In the case of a patient with a high *TES* can be expected to have a larger *area*, so both tests are consistent. In addition, it should be noted that the older the patient, the higher the *TES* and the larger the *area*.

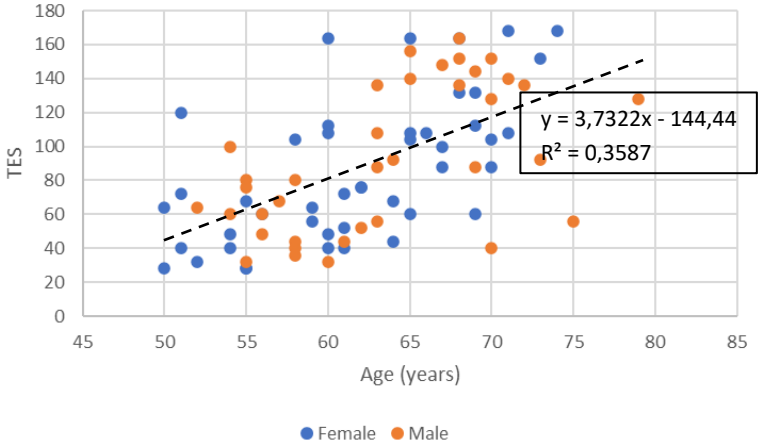

Figure 1: Scatter plot of TES value by age (years).

Table 1: Descriptive measures of centrality and dispersion (η: percentile).

	Age (years)	a	b	θ	TES	PTESRG	PTESBY	PTESBY-PTESRG	PTESRG/TES	Area
Median	62.5	0.02	0.0075	72.57	80	31.5	49.5	1.57	0.37	0.00012
Range	29	0.11	0.0109	161.24	140	92	107	8.96	0.68	0.00081
η_{25}	56.75	0.015	0.006	68.48	52	17	32	0.72	0.31	0.00080
η_{50}	62.5	0.02	0.0075	72.57	80	31.5	49.5	1.57	0.37	0.00012
η_{75}	68	0.026	0.0087	74.97	128	46	75	2.43	0.43	0.00016

[1]Luque-Cobija, Díez-Ajenjo, García-Domene and Fez-Saiz; *MUC, colour threshold measurement software*. https://www.deepl.com/es/translator Last visited: 08/05/2023

[2]Smith, Pokorny and Pass; *American Journal of Ophthalmology,* **100(1)**, 176 (1985).

[3]García-Domene, Díez-Ajenjo, Fez-Saiz and Luque-Cobija; *XI Congreso Nacional del Color*. 978-84-608-9872-6 (2016).

[4]Kinnear and Sahraie; *The British journal of ophthalmology*, **86(12)**, 1408 (2002).

Assessmet of the optical performance of presbyopic intraocular lenses by measuring of the Through the Focus Point Spread Function

Anabel Martínez-Espert[1], Vicente Ferrando[2], Juan A. Monsoriu[2] and Walter D. Furlan[1]

[1] Departamento de Óptica y Optometría y Ciencias de la Visión, Universitat de València, Dr. Moliner 50, 46100, Burjassot, Spain.

[2] Centro de Tecnologías Físicas, Universitat Politècnica de València, Camí de Vera s/n, 46022, Valencia, Spain.

Contact: anabel.martinez@uv.es

In this study we present an improvement of the experimental device[1], which is based on ISO 11979-2, 2014[2]. The new approach allows the assessment of the optical quality of full-range vision intraocular lenses (FRV-IOLs) by capturing Through Focus Point Spread Function (TF-PSF). The system, depicted in Figure 1, automatically records the PSF generated by the artificial eye of a 15 µm pinhole that moves axially with a stepper motor to generate different object vergences. It is a modular system in which the chromatic filter, the pupillary diameter, and the artificial cornea can be changed to evaluate different IOL properties. The images of the PSFs recorded by the CCD camera are processed to compute the Modulation Transfer Function (MTF) for all frequencies in a wide range of frequencies, in our case from 0 to 50 lp/mm. In this way, a two-dimensional map of the MTF values as a function of vergence (2D MTF) can be obtained.

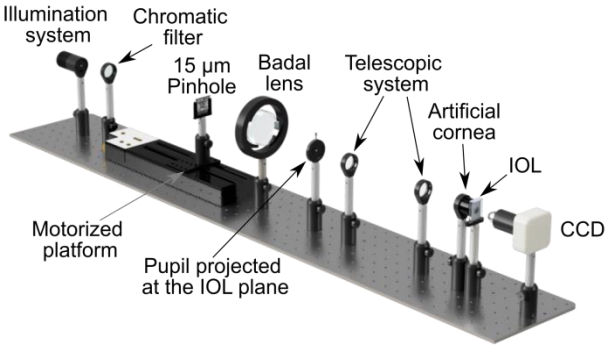

Figure 1: Optical Setup.

Figures 2 and 3 show the 2D MTF maps obtained for two FineVision POD F trifocal IOLs (PhysIOL, Liège, Belgium). Both lenses (with 13 D and 35 D, base power) were evaluated with monochromatic light (550 nm) and two different pupil diameters.

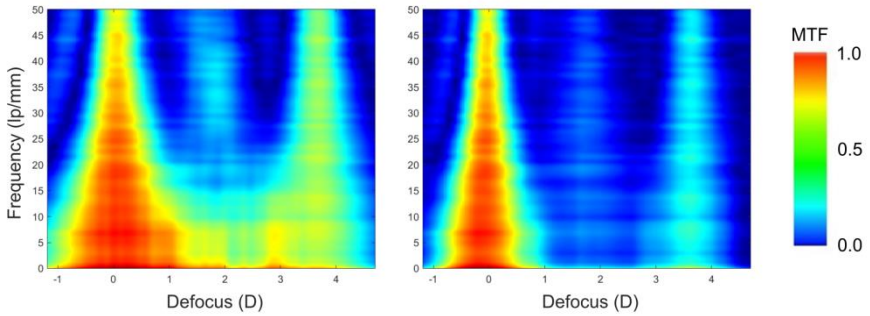

Figure 2: 2D MTF map of the FineVision IOL with 13 D power for 3.0 mm (left) and 4.5 mm (right) pupil diameters.

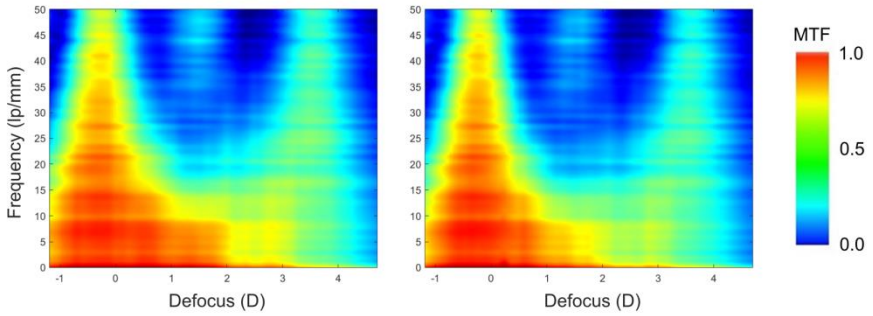

Figure 3: 2D MTF map of the FineVision IOL with 35 D power for 3.0 mm (left) and 4.5 mm (right) pupil diameters.

From these representations the Through Focus MTF (TF-MTF) can be obtained by taking a horizontal slice of the 2D MTF function at a desired frequency. Figure 4 shows the TF-MTFs at 50 lp/mm. On the other hand, the Through Focus area under the MTF curve (TF-MTFa) can also be calculated by performing the integral of the MTF values along the vertical lines at each vergence. In conclusion, we have presented versatile opto-mechanical system that offers a significant improvement on the assessment of FRV-IOLs. Its main feature relies on the recording the TF-PSF, from which a 2D MTF map and other metrics of the optical quality of FRV-IOLs can be obtained.

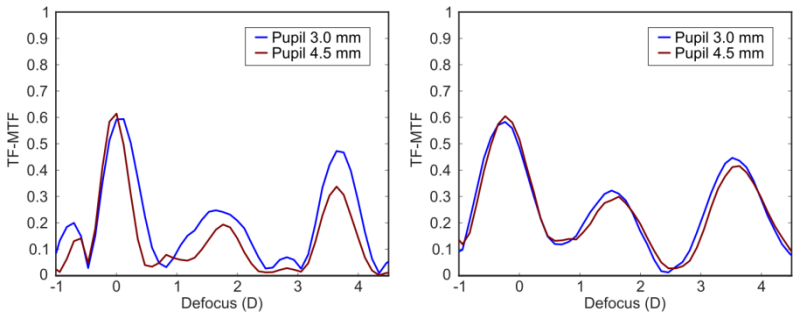

Figure 4: TF-MTF at a frequency of 50 lp/mm for the FineVision IOL with powers of 13 D (left) and 35 D (right), for pupil diameters of 3.0 and 4.5 mm.

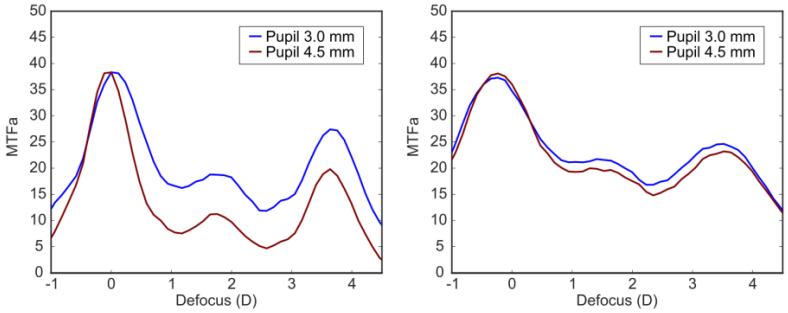

Figure 4: MTFa (0 to 50 lp/mm) for the FineVision IOL with powers of 13 D (left) and 35 D (right), for pupil diameters of 3.0 and 4.5 mm.

ACKNOWLEDGEMENTS: A. M.-E. acknowledges financial support from Universitat de València (programa Atracció de Talent 2021).

[1]V. Ferrando; 2022 Young researchers biophotonics summer meeting. https://www.youtube.com/watch?v=dutDqSfakzE

[2]ISO 11979-2; Ophthalmic Implants-Intraocular Lenses-Part 2: Optical Properties and Test Methods; International Organization for Standardization: London, UK, 2014.

Contribution of the anterior corneal topography to off-axis wavefront aberration: a pilot study

Iñaki Blanco-Martínez[1], Sara Silva-Leite[1], Juan Queiruga-Piñeiro[2], José M. González-Méijome[1] and Miguel Faria-Ribeiro[1]

[1] Clinical & Experimental Optometry Research Lab (CEORLab), Physics Center of Minho and Porto Universities (CF-UM-UP), School of Sciences, University of Minho (4710-057 Braga, Portugal)
[2]Ophtalmologic institute Fernandez-Vega (Oviedo, Spain)

Contact: Iblanco@fisica.uminho.pt

Introduction: Off-axis wavefront aberrations have become increasingly relevant in visual sciences as a way to estimate the imaging properties of the eye in the perifoveal and peripheral retina. Applications go from understanding the mechanisms of myopia progression to the development of ophthalmic lenses, contact lenses and intra-ocular lenses[1]. The anterior corneal surface is the main contributor to the ocular refraction and its measurement is easily accessible. This study aimed to evaluate the influence of considering realistic anterior corneal surfaces versus more general conic models[2] when determining off-axis wavefront aberrations from eye models with ray tracing software.

Methods: For this study, the anterior corneal elevation from 20 eyes of 10 young adults was evaluated with the Placido-based corneal topographer Medmont E300 (Medmont, Australia). Inclusion criteria required participants to have no ocular conditions other than refractive error. The anterior surface of the cornea was modelled in Zemax OpticStudio 22.2 (Ansys, USA) using the standard Zernike sag surface, defined by a base parabola, with its apical radius of curvature and conic constant, plus a Zernike expansion up to 6th order, to account for the residual deformations of the surface. The data analysis, fitting, and other computational processes were performed using Matlab (The MathWorks Inc., USA). Once the surface was imported, rays were traced along the horizontal field of view, from -40° to 40° of eccentricity, in steps of 5°. Zernike standard coefficients were obtained directly from Zemax for a 5 mm entrance pupil diameter at all eccentricities, using the pupil stretching method to address the issue of elliptical pupils[3]. The analysis of peripheral aberrations was focused on the polynomial terms expected to have the most relevance in the periphery along the horizontal meridian, which are horizontal astigmatism (C_2^2 and C_2^4), and horizontal coma (C_1^3 and C_1^5). Finally, the outcomes between the full theoretical and the semi-customized model were compared.

Results: Figure 1 depicts the results from the comparison between the full theoretical Navarro Eye model and the models semi-customized with the 20 realistic anterior corneal surfaces, for second-order astigmatism and third-order horizontal coma. On-axis values were subtracted from off-axis values to obtain the relative change induced by the oblique incidence of the light.

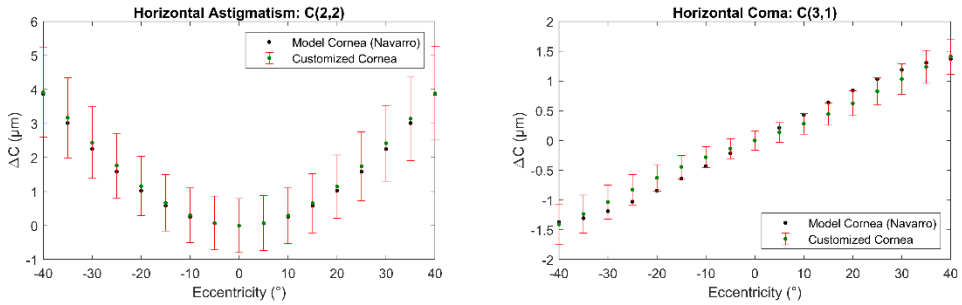

Figure 1: Low-order coefficients comparison as a function of angle between the theoretical and semi-customized models.

Figure 2 shows the results for fourth-order astigmatism and fifth-order horizontal coma.

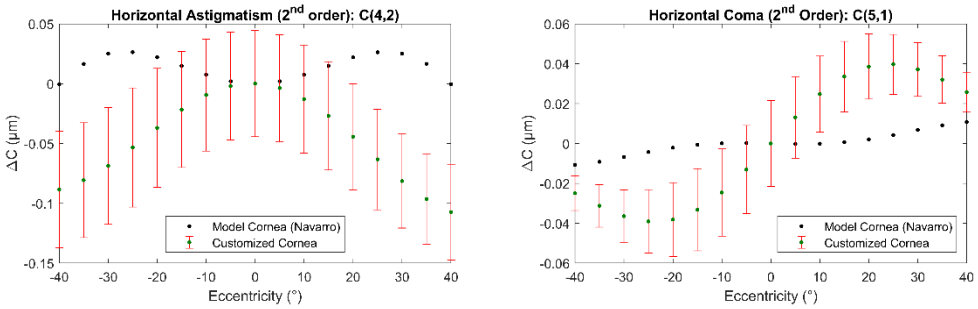

Figure 2: High-order coefficients comparison as a function of angle between the theoretical and semi-customized models.

Conclusions: The results obtained from the evaluation of off-axis wavefront aberrations demonstrate a close correspondence from theoretical and semi-customized models for C_2^2 and C_1^3. However, for C_2^4 and C_1^5, it shows different values and trends between the two modelling approaches, which may be attributed to the inclusion of a larger number of aspheric terms and irregularities when considering individual corneas. In conclusion, approximating the anterior corneal surface with a conic surface provides a good approximation for C_2^2 and C_1^3. However, when examining higher-order terms, C_2^4 and C_1^5, variations and discrepancies become evident.

ACKNOWLEDGEMENTS: This project has received funding from the European Union's Horizon 2020 research and innovation programme under the Marie Skłodowska-Curie grant agreement No 956720.

---

[1] D. Romaschenko; *KTH Royal Institute of Technology,* Doctoral Thesis in Physics (2021).
[2] R. Navarro; *Journal of Optometry*, **2**, 3 (2009).
[3] L. Lundström, J. Gustafsson & P. Unsbo; *Journal of the Optical Society of America*, **26**, 2192, (2009).

EFFECT OF ABERROMETRY IN INTRAOCULAR LENSES ON VISUAL QUALITY.

Inas Baoud Ould Haddi[1], Dayan Flores Cervantes[1,2], Emilio Dorronzoro Ramirez[2], Vanesa Blazquez Sanchez [1] y Cristina Bonnin Arias[1].

[1] Departament of Optometry and Vision, Faculty of Optics and Optometry, Universidad Complutense de Madrid, C. de Arcos de Jalón, 118 (28037, Madrid, Madrid)

[2] Hospital Universitario Sanitas La Moraleja, Ana de Austria, C. Arroyo de Valdebebas, 5 (28050, Madrid, Madrid)

Contact: ibaoud@ucm.es

Introduction.

Corneal aberrations influence visual quality outcomes after multifocal intraocular lens (IOL) implantation. Therefore, surgeons are increasingly considering these higher order aberrations (HOA) when implanting multifocal IOLs. Equipment such as the Pentacam HR® (Oculus Optikgeräte GmbH, Germany), allows these parameters to be obtained quickly and efficiently, calling them "Total Cor Irregular Astig" in its software. According to the latest studies, it is established that if this value is RMS HOA<0.3 µm the patient is indicated to implant a multifocal lens, but if 0.3µm<RMS HOA< 0.5µm care should be taken when implanting the multifocal IOL.1,2 So far the published works analyze the relationship between HOAs and multifocal IOLs, but there are no studies that relate it to the new models of extended depth of focus (EDOF) and monofocal plus IOLs.

Objective.

To analyze the effect of higher order aberrations on the choice of intraocular lenses to optimize the visual quality of patients.

Setting.

The study was performed at the Hospital Universitario Sanitas la Moraleja in Madrid. All surgeries were performed by the same experienced surgeon (E.D.R). The study followed the principles of the Declaration of Helsinki.

Material and method.

Observational, prospective, cross-sectional study. A total of 56 eyes of 28 patients operated on for cataract or lensectomy, with bilateral implantation of one of the three study intraocular lenses (IOLs) were included in the sample: 16 eyes with PhysiOL® IsoPure 123™ implant (BVI Medical/PhysIOL, Liége, Belgium), 20 eyes with AcrySof ® IQ Vivity™ (Alcon Laboratories, Inc, Fort Worth TX) and 20 eyes with Tecnis® Eyhance™ (Johnson & Johnson Surgical Vision, Inc, Santa Ana, CA). In the preoperative study, in addition to biometry, endothelial count and optical coherence tomography (OCT) and corneal. In addition, with the Pentacam HR® (Oculus Optikgeräte GmbH, Germany), analysis of higher-order aberrations was performed.

After 30 days after surgery, an evaluation of photopic visual acuity (VA) in monocular and binocular, for far distance (4 meters) and near distance (40 cm) was performed with the ETDRS test, as well as halometry and the VFQ-14 questionnaire to determine patient satisfaction. A p value < 0.05 was considered a criterion of statistical significance and the correlation was performed with Spearman's test.

Results.

VA analysis under photopic conditions showed no significant differences between the Tecnis® Eyhance™, PhysiOL® IsoPure 123™ and AcrySof® IQ Vivity™ lenses (-0.09 ± 0.09), (-0.10 ± 0.09) and

(-0.14 ± 0.07), respectively for distance far distance. No statistically significant differences were found when comparing HOA, as the p-value between Tecnis® Eyhance™ and AcrySof® IQ Vivity™ (0.972), Tecnis® Eyhance™ and PhysiOL® IsoPure 123™ (0.997) and AcrySof® IQ Vivity™ with PhysiOL® IsoPure 123™ (0.980) lenses. In addition, there was also no positive correlation when relating VA or the presence of photic effects to HOA aberrometry values.

Conclusions.

All three IOL designs, AcrySof® IQ Vivity™, PhysiOL® IsoPure 123™ and Tecnis® Eyhance™ provide optimal VA for the distance distance, although the AcrySof® IQ Vivity™ lens performed better. The subjects did not have a presence of photic effects, and therefore, these lenses have been shown to be indicated in patients with higher order aberrations, as it does not influence the patient's visual quality.

Authors' conflict of interest.

There is no funding or conflict of interest on the part of any of the authors of this study.

References.

1. Maeda N. Evaluación de la calidad óptica corneal para los LIOs Premium con el Pentacam HR. En: Michael W, Stephen S, Renato A Jr. Tomografía corneal basada en la Elevación. Segunda Edición. Republica de Panamà:Jaype-Highlights Medical Publishers,Inc. Ciudad del Saber;2012. 197-204.

2. A Bartol-Puyal FD, Giménez G, Altemir I, Larrosa JM, Polo V, Pablo L. Optical aberrations in three different intraocular lens designs of a same platform. Saudi J Ophthalmol. 2022 Feb 18;35(2):126-130. doi: 10.4103/1319-4534.337865. PMID: 35391809; PMCID: PMC8982946.

Calibration of a Tunable Lens for Optometric Applications

Raquel Salvador-Roger[1], José J. Esteve-Taboada[1] and Vicente Micó[1]

[1] Department of Optics, Optometry and Vision Sciences, Faculty of Physics, University of Valencia (Dr. Moliner, 50, 46100, Valencia, Spain)

Contact: raquel.salvador@uv.es

Aim: Tunable lenses are becoming a crucial component in both adaptive optics and ophthalmic optics. Their manufacturing allows for changes in their dioptric power, reducing the need for multiple lenses.[1] This power variation can be achieved through different strategies, such as mechanical deformation of a membrane containing a liquid with a different refractive index, manual application of voltages on the interface of two liquids with different refractive indexes (electrowetting), or using other elements such as temperature, sound, and/or dielectric elastomers to control the interface.[2] As they are variable in dioptric power, it is important to know their optical properties before its use. This study characterizes a manual liquid lens under various environmental and geometric conditions.

Methodology: For this characterization, an Optotune ML-20-37 manual liquid lens (Optotune, Switzerland) was considered. This lens permit to be rotated over itself so as to change its orientation; as a result, its dioptric power also changes. A Hartmann-Shack WFS40-K2/M aberrometer (Thorlabs) was employed. Measurements were taken under four different conditions. Firstly, the stability of the lens was evaluated by maintaining the laboratory temperature constant for a wavelength of 520 µm for three lens orientations. Next, while maintaining the previous measurement conditions, the lens's reaction time was assessed. The changes produced by a change in ambient temperature were also characterized for the same three lens orientations. Finally, the influence of gravity on the lens was examined changing the lens from a vertical position to a horizontal one.

Results: When measuring the stability of the lens keeping the laboratory temperature constant, its spherical equivalent power (M) varies between 0.03 µm (0.01 D) in Orientation 1, 0.10 µm (0.03 D) in Orientation 2, and 0.06 µm (0.02 D) in Orientation 3 (see Figure 1). The average reaction time of the lens is 1.2 ± 0.3 s (see Figure 2a). With changes in ambient temperature, the lens in Orientation 1 varies a total of 0.9 µm (0.25 D), Orientation 2 changes by 1.82 µm (0.5 D), and for Orientation 3 M varies by 1.74 µm (0.48 D). Additionally, this change does not follow the same trend for all orientations (see Figure 2b). Figures 2c-f show variations in some Zernike coefficients when changing the orientation of the lens.

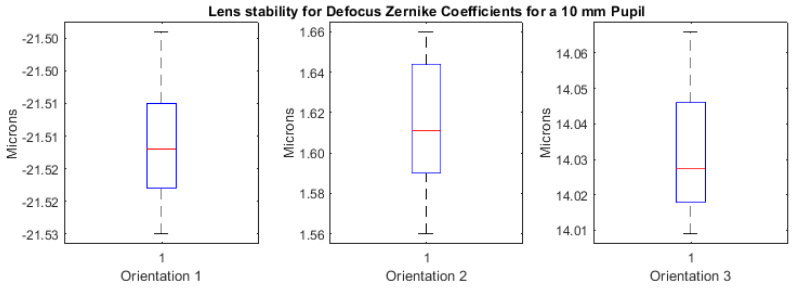

Figure 1: Boxplot for coefficient C(2,0) in three orientations.

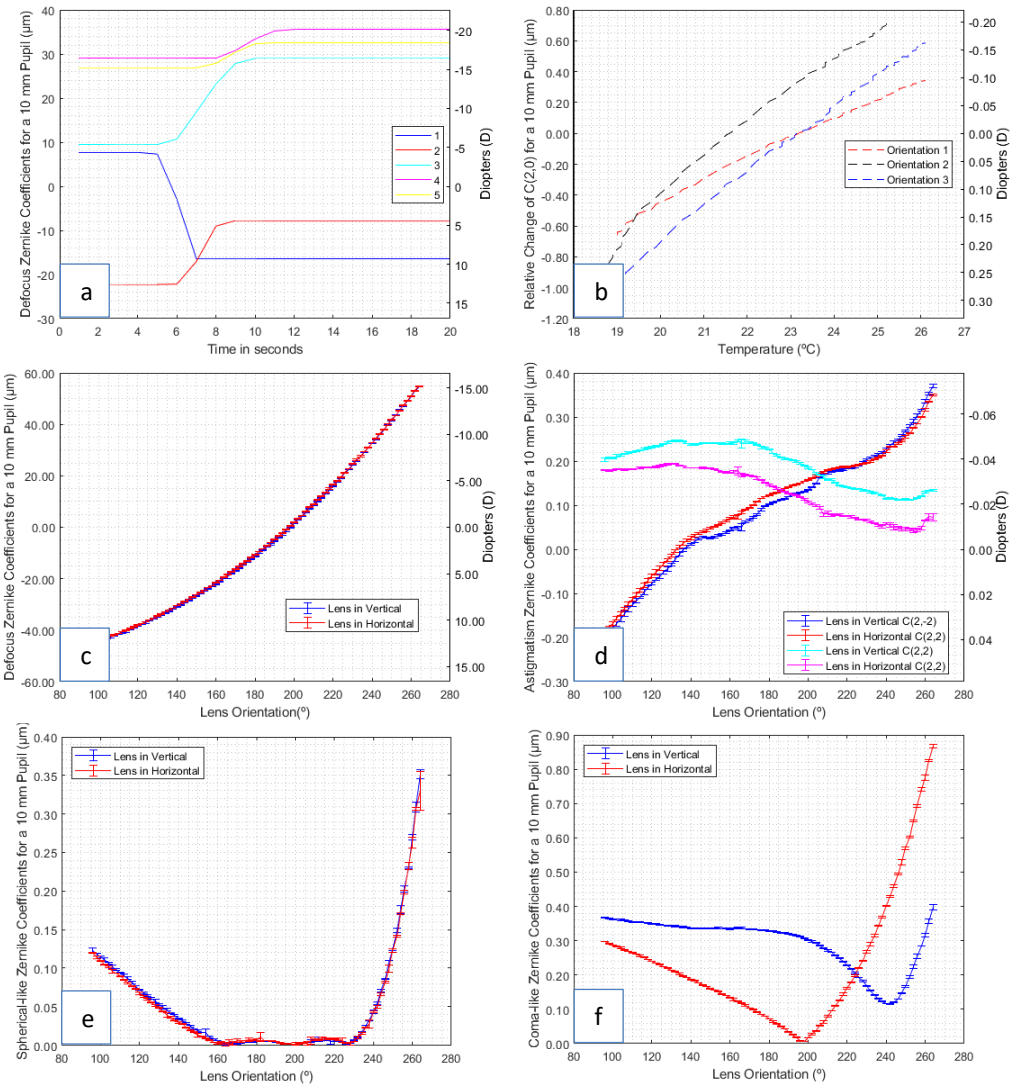

Figure 2: Results of a) lens response time to different M changes, b) change in relative M as a function of temperature, c) C(2,0) in lens horizontal and vertical positions , d) C(2,-2) and C(2,2) in lens horizontal and vertical positions, e) Spherical-like (RMS of C(4,0) and C(6,0)) in lens horizontal and vertical positions, and f) Coma-like (RMS of C(3,-1), C(3,1), C(5,-1), and C(5,1)) in lens horizontal and vertical positions.

Conclusions: The properties of the liquid lens remain stable over time as long as ambient conditions remain constant. It has also been observed that a change in ambient temperature can cause a change of up to 0.5 D in M. The average reaction time could be negligible in fields such as optometric applications. Finally, the influence of gravity is shown on certain coefficients such as C(2,2) and C(3,-1). In summary, maintaining constant measurement environmental conditions, as well as the lens position, are fundamental factors to consider when using the lens for ophthalmic applications.

ACKNOWLEDGEMENTS: This work was supported by the Spanish Ministerio de Universidades Grant FPU20/05624 awarded to Raquel Salvador-Roger

[1]R. Marks et al. *Optics letters,* **34**, 515 (2009).
[2]L. Chen et al. *Frontiers in Robotics and AI,* **8**, 678046 (2021).

Low-cost manually tunable lens for astigmatic compensation in optical instruments

Sara Ferrer-Altabás[1] and Vicente Micó

[1] Department of Optics and Optometry and Vision Sciences, Faculty of Physics, University of Valencia, Street Dr. Moliner, 50, 46100 Burjassot, Valencia (Spain)

Contact: Sara.Ferrer@uv.es

Astigmatism is a well-known refractive error and the most common among the population and have important implications in visual performance and comfort[1,2]. However, while spherical refractive errors as myopia and hyperopia can be easily corrected by adjusting the eyepiece in optical instruments, astigmatism is still not considered in the same way for commercial eyepieces[3].Several tunable astigmatic lenses have been presented over the years, from mechanical rotation of refractive optical elements as cylinder or cross-cylinder lenses[3,4]. Additionally, the field of research in tunable fluidic lenses has been experiencing continuous advances in recent years. Based on different principles as electrowetting, membranes, plates or gradient refractive index elements, tunable fluidic lenses allow to generate different types of optical aberrations as spherical and astigmatic power. Despite that, they still have some non-neglectable drawbacks to be used in instruments as binoculars or microscopes, since they are generally sensitive to changes in the environment as temperature[5].

The aim of this work is to present the construction and characterization of a low-cost compact tunable astigmatic lens (modified Stokes lens) with an expanded range of astigmatism compensation to be used in optical instruments for measurement and/or compensation of astigmatism. Our objective parameters were to be able to measure small changes as 0,25D, and to cover a cylindrical range compensation up to 6D of cylinder (3D of J component), which match with the features of ophthalmic instruments for subjective refraction as phoropters. The treatment of the dioptric power is conducted with power vectors (M, J), which allow a clear statistical analysis[6].

As a first approach, the construction of a Stokes lens using a Risley prism mount from a lensmeter is made by exchanging the prism lenses by cylinder lenses of C= +/- 1,50D. The lens is characterized with an automatic lensmeter. The results in Figures 2 and 4 show that the dioptric power range allows to compensate up to 3D of cylinder (1,5D in J component), and the accuracy allows to measure small values as 0,25D steps[6]. Finally, to expand up the cylindrical range, a modified Stokes lens is proposed as the combination of the previous Stokes lens with a cross-cylinder lens (CCL) (Figure 1). In the presented implementation, the CCL is fixed while the lenses in the Risley prism mount are rotated for the astigmatism variation. The characterization is also carried out with an automatic lensmeter. The results in Figures 3 and 5 show the same accuracy as the previous Stokes lens, while the range has been increased up to 6D of cylinder (3D in J component)[6].

Stokes lenses can be widely applied to, for instance, allow compensation or measurement of astigmatism in optical instruments as microscopes or binoculars as well as for optometric

applications as lensometry or subjective refraction[6-9]. A main advantage is that the value and orientation of astigmatism generated are both tunable, allowing to find the position that best fits for a given purpose, without the need of buying a customized astigmatic lens and allowing to use optical instruments without other compensating elements as spectacles or contact lenses.

In conclusion, the modified Stokes lens fulfills the requirements stablished and is compact and robust for being used in optical instruments for astigmatism compensation.

Figure 1: Modified Stokes lens

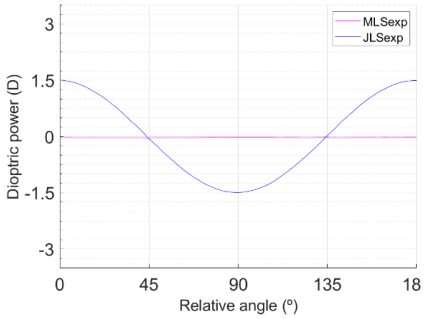

Figure 2: Characterization of a a conventional Stokes lens using power vectors (MLSexp) and (JLSexp).

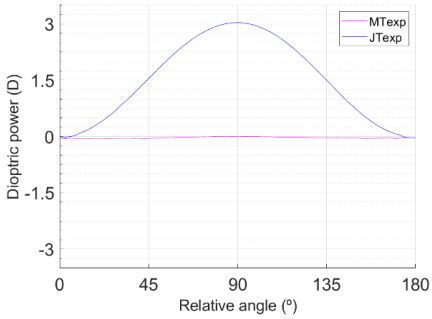

Figure 3: Characterization of the modified Stokes lens using power vectors (MTexp) and (JTexp).

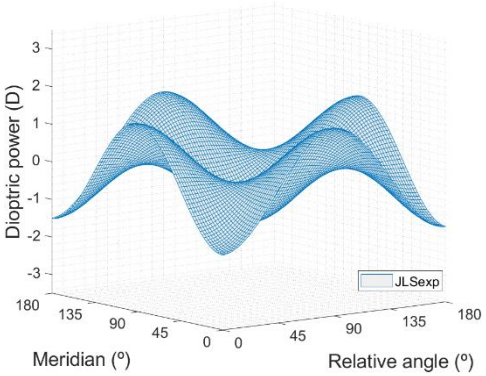

Figure 4: Representation of the conventional Stokes lens regarding relative angle and meridian.

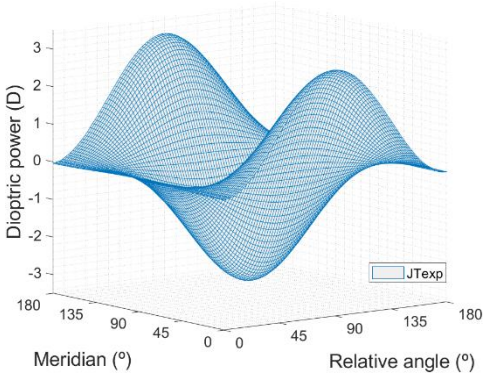

Figure 5: Representation of the modified Stokes lens regarding relative angle and meridian.

ACKNOWLEDGEMENTS: This research has been granted by the Grant PID2020-120056GB-C21 funded by MCIN/AEI/10.13039/501100011033 and by the Spanish Ministerio de Universidades Grant FPU21/00985.

[1]H. Hashemi and A. Fotouhi et al.; *Journal of Current Ophthalmology*, **30**, 3 (2018).
[2]S. Read, S. Vincent, M. Collins; *Ophthalmic and Physiological Optics*, **34**, 267 (2014).
[3]J. Arines and E. Acosta; *Optometry and Vision Science*, **88**, 1524 (2011).
[4]J. Foley and C. Campbell; *Optometry and Vision Science*, **76**, 664 (1999).
[5]C. Dorronsoro and X. Barcala et al.; *Optics Express*, **27**, 2085 (2019).
[6]S. Ferrer-Altabás , L. Thibos and V. Micó ; *Optics Express*, **30**, 8974 (2022)
[7]S. Ferrer-Altabás and V. Micó; *Applied Optics*, **59**, 3347 (2020).
[8]S. Ferrer-Altabás, M- Sanz-Sabater and V. Micó; *Optics and Lasers in Engineering*, **146**, 106703 (2021).
[9]J. Albero-Moreno, C. Albarrán-Diego and V. Micó; *Optical Engineering*, **61**, 1 (2022).

Optical imaging quality and expected range of vision of two presbyopia-correcting intraocular lens designs

Fátima Cuéllar[1], Fidel Vega[1], David Madrid[2] and María S. Millán[1]

[1] Grupo de Óptica Aplicada y Procesado de Imagen. Departamento de Óptica y Optometría. Universitat Politècnica de Catalunya – BARCELONA**TECH.** Terrassa (Barcelona).
[2] Optometry and Vision Department, Faculty of Optics and Optometry, Universidad Complutense de Madrid, Spain.

fatima.cuellar@upc.edu

This work is based on the prediction of the expected visual acuity (VA) from the optical imaging quality obtained with an on-bench MTF-based metric, named area under the MTF curve (MTFa). Previous studies have shown that the average visual performance of a pseudophakic subject, after IOL implantation, can be correlated with this metric through the expression:[1]

$$VA(MTFa) = a * (\frac{1}{MTFa}) + c \quad \text{Where a = 0.085 and c = -0.21 logMAR} \quad (1)$$

For the development of this study, two intraocular lenses (IOL) were considered, whose basic features are summarized in Table 1.

Intraocular lens (IOL)	Power (D)	Design
Asquelio	19 D	EDOF
OptiFLEX TRIO	22 D (+1.85 D / +3.50 D)	Trifocal

Table 1: Characteristics of the IOLs studied in this work

The optical image quality of the IOLs was measured in vitro following the recommendations of ISO 11979-2:2014[2] and ANSI Z80.35-2018[3], with model eye type 2 (i.e., artificial cornea with spherical aberration of +0.27 µm for 5.15 mm IOL pupil).

Figure 1 shows the TF- MTFa curves for Asquelio vs OptiFLEX IOLs for 3.0 mm and 4.5 mm pupils, respectively. The useful range of vision extends from 0.0 D defocus (far vision) to the negative defocus values (intermediate and near vision). Defocus and pupil are referred to the IOL plane.

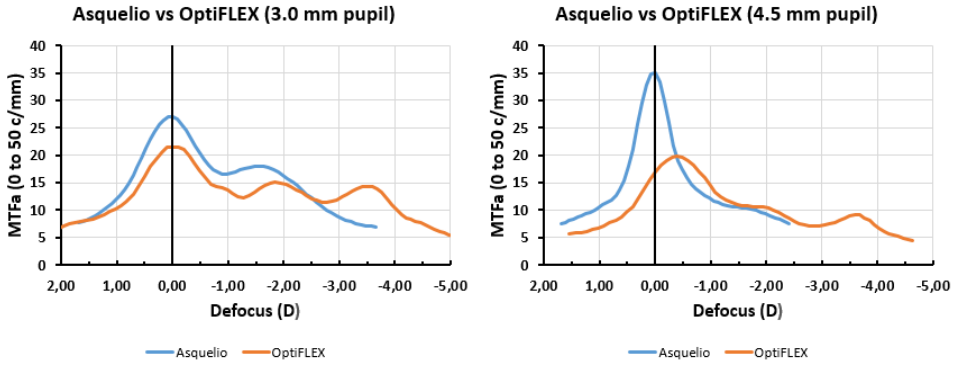

Figure 1: TF-MTFa obtained with 3.0 mm and 4.5 mm pupils.

With the 3.0 mm pupil, the MTFa curves of both lenses show the characteristic shape of their respective design. The Asquelio shows little better MTFa and thus better optical imaging quality in far focus and up to an intermediate vision of -1.25 D approximately.
When the pupil increases, the behavior of both lenses changes. Thus, while the Asquelio forms a single highly focused peak of better quality for distance vision, the OptiFLEX optical quality decreases with a flattened curve where it is still possible to distinguish three peaks for distance, intermediate and near vision. The far focus of the OptiFLEX shifts towards negative vergence more likely due to an overall increase of the (positive) spherical aberration of the model eye.

We calculated the expected visual acuity (logMAR) from the through-focus (TF) MTFa values of each lens using equation 1. Figure 2 shows the results (expected visual acuity versus defocus) for both IOLs obtained with the 3.0 mm pupil. The defocus values in the calculated TF-VA curves are referred to the spectacle plane.

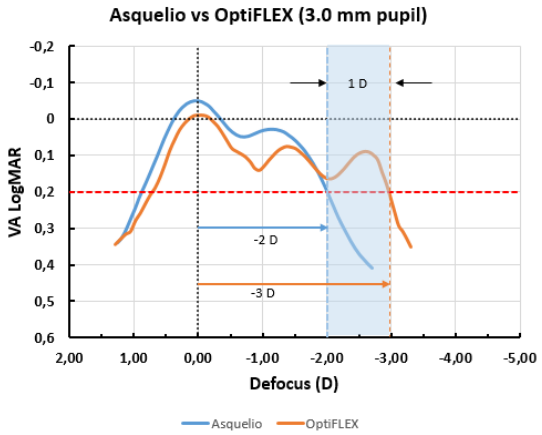

Figure 2: Expected VA (LogMAR) defocus curves of Asquelio and OptiFLEX IOLs

With both IOLs, the best VA is predicted for 0.0 D defocus (at the focus for distance vision) and, consistently with the differences in MTFa between lenses at far distance (Figure 1), the expected VA with Asquelio is slightly better (although less than 1 line).

In conclusion, Asquelio would have better VA from far to intermediate vision, -1.25 D approximately. In closer distances, the near focus of the OptiFLEX would lead to better AV expectancy.
The expected range of vision, defined as the defocus range for which the expected VA has the logMAR value 0.2 or better as specified in the ANSI Z80.35:2018[3], obtained for each lens are -2 D for Asquelio and -3 D for OptiFLEX (Figure 2). Therefore, OptiFLEX has a range of vision of (negative) 1 D over Asquelio.

ACKNOWLEDGEMENTS:
Ministerio de Ciencia e Innovación, Agencia Estatal de Investigación (PID2020-114582RB-I00/AEI/ 10.13039/501100011033)

References

[1]Alarcon, A., Canovas, C., Rosen, R., Weeber, H., Tsai, L., Hileman, K., Piers, P. (2016). Preclinical metrics to predict through-focus visual acuity for pseudophakic patients. Biomedical Optics Express, 7(5), 1877
[2] Ophthalmic implants. Intraocular lenses. Part 2: Optical properties and test methods. ISO 11979-2:2014.
[3] American National Standards Institute, ANSI Z80.35-2018. (2019). Extended depth of focus intraocular lenses. Alexandria, VA U.S.A.: The Vision Council.

DEVELOPMENT OF A PORTABLE AND LOW-COST MULTISPECTRAL FUNDUS CAMERA

Marina Bou[1], Francisco J. Burgos[1] and Meritxell Vilaseca[1]

[1] Center for Sensors, Instruments and Systems Development, Universitat Politècnica de Catalunya, Rambla Sant Nebridi 10, Terrassa 08222 (Barcelona), Spain

Contact: marina.bou@upc.edu

Fundus imaging is a fundamental tool widely used in clinics for retinal screening, which makes the diagnosis of fundus diseases faster and easier. Examination of the eye fundus with fundus cameras provides fast and accurate information by means of a non-invasive technique. However, their spectral resolution is limited because they include colour cameras with only three spectral bands (R, G, and B). As a consequence, some fundus structures and substances with different spectral properties related to specific ocular diseases cannot be detected sometimes because they are metameric (i.e., they produce the same R, G and B signals)[1]. Moreover, since conventional colour cameras have a spectral sensitivity limited to the visible (VIS) range, it is difficult to image other structures, especially those located at the deepest layers of the ocular fundus, where VIS light cannot penetrate due to the higher absorption and scattering from previous tissues[2]. Recently, multispectral imaging has been applied to this purpose, since it can acquire images for more than three channels in the VIS and also from other ranges of the electromagnetic spectrum, allowing spectral data to be obtained and not only colour information. This analysis has been proven to be very useful, since the spectral response depends on the chemical composition of the tissue, providing better discrimination between healthy and diseased structures[3].

On the other hand, recent developments have focused on the use of smartphones to evaluate the eye fundus, especially for screening purposes, since images with high spatial resolution can be obtained, and they are economically more affordable and easier to use than conventional fundus cameras[4]. Accordingly, the goal of this work was to develop a smartphone-based multispectral fundus camera that allows obtaining images of the fundus in the VIS and near-infrared (NIR) range, to improve the diagnosis of certain diseases that affect the eye fundus.

The developed prototype (Figure 1) is composed of: a set of 7 fiber-coupled LEDs with peak wavelengths ranging from 400 nm to 1000 nm, which are used to illuminate the eye fundus; a modified PanOptic ophthalmoscope to image and contribute to the illumination of the eye fundus throughout the required spectral range; and a smartphone that serves as the imaging system and the device control tool, including an especially designed application. The LEDs are connected to the PanOptic ophthalmoscope through a custom-made optical fiber that has 7 inputs and 1 output. The components were characterized to evaluate their ability to operate within the required spectral range, and the spectral imaging capability of the whole system was evaluated. To conduct laboratory tests, an artificial eye (Ocular Imaging Eye Model OEMI-7, Ocular Instruments Inc.) was used to simulate the patient's eye. In addition, to verify that the detection system was capable of obtaining eye fundus images of patients, images of a real eye were taken using the smartphone attached to the PanOptic ophthalmoscope with its original lamp.

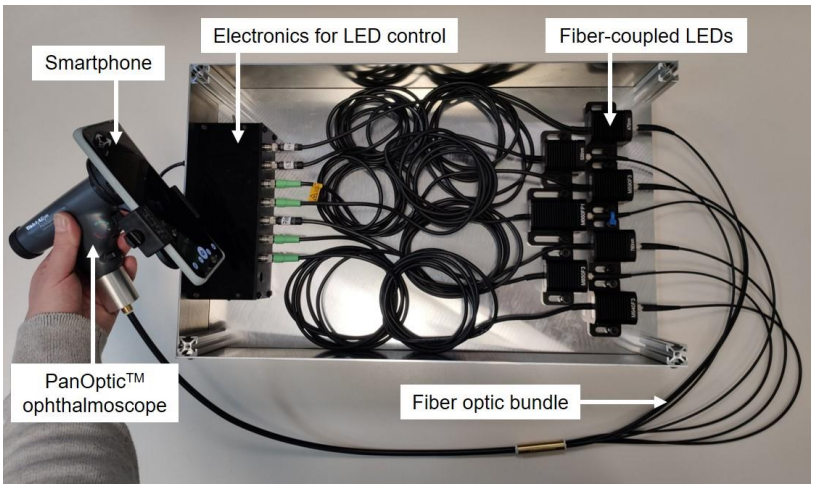

Figure 1 Prototype of the smartphone-based multispectral fundus camera

The tests performed with the setup and the artificial eye confirmed the spectral imaging capabilities of the complete system. The main components such as the illumination, optics and smartphone have been evaluated, considering that the complete system must be portable, economically affordable, and offer spectral data of eye fundus in the VIS and NIR ranges. Regarding the optical system, the transmittance of the PanOptic ophthalmoscope has been studied carefully, and a filter included in the system which blocks light above 700 nm has been removed in order to be able to work in the whole spectral range of interest. The spectral illumination by means of fiber-coupled LEDs has shown good performance when attached to the PanOptic ophthalmoscope. Regarding the detection system, the smartphone's monochromatic camera also showed good performance for the whole spectral range. Finally, images from real eye fundus have been obtained using the smartphone attached to the PanOptic ophthalmoscope with its original lamp.

ACKNOWLEDGEMENTS: This publication is part of the project PID2020-112527RB-I00, funded by MCIN/AEI/10.13039/501100011033. The first author gratefully acknowledges the Universitat Politècnica de Catalunya and Banco Santander for the financial support of her predoctoral grant FPI-UPC.

---

[1] I. B. Styles, A. Calcagni, E. Claridge, F. Orihuela-Espina and J. M. Gibson; Quantitative analysis of multi-spectral fundus images. *Medical Image Analysis* 10, 578–597 (2006).

[2] T. Alterini, F. Díaz-Doutón, F. J. Burgos-Fernández, L. González, C. Mateo, and M. Vilaseca; Fast visible and extended near-infrared multispectral fundus camera, *J. Biomed. Opt.* 24, 1 (2019).

[3] F. J. Burgos-Fernández et al.; Reflectance evaluation of eye fundus structures with a visible and near-infrared multispectral camera, *Biomed. Opt. Express* 13, 3504 (2022).

[4] N. Panwar et al.; Fundus Photography in the 21st Century—A Review of Recent Technological Advances and Their Implications for Worldwide Healthcare, *Telemedicine and e-Health* 22, 198–208 (2016).

Repeatability in wavefront measurement at different pupil sizes in young subjects

María Mechó-García[1], José Manuel González-Méijome[1], Elvira Orduna-Hospital[2] and Ana Sánchez-Cano[2]

[1] Clinical & Experimental Optometry Research Lab, Center of Physics (Optometry), School of Sciences, University of Minho, Braga, Portugal.
[2] Department of Applied Physics, University of Zaragoza, Zaragoza, Spain

Contact: mmechogarcia@fisica.uminho.pt

Purpose: It is of interest to know information about the repeatability of an instrument under normal conditions to establish validation of the instrument in clinical practice[1-3], as well as the impact of pupil size on data analysis. The IRX3 aberrometer uses a Hartmann-Shack sensor to obtain the wavefront of the human eye. The aim of this work was to investigate the effect of pupil size on the repeatability of the different Zernike coefficients that describe the wavefront error.

Methods: A total of 63 eyes (30 right eyes and 33 left eyes) from 37 healthy young volunteers (25.17 ± 3.55 years old, 24 women and 12 men) were enrolled.
Three measurements were made for each eye with the aberrometer Hartmann-Shack (IRX3, Imagine Eyes, Orsay, France). During the measurement the contralateral eye was occluded to ensure that the subject fixes the gaze on the stimulus inside the aberrometer.
The results were exported with a maximum pupil and then rescaled for 5 different pupil sizes (4.0 mm, 4.5 mm, 5.0 mm, 5.5 mm and 6.0 mm) based on the formulas described by Jim Schwiegerling (2002)[4].
Wavefront aberrations, including defocus (C (2,0)), primary spherical aberration (C (4,0)), secondary spherical aberration (C (6,0)), vertical coma (C (3, -1)) and horizontal coma (C (3, 1)) were analysed. To allow for mirror symmetry between right and left eyes, the sign of left eye ocular aberration coefficient C (3,1) was changed to perform the calculations. The repeatability was evaluated using one-way ANOVA method, within-subject standard deviation (Sw), intraclass correlation coefficient (ICC), limits of agreement (LoA), coefficient of variation (CoV) and coefficient of repeatability (CoR) were obtained for each Zernike coefficient at each pupil size.

Results: The CoR increases with increasing pupil size for all Zernike coefficients analysed (CoR< 0.88). The CoV of the different Zernike coefficients decreased with the increasing order. The higher CoV was obtained for the third-order Zernike coefficients (Table 1).

The mean defocus, C (2,0), changed from 1.438 ± 1.404 µm to 3.459 ± 3.282 µm, from the minimum to the maximum pupil diameter analysed (Figure 1).

As expected, the magnitude of the higher-order Zernike coefficients (Figure 2 and 3) increased with larger pupil diameter. The rotationally symmetric Zernike coefficients C (4,0) and C (6,0) have larger changes with pupil diameter (Figure 3). Primary spherical aberration had the largest changes from 0.004 µm to 0.131 µm. The non-rotationally symmetric Zernike coefficients (Figure 2) C (3,1) and C (3, -1) had a trend towards more negative values with increasing pupil diameter. Although the magnitude was of lesser with respect to C (2, 0) and C (4, 0).

Ocular higher-order aberrations (HOA) measured by the IRX showed Sw < 0.319 µm (Table 1). The 95% LoA increased for low and high order terms as increasing the pupil size.

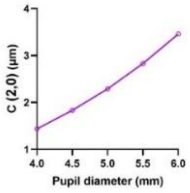

Figure 1. C (2,0) representation as a function of pupil size.

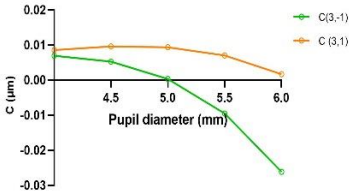

Figure 2. C (3, -1) and C (3,1) representation as a function of pupil size.

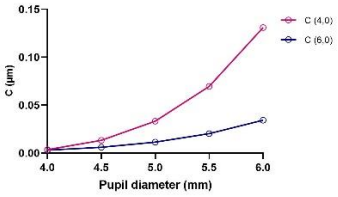

Figure 3. C (4,0) and C (6,0) representation as a function

	C (2,0)		C (4,0)		C (6,0)		C (3,-1)		C (3,1)	
	Pupil 4 mm	Pupil 6 mm	Pupil 4 mm	Pupil 6 mm	Pupil 4 mm	Pupil 6 mm	Pupil 4 mm	Pupil 6 mm	Pupil 4 mm	Pupil 6 mm
Sw	0.116	0.305	0.011	0.099	0.003	0.034	0.022	0.214	0.024	0.319
CoV	0.080	0.088	3.138	0.762	0.996	0.996	3.132	-8.173	10.840	-25.477
CoR	0.320	0.846	0.031	0.276	0.009	0.095	0.059	0.593	0.066	0.882

Table 1. Values of Sw, CoV and CoR obtained for each Zernike coefficient with the minimum pupil analysed (4 mm) and maximum pupil analysed (6 mm).

Conclusions: Consistent with the results of other studies[5,6], when pupil size increases from 4 mm to 6 mm, defocus increases becoming more myopic on average in this healthy young population. Also, similar trends from other studies were found for spherical aberration[6]. A positive trend was observed in the vertical and horizontal coma, as different studies report[5-7].
Intersubject variability increases with increasing pupil size. And repeatability increases in larger pupils.
The IRX3 provides good repeatability in the measurement of the ocular wavefront. However, repeatability is affected with increasing pupil size. Therefore, smaller pupil diameter values will give more precise data of the measurements.

ACKNOWLEDGEMENTS: This project has received funding from the European Union's Horizon 2020 research and innovation programme under the Marie Skłodowska-Curie grant, agreement No. 956720.

[1]N. Visser, T.T. Berendschot, F. Verbakel, A.N. Tan, J de Branbander and R.M. Nuijts; *Investigative ophthalmology & visual science*, **52**, 1302 (2011).
[2]R.P. Hughes, S.J. Vicent, S.A. Read and M.J. Collins; *Clinical Experimental Optometry*, **103**, 68 (2020).
[3]G. Carracedo, C. Carpena-Torres, L. Batres, M. Serramito and A. González- Bergaz; *Journal of Ophthalmology*, **3** (2020).
[4]J. Schwiegerling**;** *Journal of the Optical Society of America. A, Optics, image science*, and vision**, 19,** 1937 (2002).
[5]Y. Levy, O. Segal, I. Avni and D. Zadok; *American Journal of Ophthalmology*, **139**, 225 (2005).
[6]X. Liao, M.J. Wang, Q.Q. Tan and C.J. Lan; *International ophthalmology*, **42,** 2525 (2022).
[7]M.A. Miranda, C. O'donnell and H. Radhakrishnan; *Clinical and Experimental Optometry*, **92,** 253 (2009).

A compact binocular adaptive optics visual simulator for clinical use in highly aberrated patients

Santiago Sager[1,2], Pedro M. Prieto[1,2], Alba M. Paniagua-Diaz[1], Adrián Gambín[1], Debajyoti Debnath[3], Sabyasachi Goswami[3], Shrikant R. Bharadwaj[3] and Pablo Artal[1,2]

[1] Laboratorio de Óptica, Universidad de Murcia, Murcia, Spain
[2] Voptica SL, Murcia, Spain
[3] L V Prasad Eye Institute, Hyderabad, India

Contact: santiago.sagerg@um.es

The impact of Higher Order Aberrations (HOAs) on monocular vision has been extensively researched, but their influence on binocular vision is to be thoroughly assessed. We developed a Binocular Visual Adaptive Optics (VAO) simulator capable of measuring objective refraction and HOAs, as well as to perform subjective vision measurements. From the binocular visual acuity and stereoacuity on highly aberrated patients with full correction, to the influence of different amounts of spherical aberration on each eye on the depth of focus, the proposed binocular VAO will allow for impactful research in a wide field of study.

The design of this device has been adapted from the commercial monocular version available from Voptica. Two HD stimulus screens are used in a system with a single phase modulator and a Hartmann-Shack (HS) wavefront sensor for aberration correction and measurement respectively. An intensity modulator screen allows for artificial pupil control while an electrically tunable lens increases measurement and correction range. The pupil camera and the periscope with eye separation and tilt control are used for precise patient positioning. A schematic of the optical design can be seen in Figure 1.

The first prototype of the device allows for an objective measurement range of +/- 15D in defocus, or 1µm for HOAs with a 4.5mm diameter pupil, due to the combination of the tunable lens and wavefront sensor. GPU Hartmann-Shack processing allows for simultaneous measurements in real time for both eyes and for pupils up to 7mm in diameter. The LCOS screen used for phase modulation is full HD, with a resolution that allows for an even larger correction range than the HS sensor. The system has been completed with a control software that allows for pupil tracking, subjective visual acuity tests, and stereoacuity tests. The device and software can be seen at work in Figure 2.

The first prototype of the Binocular Visual Adaptive Optics simulator has been successfully completed, improving over the current visual simulators available. This device will allow for more exhaustive research on the impact of higher order aberrations on binocular vision.

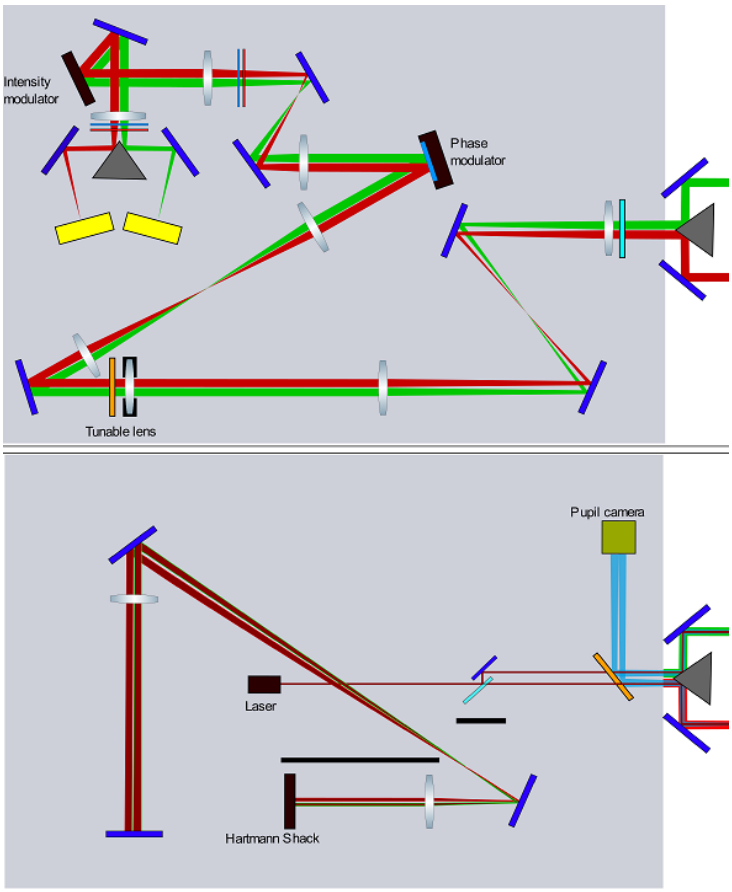

Figure 1: Schematics of the binocular VAO simulator

Figure 2: First prototype of the proposed Binocular VAO with control software

ACKNOWLEDGEMENTS: Fundación Séneca, Ministerio de Ciencia e Innovación, Voptica SL, LV Prasad Eye Institute

Visual Function of Myopic Young Adults with a Novel Ophthalmic Lens for the Control of Myopia Progression

Sara Silva-Leite[1], Ana Amorim-de-Sousa[1], Paulo Fernandes[1] and José Manuel González-Méijome[1]

[1] Clinical & Experimental Optometry Research Lab (CEORLab), Physics Center of Minho and Porto Universities (CF-UM-UP), School of Sciences, University of Minho, Gualtar (4710-057 Braga, Portugal)

Contact: saracsleite@gmail.com

Purpose: Several methods are currently available to control myopia progression and some of them show an impact on the visual function of myopes[1-3]. The purpose of this study was to evaluate the impact of a novel perifocal ophthalmic lens for the control of myopia progression on the visual function of young myopes.

Methods: This experimental, non-dispensing crossover study evaluated 17 myopic adults (mean age of 24.0 ± 3.5 years). The participants were myopes below 6.00 D (right eye (RE) -2.80 ± 1.75 D and left eye (LE) -2.81 ± 1.82 D). The visual function was assessed through visual contrast sensitivity (VCS) function and light disturbance (LD) analysis. VCS was measured in five spatial frequencies (1.5; 3; 6; 12 and 18 cycles/degree—cpd) at a 3.00 m distance, with the Vistech system VCTS 6500, in a low-light condition, to simulate the vision under challenging conditions. LD was assessed with the Light Distortion Analyzer (LDA)[4] 2.00 m away from the device. The software provides two metrics that allow quantifying the size of the LD - the light disturbance index (LDI), and the best-fit circle (BFC) radius (BFCRad) - and two metrics that evaluate the irregularity of the distortion - the BFC irregularity (BFCIrreg) and the standard deviation of the BFC irregularity (BFCIrregSD). VCS and LD were measured with a monofocal lens (control condition) and a perifocal lens (test condition) with an add power of +2.50 D on the temporal side of the lens and +2.00 D on the nasal side[5], as shown in Figure 1.

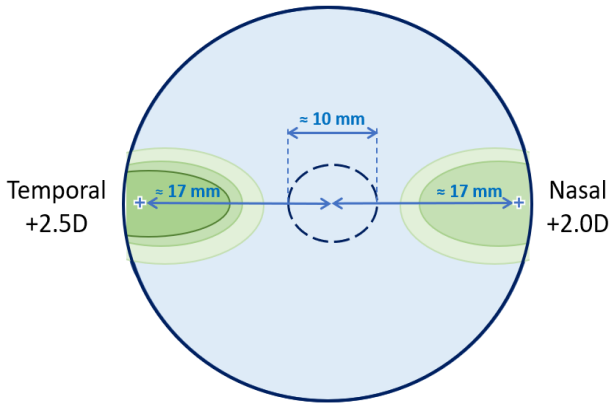

Figure 1: Schematic figure of the lens design according to the manufacturer. This represents the lens for the right eye, with a diameter of 38 mm. The central monofocal correction circle is 10 mm in diameter.

Results: The right eyes of the participants were analysed. Low-light VCS did not suffer any statistically significant changes when patients were using the perifocal lenses (p-value > 0.005), compared to the monofocal lenses, as shown in Table 1. The LD analysis showed no statistically

significant differences in the subject's light perception in the test condition (*p*-value > 0.005), compared to the control condition (Figure 2).

Spatial Frequency (cpd)	Control	Test	*p*-Value
1.5	1.36 ± 0.36	1.38 ± 0.38	0.194
3	1.61 ± 0.42	1.62 ± 0.43	0.322
6	1.42 ± 0.40	1.35 ± 0.39	0.192
12	0.79 ± 0.44	0.77 ± 0.52	0.844
18	0.13 ± 0.26	0.21 ± 0.31	0.257

Table 1: Mean ± standard deviation of log visual contrast sensitivity (VCS) for five spatial frequencies, for both control and test conditions. All *p*-values were calculated using the Wilcoxon test.

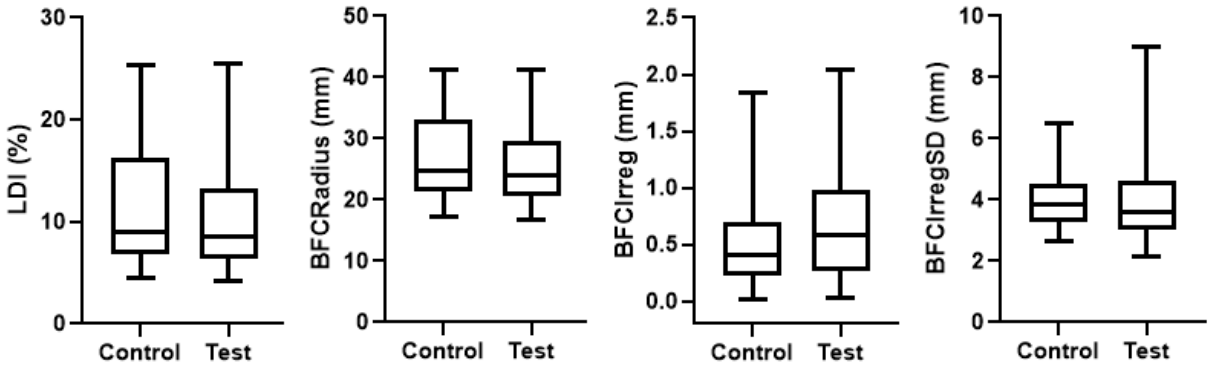

Figure 2: Light disturbance (LD) parameters obtained with LDA device for both control and test conditions. The median with 95% CI is shown for LDI, BFCRadius, BFCIrregularity and BFCIrregularitySD.

Conclusion: Although this novel perifocal ophthalmic lens modifies peripheral refraction for myopia management[5], this work shows that it does not affect the visual function of myopic young adults.

ACKNOWLEDGEMENTS: This work was supported by the Portuguese Foundation for Science and Technology (FCT) in the framework of the Strategic Funding UIDB/04650/2020 at the Center of Physics, UMinho, and predoctoral grant SFRH/BD/136684/2018 to Ana Amorim-de-Sousa. We acknowledge Indo Optical, S.L.U. for supplying the lenses used in this study.

[1]Y. Gao, E. Lim, A. Yang, B. Drobe and M. Bullimore; *Ophthalmic & Physiological Optics*, **41**, 1320 (2021).
[2]C. Lam, W. Tang, H. Qi, H. Radhakrishnan, K. Hasegawa, C. To and W. Charman; *Translational Vision Science and Technology*, **9**, 1 (2020).
[3]J. García-Marqués, R. Macedo-de-Araújo, A. Cerviño, S. García-Lázaro, C. McAlinden, J. González-Méijome; *Ophthalmic & Physiological Optics*, **40**, 718 (2020).
[4]H. Ferreira-Neves, R. Macedo-de-Araújo, L. Rico-del-Viejo, A. Silva, A. Queirós, J. González-Méijome; *Journal of Biomedical Optics*; **20**, 75002 (2015).
[5]E. Tarutta, O.Proskurina, N. Tarasova, S. Milash, G. Markosyan; *Vestnik Oftalmologii*, **135**, 46 (2019).

Dynamic accommodation from wavefront aberrometry in symptomatic and asymptomatic subjects

Jessica Gomes[1], Aina Turull-Mallofré[2], Nestor Gonzalez[2], Jaume Pujol[2] and Sandra Franco[1]

[1] Centre of Physics, University of Minho, Campus de Gualtar, 4710-407, Braga, Portugal
[2]Centre for Sensors, Instruments and Systems Development (CD6), Universitat Politècnica de Catalunya, Rambla Sant Nebridi 10, 08222, Terrassa, Spain

Contact: sfranco@fisica.uminho.pt

Introduction

Excessive time spent performing near tasks can cause symptoms in some people, such as headaches, eye strain or blurred vision, and it is important to assess these symptoms to help identify and monitor visual problems. However, some people sometimes present with symptoms without any evident changes on clinical examination.[1]

Wavefront aberrometry can be used to objectively measure the accommodative response (AR) and, if performed in real-time, it is possible to calculate several parameters of the AR and have detailed accommodative behaviour.[2]

The aim of this study was to evaluate the dynamic AR in subjects with and without near-related symptoms.

Methods

To select the subjects, a questionnaire was first administered that included the questions from the CISS survey to assess the symptomatology associated with near work. A score ≥21 was considered symptomatic and <21 was considered asymptomatic. Five symptomatic and five asymptomatic subjects, aged between 21 and 31 years, were then selected. In both groups, corrected visual acuity was 20/20 or better, mean sphere -1.08±1.40D and astigmatism -0.50±0.41D. The amplitude of accommodation was 13.90±3.22D and 12.88±2.57D and the accommodative facility was 17.20±1.789cpm and 17.60±2.80cpm in the symptomatic and asymptomatic subjects, respectively.

Aberrometry was performed in real-time using a Shack-Hartmann aberrometer[3]. Measurements were taken initially in the relaxed state of accommodation and then the target was moved to 1m, 0.40m, 0.25m and 0.20m, producing accommodative stimuli of 1.00D, 2.50D, 4.00D and 5.00D. The accommodative stimulus target was the letter 'E', which was resized for each distance. All subjects were fully corrected with spectacle lenses during the procedure and measurements were taken under mesopic lighting conditions.

AR was obtained from defocus aberration and using the software Wolfram Mathematica 12.2, a sigmoid function was fitted to the data:

$$AR = \frac{Af - Ai}{1 + e^{\frac{-(x-x_0)}{w}}} + Ai$$

Where x is the time in seconds, Af and Ai are the initial and final asymptotic values, w is the width of the x values between these two asymptotes and x_0 is located roughly at the centre of w. To obtain AR time, we started the measurement and after a few seconds the subjects opened their eyes and focused on the target. AR time was defined as the time between the moment the onset of the accommodative response (deleting the eye-opening values) and when the Boltzmann sigmoid fit

reached 98% of the total change in accommodation. AR and AR time were compared between subjects with and without symptoms.

Statistical analysis was performed using version 4.1.3 of the R software. Shapiro-Wilk was used to test the normality of the data and to analyse the differences between the groups, using the t-test for parametric data and the Wilcoxon test for non-parametric data. Data were considered statistically significant when $p<0.05$.

Results

The AR over time of symptomatic and asymptomatic subjects for the different distances are shown in Figure 1. The AR of the symptomatic subjects was observed to be lower than those of the asymptomatic subjects. This was verified for all accommodative stimuli and statistically significant for the target at 0.25m and 0.20m.

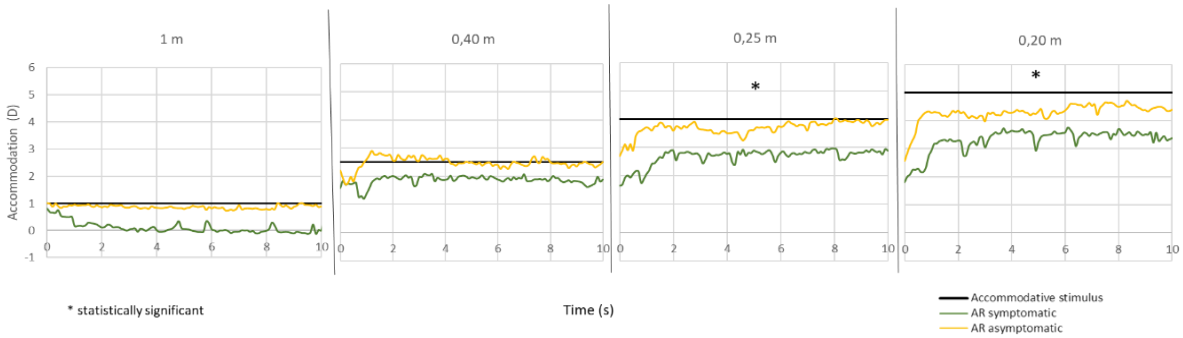

Figure 1. AR over time in symptomatic and asymptomatic subjects for different distances.

AR times were obtained for all distances and are shown in Table 1. They were higher in symptomatic than in asymptomatic subjects for all stimuli and these differences were statistically significant when the target was at 1 m. The dispersion was higher for the shorter distances, which may explain the lack of statistically significant differences for these distances.

Table 1. AR times of symptomatic and asymptomatic subjects for different distances.

	1 m	**0.40 m**	**0.25 m**	**0.20 m**
Symptomatic	870.8±164.95	794.0±416.84	1194.8±981.11	946.0±558.61
Asymptomatic	525.8±69.11	638.6±137.34	775.6±230.39	847.6±183.69
p-value	<0.01	0.47	0.40	0.72

Conclusions

In this study, it was observed that subjects with symptoms during near vision tasks may have normal results on clinical examinations, but changes in the AR when observed with a real-time wavefront aberrometer, in particular the amplitude of the AR and the AR time. This objective tool can be used as a diagnostic method in subjects presenting with symptoms during near vision tasks.

ACKNOWLEDGEMENTS: This work was supported by the Portuguese Foundation for Science and Technology (FCT) in the framework of the Strategic Funding UID/FIS/04650/2019 and by the project PTDC/FISOTI/31486/2017. The author Jessica Gomes is also supported by the PhD grant 2020.08737.BD from FCT. The author Aina Turull-Mallofré acknowledges Universitat Politècnica de Catalunya and Banco Santander for the financial support of her predoctoral grant FPI-UPC. This publication is part of the project PID2020-112527RB-I00, funded by MCIN/AEI/10.13039/501100011033

[1]S. Franco and J. Gomes. *Biomed Res Int,* **29**, 9415751 (2018)
[2]J. Tarrant, A. Roorda and C. Wildsoet; *Journal of Vision*, **10**, 4 (2010).
[3] C. E. García-Guerra, et al, Transl Vis Sci Technol., accepted for publication

Adaptive Optics vision simulator for 2-photon vision

Xinyu Wang[1], Silvestre Manzanera[1] and Pablo Artal[1]

[1] Laboratorio de Óptica, Universidad de Murcia, Murcia, Spain

Contact: xinyu.w@um.es

With normal vision, the sensitivity of the human eye to infrared (IR) light declines rapidly as the wavelength increases[1]. This sensitivity can be several orders of magnitude lower than for visible light. But when a pulsed IR source is used, the eye can perceive IR light as visible with a color corresponding to approximately half wavelength of the IR. Several studies[2-4], have attributed this phenomenon to a non-linear 2-photon (2P) absorption process.

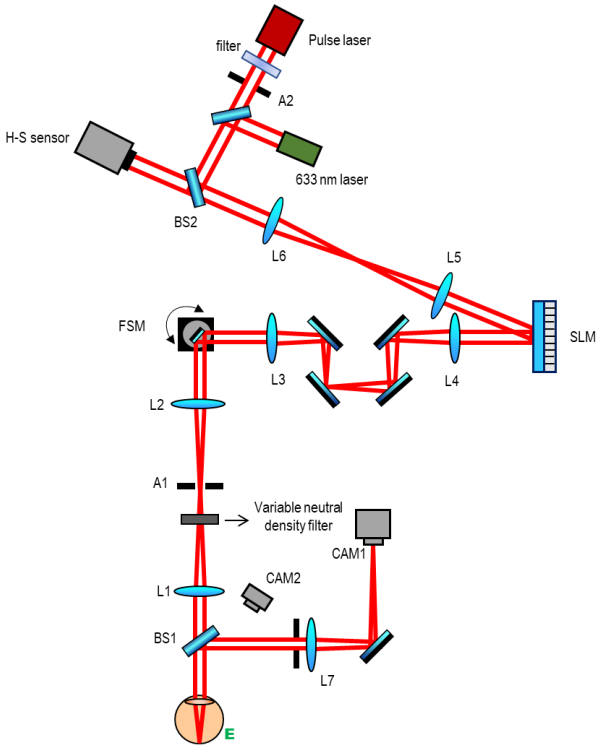

Figure 1: Schematic of the adaptive optics vision simulator

Applications of this phenomenon are still being investigated. For example, the perception of infrared light through two-photon (2P) excitation of visual pigments[5] will improve sensitivity when applied to older eyes with increased optical opacity[6]. Near-infrared light is less likely to be scattered by the ocular medium and less affected by scatter. The ability to use infrared light to produce visual perception[4] and to penetrate deeply into the scattering medium can be exploited in certain applications, for instance, to test the retinal response of eyes with severe cataracts[7]. Cataracts can block or scatter light as it passes through the lens of the eye, resulting in severe vision loss. Two-

photon excitation can penetrate the opaque ocular medium, allowing to test the visual field even when conventional methods may not be effective[8]. In this case, the combination with adaptive optics imaging might allow for a better assessment of not only the retina but also the neural pathways.

We have developed an adaptive optical vision simulator (AOVS) that uses pulsed IR light. It is based on a spatial light modulator (SLM)[9-11] and a Hartmann-Shack (HS) wavefront sensor [12-14] to correct aberrations in the optical system in real-time. A fast steering mirror is used to scan the beam and produce images on the retina for vision testing. In addition, a Badal system can correct defocus, releasing the SLM for control of higher-order aberrations. Fig 1 shows a schematic of the optical setup. A description of the current device and initial uses will be presented.

ACKNOWLEDGEMENTS:
Chinese Scholarship Council. Agencia Estatal de Investigación, Spain (PID2019-105684RB-I00/AEI/10.13039/501100011033).

---

[1]Griffin D R, Hubbard R, Wald G. The sensitivity of the human eye to infra-red radiation[J]. JOSA, 1947, 37(7): 546-554.
[2]Savin B M, Kovach R I, Kolchin E E. Role of nonlinear optical effects in the process of photoreception of laser radiation[J]. Doklady Akademii Nauk SSSR, 1975, 221(1): 225-226.
[3]Palczewska G, Vinberg F, Stremplewski P, et al. Human infrared vision is triggered by two-photon chromophore isomerization[J]. Proceedings of the National Academy of Sciences, 2014, 111(50): E5445-E5454.
[4]Artal P, Manzanera S, Komar K, et al. Visual acuity in two-photon infrared vision[J]. Optica, 2017, 4(12): 1488-1491
[5]Ruminski D, Palczewska G, Nowakowski M, et al. Two-photon microperimetry: sensitivity of human photoreceptors to infrared light[J]. Biomedical optics express, 2019, 10(9): 4551-4567.
[6]Zielińska A, Kiluk K, Wojtkowski M, et al. System for psychophysical measurements of two-photon vision[J]. Photonics Letters of Poland, 2019, 11(1): 1-3.
[7]Komar K, Marzejon M, Matuszak A, et al. Two-photon visual sensitivity of cataract patients[C]//Bio-Optics: Design and Application. Optica Publishing Group, 2021: DF2A. 4.
[8]M. Crossland, M.-L. Jackson, and W. H. Seiple, "Microperimetry: a review of fundus related perimetry," Optometry Rep. 2(1), 2 (2012).
[9]F. Vargas-Martn, P. M. Prieto, and P. Artal, "Correction of the aberrations in the human eye with a liquid-crystal spatial light modulator: limits to performance," J. Opt. Soc. Am. A 15, 2552–2562 (1998).
[10]P. M. Prieto, E. J. Fernández, S. Manzanera, and P. Artal, "Adaptive optics with a programmable phase modulator: applications in the human eye," Opt. Express 12, 4059–4071 (2004).
[11]E. J. Fernández, P. M. Prieto, and P. Artal, "Wave-aberration control with a liquid crystal on silicon (LCOS) spatial phase modulator," Opt. Express 17, 11013–11025 (2009).
[12]J. Liang, B. Grimm, S. Goelz, and J. F. Bille, "Objective measurement of wave aberrations of the human eye with the use of a HartmannShack wave-front sensor," J. Opt. Soc. Am. A 11, 1949–1957 (1994).
[13]P. M. Prieto, F. Vargas-Martn, S. Goelz, and P. Artal, "Analysis of the performance of the Hartmann-Shack sensor in the human eye," J. Opt. Soc. Am. A 17, 1388–1398 (2000).
[14]E. Chirre, P. M. Prieto, and P. Artal, "Binocular open-view instrument to measure aberrations and pupillary dynamics," Opt. Lett. 39, 4773–4775 (2014).

Restoration of retinal images using dictionary learning-based methodology

Erik M. Barrios[1,2], María S. Millán [3] and Andrés G. Marrugo[2]

[1] Escu. de Ciencias Básicas, Tecnología e Ingeniería, Universidad Nacional Abierta y a Distancia (Corozal, Colombia.)
[2] Facultad de Ciencias Básicas, Universidad Tecnológica de Bolívar (Cartagena, Colombia)
[3] Dept. de Óptica y Optometría, Universitat Politècnica de Catalunya - BARCELONATECH (Terrassa, Spain)

Contact: embm32@gmail.com

Fundus images acquired using retinal cameras are crucial for diagnosing various eye diseases[1]. However, the accumulation of dust particles in sensors is a significant problem in ophthalmology, as it is inevitable and routine cleaning is not usually performed. Dust particles in camera sensors often produce image artifacts that can be mistaken for small lesions. In this study, we propose a sparse representation and dictionary learning-based methodology for the removal and inpainting of artifacts from retinal images.

The presence of artifacts in retinal images can cause problems in both diagnosis and subsequent digital processing[2]. Therefore, several inpainting methods have been used to digitally remove these artifacts from the images[3]. We classified these methods into three categories: diffusion-based methods, exemplar-based inpainting methods, and hybrid methods[4,5]. We chose an exemplar-based approach to remove dust artifacts from retinal images.

Our proposed methodology consists of three stages: (i) generating a patch-based sparse representation of the image, (ii) generating a dictionary from image patches that do not contain artifacts and a predefined basis, such as the Discrete Cosine Transform (DCT), and (iii) predicting the values of the missing regions (artifacts) by constructing an approximate image without artifacts. A mask is used to avoid the pixels of the artifacts in the dictionary learning process and to identify the pixels that need to be replaced (Figure 1).

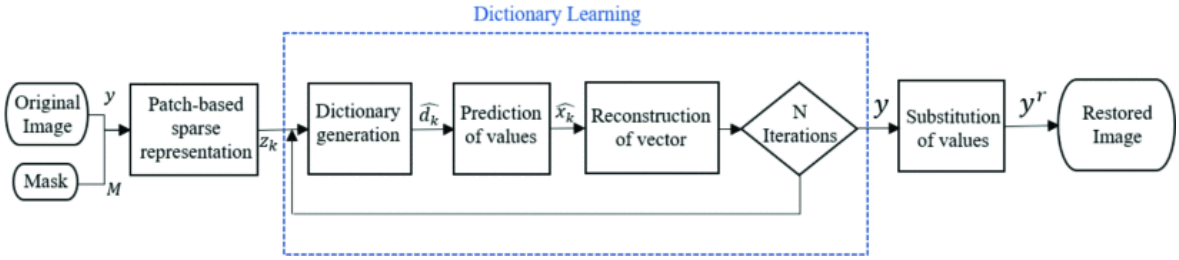

Figure 1: Flowchart of the proposed method.

We tested our method with real retinal images with actual dust artifacts and compared our results with those from a diffusion-based inpainting technique. The encouraging experimental results show that our method can successfully remove artifacts while maintaining the continuity of retinal structures such as blood vessels (Figure 2). Our proposed methodology using dictionary learning and sparse representations effectively restores real fundus images by removing artifacts without altering surrounding pixels. The learned dictionary is effective in replicating the texture and structure of the considered regions, and the low and medium frequencies contain the relevant information, whereas high frequencies remain relatively unchanged to avoid learning noise.

Therefore, our approach offers a promising solution for the digital restoration of fundus images for better diagnosis and treatment. The proposed methodology can be a useful tool for ophthalmologists to obtain accurate diagnoses and subsequent digital processing.

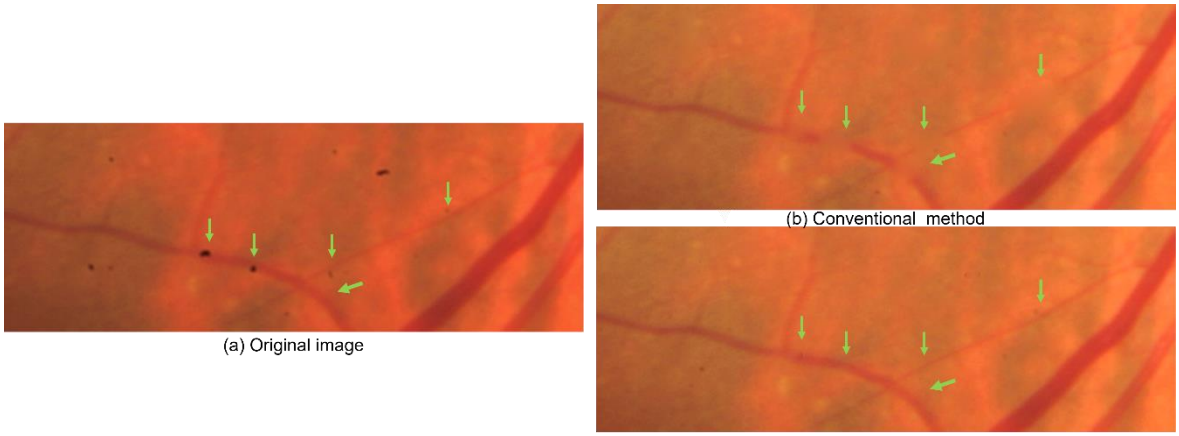

Figure 2: Comparison of Inpainting Methods for Dust Artifact Removal in Retinal Images:(a) Original image, (b) Conventional method, (c) Proposed method. The regions of interest are indicated by arrows.

ACKNOWLEDGEMENTS: The authors acknowledge the financial support from the Universidad Technológica de Bolívar (project CI2021P04) and Agencia Estatal de Investigación (España) (PID2020-114582RB-I00/ AEI / 10.13039/501100011033). Authors are grateful to J. L. Fuentes from the Miguel Servet University Hospital (Zaragoza, Spain) for providing images. E. M. Barrios thanks Minciencias and Sistema General de Regalías (Programa de Becas de Excelencia) for a PhD scholarship.

---

[1] M. D. Abramoff, M. K. Garvin, and M. Sonka; "Retinal imaging and image analysis," IEEE Reviews in Biomedical Engineering, vol. 3, pp. 169-208 (2010).
[2] K. V. Chalam and S. Sambhav; Expert Review of Ophthalmology, vol. 7, no. 3, pp. 287-302 (2012).
[3]E. M. Barrios, E.Sierra, L. A. Romero, M. S. Millán, and A. G. Marrugo; Óptica pura y aplicada, 54(3), 1-14 (2021).
[4]M. Elad and M. Aharon; IEEE Transactions on Image Processing, 15, 3736 (2006).
[5] J. M. Bueno, J. F. Vélez, M. E. Gegúndez-Arias, J. M. García, and J. M. Marín; Journal of Visual Communication and Image Representation, vol. 25, pp. 137-152 (2014).

Towards a low-cost optical biometer: development of a low-cost optical delay line for axial scans and a whole-eye beam scanner for fixation checks.

María Pilar Urizar[1,2], Álvaro de la Peña[2], Enrique Gambra[1], Alberto de Castro[2], Onur Cetinkaya[3], Susana Marcos[2,4] and Andrea Curatolo[3]

[1] 2EyesVision, Madrid, Spain
[2] Instituto de Óptica "Daza de Valdés", Consejo Superior de Investigaciones Científicos (IO-CSIC), Madrid, Spain
[3] International Center for Translational Eye Research and Institute of Physical Chemistry, Polish Academy of Science, Warsaw, Poland
[4] Center for Visual Science, The Institute of Optics: Flaum Eye Institute. University of Rochester, New York, USA

Contact: purizar@2eyesvision.com

1. Introduction

Optical coherence tomography (OCT) is a non-invasive biomedical imaging technique widely used in ophthalmology for ocular biometry[1] to measure the intraocular distances of an eye. Ocular biometry is indispensable in cataract surgery planning to select the intraocular lens to implant. However, either due to the use of high-cost components or to the limited transportability of OCT-based optical biometers, there is still reduced accessibility to this technology in remote and low-resource settings[2]. To increase patients' access to optical biometry we propose the low-cost development of two of the main components of an OCT-based optical biometer.

On one side, we propose a novel low-cost frequency-domain optical delay line (FDODL) which, integrated into a time-domain (TD)-OCT system, performs 1-D axial eye scans. FDODLs, typically based on galvanometric scanners, have been used for rapid and long-range scanning as they only involve varying the tilt of a small mirror to generate an axial scan. To reduce the FDODL cost, we propose a redesign of the delay-actuator axis, prompting the replacement of the expensive galvanometric scanner by an inexpensive stepper motor spinning a mirror at a constant tilt to the motor's axis[3]. The novel low-cost FDODL allows to independently select the scan range and frequency by changing the mirror tilt angle and motor speed respectively, unlike in galvanometer mirror-based FDODLs.

On the other hand, whole-eye 2-D cross-sectional scans are also of high interest in ocular biometry as they allow to obtain structural information of the anterior and posterior segments of the eye as well as checking proper fixation for improved measurement repeatability[4]. However, conventional OCT systems cannot switch between both eye segment scan configurations unless some optical components are changed to account for the eye refraction. In this work, we propose a versatile and low-cost whole-eye beam scanner based on three ETLs capable of non-mechanically switching between anterior and posterior segment imaging configurations, *i.e.*, performing dynamic focusing and control of the beam direction[5]. We experimentally validated both scanning components when integrated into different OCT systems to image various ocular samples.

2. Methods and results

The optical design of the proposed spinning tilted mirror (STM)-based FDODL is shown in Figure 1(a). The optical pathlength (OPL) is varied during the STM rotation along a circular path generated by the light beam reflected from the STM on the diffraction grating (DG). The axial scan range for a given rotation is proportional to the diameter of the circle at the DG. The STM-FDODL was integrated into a TD-OCT system with a dual-sample arm with a fixed delay between the two arms, allowing to focus on both ocular segments to improve the signal collection and to compensate for the vitreous body length. The STM was mounted with a tilt of 1.5 deg, resulting in a scan range of 7.31 mm at 10 Hz. The experimental measurement of the intraocular distances of a model eye (Modell-Augen Manufaktur) is shown in Figure 1(b) after analogue signal processing to extract its

envelope. By considering the delay introduced between the two sample arms (see Figure 1(c)) the measured central corneal thickness (CCT), anterior chamber depth (ACD) and axial length (AXL) of the model eye were 0.504 mm, 3.513 mm and 23.973 mm respectively, in good agreement with the specifications from the manufacturer.

The working principle of the proposed low-cost whole-eye beam scanner is presented in Figure 1 (d),(e). It combines three ETLs arranged in a double pass configuration, such that the light beam firstly propagated on-axis through the three ETLs and then it propagates off-axis through two of the ETLs due to a crucial offset $\mathrm{h_{in}}$ induced by a hollow-roof mirror HRM. By setting a combination of the focal lengths of $\mathrm{ETL_1}$ and $\mathrm{ETL_2}$ the scanning configuration is dynamically changed from a parallel displacement of the beam axis to an angular displacement pivoting the beam axis at the eye pupil. The additional combination of the focal length of $\mathrm{ETL_3}$ allows for a simultaneous dynamic focusing. After an analytical characterization and an experimental calibration of the focal length and scanning capability, the low-cost whole-eye beam scanner was connected to a custom swept source (SS)-OCT system. We imaged an *ex vivo* rabbit eye in both imaging configurations (see Figure 1 (c)). A wealth of details are visible in the cornea, iris and lens in the anterior segment scan, while the visibility of details of the retina is restored with the posterior segment scan.

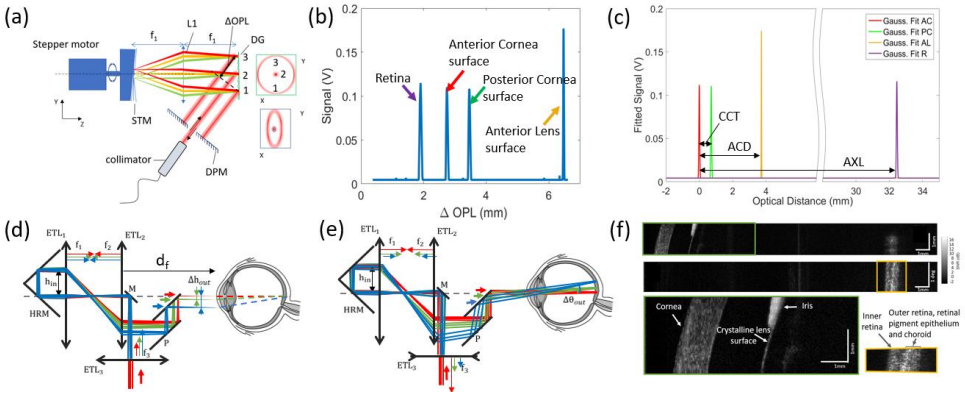

Figure 1 – (a) Schematic of the STM-FDODL. (b) Recorded A-scan OCT envelope for a model eye as a function of the scanned OPL in the dual-sample arm TD-OCT biometer. (c) Plot of the gaussian fits to the OCT envelope of each ocular surface. Schematic of the whole-eye scanner for (d) the anterior and (e) posterior segment imaging configurations. (f) *Ex vivo* rabbit eye images acquired with the whole-eye OCT system. Anterior (top) and posterior (bottom) segment scans with close-up in green and yellow boxes.

3. Conclusions

We presented the development of two important components of a low-cost OCT-based optical biometer: a low-cost delay line capable of scanning long axial ranges to measure the intraocular distances of an eye, and a low-cost whole-eye beam scanner capable of dynamic focusing and scan configuration switching. We have characterized their scanning capabilities in different OCT systems and imaged various ocular samples. Sourcing components affording larger transversal and axial scan ranges and faster scan speeds will allow for *in vivo* use.

ACKNOWLEDGEMENTS: This project has received funding from the Spanish Government (PID2020-115191RB), the Madrid Government (IND2019/BMD-17262) and Fundacja na rzecz Nauki Polskiej (MAB/2019/12).

[1]Hitzenberger, C.K., et al., Investigative Ophthalmology & Visual Science, 57 (9), OCT460 (2016)
[2]Grimes, C.E., et al., World J. Surg., 35 (5), 941 (2011)
[3]Urizar, M.P., et al., SPIE BiOS, PC12367 (2023)
[4]Ma, J., et al., Clin Ophthalmol, 15 (2021)
[5]Urizar, M.P., et al., Biophotonics Congress: Biomedical Optics, CS2E.3 (2022)

Wavefront shaping and Optical Memory Effect of ex-vivo cataractous crystalline lenses

Elena Moreno[1], Alba M. Paniagua-Díaz[1], Inés Yago[2], José María Marín[2] and Pablo Artal[1]

[1]Laboratorio de Óptica, Universidad de Murcia, Campus de Espinardo, 30100 Murcia, Spain

[2] Oftalmología, Hospital Universitario "Virgen de La Arrixaca", El Palmar, Murcia, Spain

Contact: e.morenorubio@um.es

Introduction. Cataracts increase is an ocular pathology that impairs vision due to intraocular light scattering in the crystalline lens. Controlling the propagation of light through scattering media is a challenge of interest in different fields and there issubstantial effort put into overcoming this issue. In recent years Wavefront Shaping (WS) techniques appeared as an excellent tool to control the propagation of light through scattering materials[1]. WS is based on the coherent control of the wavefront incident on a scattering medium, using a spatial light modulator for the local manipulation of the phase and/or amplitude of the wavefront. Recently wavefront shaping techniques have been suggested for the optical (non-surgical) correction of scattering in cataractous lenses[2] aided by the Optical Memory Effect, to predict the optimal isoplanatic patch of the potential optimized image[3]. In this work we perform wavefront shaping optimizations on human cataractous crystalline lenses for the first time, measuring their Optical Memory Effect before and after the wavefront optimization has been performed, which allows us to perform a more rigorous prediction regarding the optimized image isoplanatic path.

Methods. A schematic for the wavefront shaping technique is shown in Fig. 1a. A 532 nm laser is expanded and sent to a spatial light modulator to shape the wavefront in phase. The shaped wavefront is then sent to an excised human cataractous crystalline lens. The lenses are mounted on kinematic mounts allowing for lateral translation and angular rotation. In this case, the wavefront optimization is performed in a single pass through the lens, simplifying the system. At the focal plane of the lens we placed a photodiode, which we also exchanged by a camera for quality checks and for the OME measurements. The transmitted intensity is then filtered by a 50 µm pinhole and collected by a photodiode, to make the optimization simpler and faster. The intensity collected by the photodiode works as feedback for an algorithm that controls the spatial light modulator, modifying the phase of the incident wavefront in order to increase the intensity at the photodiode.

The Optical Memory Effect (OME) is an intrinsic correlation of scattering media that has been known to provide the isoplanatic patch of different imaging techniques, determining how the transmitted speckle pattern changes with a tilt/shift of the incident beam[4]. Usually this is measured using a collimated laser beam impinging on a scattering medium. However, when the incident beam has been modified, i.e. by wavefront shaping, the isoplanatic patch can be different. We measured the OME for these two approaches using a 532 nm laser incident on different cataractous lenses, first by recording the transmitted speckle pattern for different values of tilt/shift of the lens and comparing them via a cross-correlation, second after the wavefront optimization was performed.

For each cataract stage, we also characterized scattering using the straylight parameter, measured with the Optical Integration Method[5], and the Michelson Contrast of the transmitted images. A total of 9 lenses of donors aged between 21 and 62 were measured.

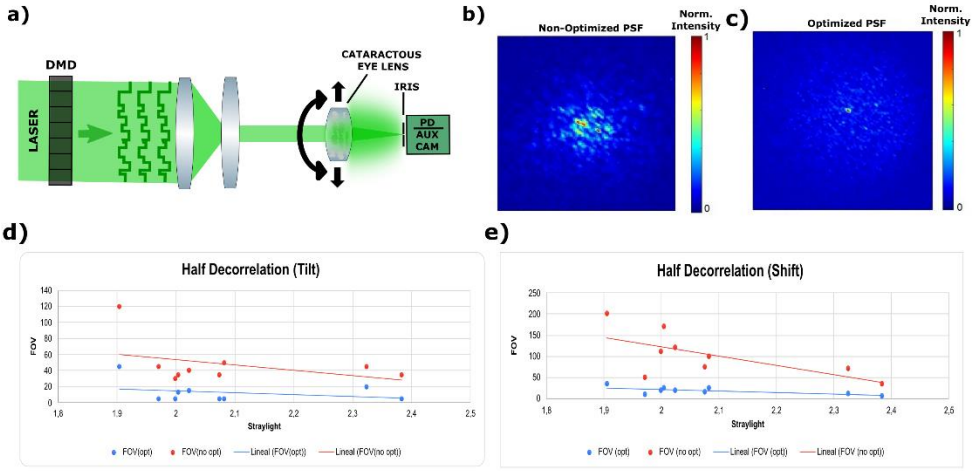

Figure 1: a) Schematic of the experimental setup of wavefront shaping through cataracts. b) Non-optimized beam passing through a cataractous crystalline lens. c) Optimized beam where the spot is diffraction-limited in size. d) Graph representing the decorrelation or maximal Field of View (FOV) of an optimized image based on the OME for angular (tilt) changes of the lens (or translation ones (e)), when using a collimated beam (red) or wavefront-optimized beam (blue) incident on the scattering medium.

Results. We demonstrated for the first time the PSF optimization through cataractous lenses using wavefront shaping techniques, with a signal to noise ratio of the order of 10 (Fig1b-c). We additionally studied the OME with the optimized wavefront and with a regular collimated beam, finding important differences in the maximal range or isoplanatic patch where the wavefront optimization is still valid, equivalent to the maximal size of the potential optimized wide-angle image through cataracts. As shown in Fig 1d-e we found the isoplanatic patch is smaller when the incident wavefront is optimized compensating the scattering process, representing a more accurate prediction for the maximal isoplanatic patch for the optimized images.

Conclusions. The PSF of ex-vivo cataractous crystalline lenses has been corrected for the first time using wavefront shaping techniques, with signal to noise ratios in the order of 10. The OME of cataractous lenses has been measured with the optimized wavefront for the first time, showing significant differences with respect to the traditional measurements with a collimated beam, providing us with a more robust approximation of the maximal isoplanatic patch for a wide-angle optimized image. This work paves the way to approaches for the non-invasive correction of cataracts using wearable devices.

---

[1]Vellekoop, I. M., & Mosk, A. P. *Optics letters*, **32**(16), 2309 (2007).

[2]Paniagua-Díaz, A. M. *et al*. *Optics Express*, **29**(25), 42208 (2021).

[3]Paniagua-Díaz, A. M. *et al*. *Biomedical Optics Express*, **14**(2), 639 (2023).

[4]Osnabrugge, G. *et al*. *Optica*, **4**(8), 886 (2017).

[5]Ginis, H. *et al*. *J. Vis*. **12**(3), 20 (2012).

Eye dominance and visual quality

Pilar Granados-Delgado[1], Miriam Casares-López[1] and José Juan Castro-Torres[1]

[1] Laboratory of Vision Sciences and Applications, Department of Optics, Faculty of Sciences, University of Granada (Prof. Adolfo Rancaño, s/n 18071, Granada, Spain)

pilargrd@ugr.es

Introduction: Ocular dominance has been extensively studied and different types have been defined: sighting, motor, orientational, sensory and visual field. So far, there is no consensus on this issue due to the complexity of the task. Dependence on the method employed for measuring dominance has been found[1] and certain functional and organic characteristics have been analysed, finding no significant differences between dominant and non-dominant eyes[2,3].

Aim: To analyse the distribution of ocular dominance measured by sensory and sighting methods, as well as the relationship between dominance and optical quality indicators in young, healthy people. To analyse the relationship between different optical quality indicators.

Material and methods: An experimental study has been carried out in healthy young people. Sighting eye was determined with Miles test. Sensory eye dominance was determined with a polarised test (Randot Stereotest). We measured optical quality with objective tests: objective scattering index (OSI) using OQAS II and higher order aberrations (HOA) using WASCA (Wavefront Supported Custom Ablation) analyzer. We also evaluated visual performance by means of different visual functions: distance and near visual acuity; contrast sensitivity using OptoTab test for 5 different spatial frequencies; contrast sensitivity thresholds with and without glare using CGT-1000; psychophysical measurement of straylight using C-Quant; and the perception of halos, analysing the visual discrimination capacity by means of the visual disturbance index (VDI) using the Halo test.

Results: Twenty-eight participants were enrolled, 6 men and 22 women (mean age 25.7 ± 5.9 years). The right eye (RE) was sensory dominant in 82.1% of the cases and sighting eye in 50%. Only nine participants presented a sensory eye different from the sighting eye; thus, the analysis of mean differences was carried out exclusively on these nine participants. The means and the results obtained in the mean comparison tests are shown in Table 1. The p-values obtained were higher than 0.05, so no statistically significant differences were found between the sensory dominant and directional dominant eye measures for all the visual variables studied. When analysing the relationship between different visual function (56 eyes in total), we obtained significant positive correlations between OSI and VDI values (rho= 0.306; p-value= 0.022), between OSI and Glare contrast threshold, GCT (rho= 0.314; p-value= 0.018), and between VDI and Glare contrast threshold (rho= 0.227; p-value= 0.038). The graphical representation of the correlations obtained is shown in Figure 1.

Discussion and Conclusions: We found no significant differences in any parameter of visual quality that would make us lean towards one type of dominance (sensory and sighting) or relate the optical quality of the image to the type of dominance. These results are in line with previous findings[3,4]. The relationship between VDI and GCT indicates that a poorer visual discrimination capacity is related to a lower contrast sensitivity under glare conditions. Moreover, the relationship found between straylight and OSI shows that the greater the intraocular straylight, the higher the intraocular scattering (i.e., the worse the optical quality). These results agree with previous research[5]. The visual variables studied to evaluate optical quality are related to each other, so we can affirm that better optical quality defines neither sensory nor sighting dominance.

	Type of ocular dominance	Mean ± SD	Statistics	Sig.
Distance VA	Sensorial DE	1.10 ± 0.14	t = -0.926	0.368
	Sighting DE	1.15 ± 0.08		
Near VA	Sensorial DE	1.18 ± 0.05	U = 48.500	0.489
	Sighting DE	1.19 ± 0.06		
Straylight (log(s))	Sensorial DE	0.88 ± 0.15	t = 0.731	0.475
	Sighting DE	0.83 ± 0.13		
Distance CSF	Sensorial DE	98.69 ± 17.36	t = 0.714	0.486
	Sighting DE	93.29 ± 14.62		
Near CSF	Sensorial DE	112.40 ± 9.84	t = -0.525	0.607
	Sighting DE	114.47 ± 6.53		
OSI	Sensorial DE	0.52 ± 0.29	t = 0.183	0.857
	Sighting DE	0.50 ± 0.23		
HOA RMS	Sensorial DE	0.55 ± 0.20	t = 0.948	0.357
	Sighting DE	0.46 ± 0.20		
VDI	Sensorial DE	0.35 ± 0.21	U = 30.000	0.387
	Sighting DE	0.26 ± 0.15		
Non-glare contrast threshold	Sensorial DE	0.04 ± 0.01	U = 43.000	0.863
	Sighting DE	0.04 ± 0.02		
Glare contrast threshold	Sensorial DE	0.07 ± 0.02	U = 41.000	1.000
	Sighting DE	0.08 ± 0.05		

Table 1: Mean monocular values of the 9 participants for the different visual variables studied and statistics

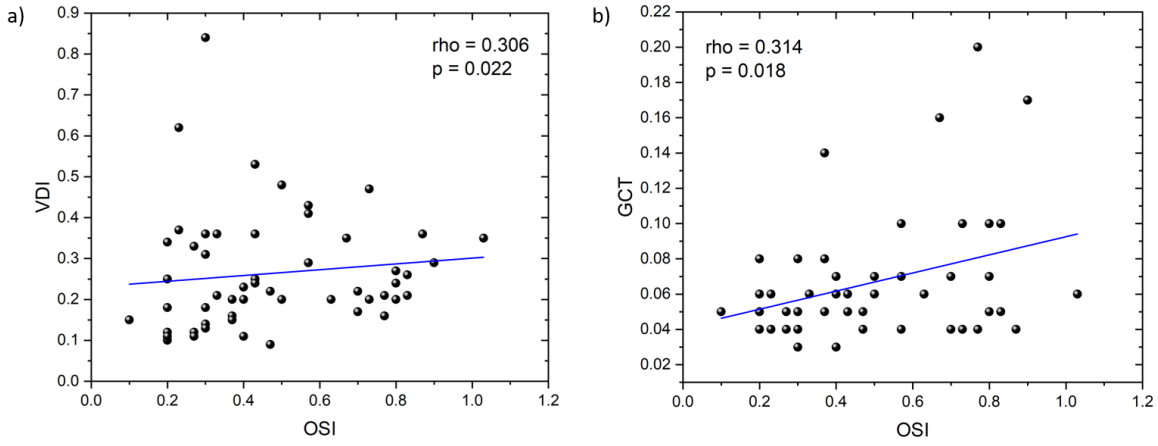

Figure 1: Correlations between visual functions (VDI and GCT) and OSI for the 28 participants

ACKNOWLEDGEMENTS: Grants PID2020-115184RB-I00, funded by MCIN/ AEI/10.13039/501100011033, and A-FQM-532-UGR20, funded by FEDER/Junta de Andalucía-CTEICU.

[1]A. Mapp and R. Barbeito; *Perception & Psychophysics*, **65**, 310 (2003).
[2]D. Lopes-Ferreira and H. Neves; *BioMed Research International*, **2013**, 7 (2013).
[3]G. Perkel and S. Akbulut; *Optometry and Vision Science*, 98, 285 (2021).
[4]. T. Ooi and Z. He; *Eye and Brain*, **2020**, 25 (2020).
[5]. L. Yao and Y. Xu; *Translational Vision Science & Technology*, **9**, 13 (2020).

Clinical validations of the SimVis binocular visual simulator

Amal Zaytouny[1], Irene Sisó-Fuertes[2], Xoana Barcala[2], Lucie Sawides[1,2], Carlos Dorronsoro[1,2], Susana Marcos[1,3]

[1]Consejo Superior de Investigaciones Científicas, Instituto de Óptica; Madrid, Spain.
[2]2EyesVision; Madrid, Spain.
[3]Center for Visual Science; Flaum Eye Institute, The Institute of Optics, University of Rochester, NY, United States.
Contact: amal.z@csic.es

Surgical lens exchange is the main treatment for presbyopia. Since not all presbyope patients accept in the same way the prescribed corrections, preoperatively selecting the optimal intraocular lens (IOL) design for each subject becomes crucial[1]. Presbyopia correcting surgery can give uncertain visual outcomes, which sometimes results on a low uptake of multifocal IOLs (MIOLs). The decision of what correction will better meet patient's particular needs is seldom based on their actual visual experience with the solutions to be offered. Both clinicians and patients would benefit from knowing the prospective vision, in an attempt to customize the IOL prescription[2].

Post-operative outcomes are assessed to study the performance of the lenses once implanted. The quality of vision provided by MIOLs, monovision approaches and combined strategies is limited to be tested using visual acuity (VA) charts at discrete distances or through questionnaires who self-report visual comfort in particular circumstances. But perception is multifactorial and complex, and it largely depends on visual conditions that require most sophisticated evaluation methods that may include the influence of pupil diameter, dominance strength, luminance conditions, contrast sensitivity of the spatial content, tridimensional vision, among others.

SimVis Gekko™ (2EyesVision, Madrid, Spain) is a binocular visual simulator that allows patients to experience the vision with different corrections before undergoing surgery.

See-through simulations allow performing clinical evaluations and study the visual perception of pseudophakic patients by combining their own ocular aberrations and perception with the simulation of presbyopic corrections[2].

After many years of technological development, several clinical studies with patients using SimVis Gekko have been performed lately to verify that the real vision through different corrections can be accurately reproduced[3-6]. Tests that assess the components that conform the final visual perception have been carried out in presbyope patients through the device to see whether the simulations can reproduce and capture the multifactorial elements of the visual function [6-12].

In a recent study, a new metric (Multifocal Acceptance Score to Evaluate Vision, MAS-2EV)[5] that allows to study the perceived visual quality under different conditions was developed. This metric demonstrated how it can be applied in combination with SimVis Gekko simulations to stablish a correction preference of prospective presbyopic corrections in patients prior to contact lens fitting or IOL implantation.

The viability of visual simulations of presbyopic corrections in patients with cataract was also assessed[10]. Cataract patients were tested preoperatively and postoperatively after bilateral implantation of monofocal intraocular lenses. From various simulated presbyopic corrections with the SimVis Gekko, results showed how the individual perceptual scores were highly correlated

preoperatively vs postoperatively ($p<0.0005$) for all corrections and distances.
From the simulation of commercial MIOLs[11], we saw from the findings the good correspondence between real and simulated through focus visual acuity (TFVA) curves in a sample of presbyope patients when mimicking commercial IOLs (Xcorr>0.90). Also, when studying the effect of the pupil diameter in the simulations, no statistical differences have been found between results under dilation or with natural pupils, exhibiting a very high similarity between both TFVA curves independently of the eye's pupil diameter (Xcorr>0.92).
The degradation of contrast sensitivity has also been proven when testing simulated monovision approaches of commercial IOLs, in which micro-monovision targets seemed to produce a larger decrease in the contrast sensitivity function (CSF) than when assessed in pure monovision corrections. The SimVis Gekko has demonstrated that eye monovision correction preference can be obtained from psycophysical tests[12], as well as the dominance strength between eyes at near and far distances. Besides, measurements performed through SimVis Gekko simulations studying stereoacuity have reported no statistical differences when compared with standard methods, which demonstrate that the device can also capture the tridimensional vision when using different tests at distance ($p>0.05$).

1. Charman WN. Developments in the correction of presbyopia I: Spectacle and contact lenses. Ophthalmic Physiol Opt 2014.
2. Radhakrishnan A, Pascual D, Marcos S, Dorronsoro C. Vision with different presbyopia corrections simulated with a portable binocular visual simulator. PLoS One 2019.
3. Radhakrishnan A, Dorronsoro C, Marcos S. Differences in visual quality with orientation of a rotationally asymmetric bifocal intraocular lens design. J Cataract Refract Surg 2016.
4. Benedi-Garcia C, Vinas M, Lago CM, Aissati S, de Castro A, Dorronsoro C, Marcos S. Optical and visual quality of real intraocular lenses physically projected on the patient's eye. Biomed Opt Express. 2021 Sep 17;12(10):6360-6374. doi: 10.1364/BOE.432578. PMID: 34745742; PMCID: PMC8548014.
5. Barcala X, Vinas M, Romero M, Gambra E, Mendez-Gonzalez JL, Marcos S, Dorronsoro C. Multifocal acceptance score to evaluate vision: MAS-2EV. Sci Rep. 2021 Jan 14;11(1):1397. doi: 10.1038/s41598-021-81059-0. PMID: 33446794; PMCID: PMC7809428.
6. Lago, C. M., de Castro, A., Benedí-García, C., Aissati, S., & Marcos, S. (2022).; Evaluating the effect of ocular aberrations on the simulated performance of a new refractive IOL design using adaptive optics. Biomedical Optics Express 2022, 13(12), 6682-6694.
7. Vinas M, Benedi C, Sissati C, Pascual D, Vias A, Dorronsoro C, et al. Visual Simulators replicate vision with multifocal lenses. Sci Rep 2019
8. Vinas M, Aissati S, Romero M, Benedi-Garcia C, Garzon N, Poyales F, Dorronsoro C, Marcos S. Pre-operative simulation of post-operative multifocal vision. Biomed. Opt. Express 10, 5801-5817 (2019)
9. Barcala X, Vinas M, Ruiz S, Hidalgo F, Nankivil D, Karkkainen T, Gambra E, Dorronsoro C, Marcos S. Multifocal contact lens vision simulated with a clinical binocular simulator. Cont

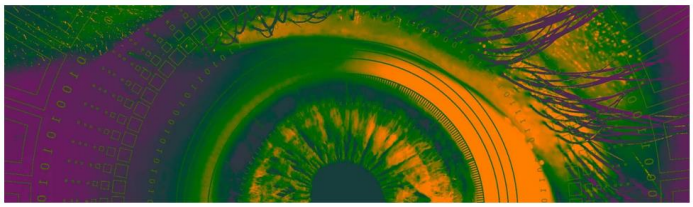

TRAVEL GRANTS AWARDEES | SPIE

1	**Alejandro Martínez Giménez**	11	**Joan Goset**
2	**André Amorim**	12	**José A.R. Monteiro**
3	**Danielle Viviana Ochoa**	13	**Lourdes Camblor**
4	**Diana Gargallo**	14	**Maria Mechó Gracia**
5	**Eduardo Esteban Ibáñez**	15	**Marina Bou**
6	**Elena Moreno**	16	**Pilar Casado**
7	**Erik Miguel Barrios**	17	**Rosa Vila Andrés**
8	**Xinyu Wang**	18	**Sara Ferrer**
9	**Iñaki Blanco**	19	**Sara Lima**
10	**Jessica Gomes**	20	**Sara Silva**

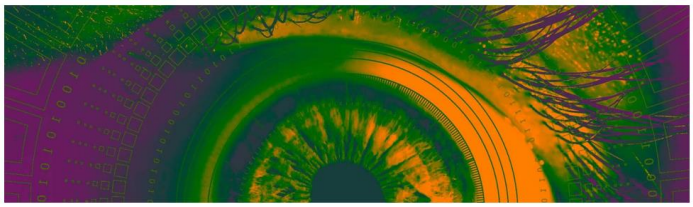

TRAVEL GRANTS AWARDEES | OPTICA

1 **Alba Herrero**
2 **Alba Paniagua**
3 **Anabel Martínez Espert**
4 **Danielle Viviana Ochoa**
5 **Inas Baoud**
6 **Victor Rodríguez Lopez**
7 **Alejandro Martínez Giménez**
8 **Paula García**
9 **Raquel Salvador**
10 **Francesco Martino**

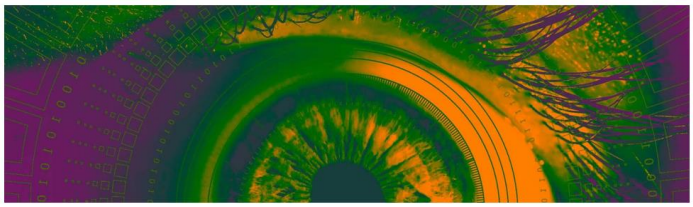

AWARDS | OPTICA-SEDOPTICA

1 **Alba Paniagua**

2 **Lourdes Camblor**

3 **Rosa Vila Andrés**

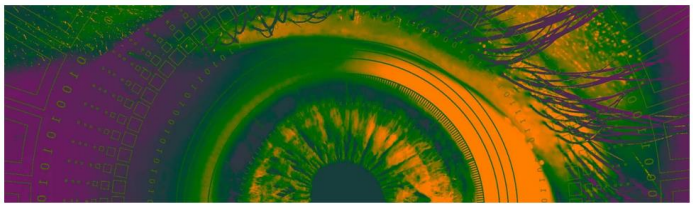

BER2023 ATTENDEES

1. *Carlos Dorronsoro*
2. *Marina Bou Marin*
3. *Aina Turull Mallofré*
4. *Fatima Cuellar Santiago*
5. *Fidel Vega*
6. *Amal Zaytouny*
7. *Joan Goset*
8. *Jaume Pujol Ramo*
9. *Clara Mestre*
10. *María Pilar Urizar*
11. *Meritxell Vilaseca*
12. *Enric Pérez Parets*
13. *Maria Viñas-Peña*
14. *Mikel Aldaba*
15. *Alejandro Martínez*
16. *Zhijian Zhao*
17. *Santiago Sager La Ganga*
18. *Pilar Casado*
19. *Miguel Gómez del Río*
20. *Brian Vohnsen*
21. *Justo Arines*
22. *Diana Gargallo Yebra*
23. *Laura Clavé*
24. *James Andrew Germann*
25. *Eduardo Esteban*
26. *Erik Miguel Barrios Montes*
27. *Jesus Armengol*
28. *María Sagrario Millán*
29. *Francesco Martino*
30. *Pilar Granados Delgado*
31. *Xinyu Wang*
32. *Alba M. Paniagua Díaz*
33. *Elena Moreno*
34. *Lourdes Camblor Navarro*
35. *Ebrahim Safarian Baloujeh*
36. *Danielle Viviana Ochoa Arbeláez*
37. *Sara Ferrer Altabás*
38. *Raquel Salvador Roger*
39. *Rosa Vila Andrés*
40. *Alba Herrero Gracia*
41. *Inas Baoud Ould Haddi*
42. *Paula García*
43. *João Manuel Maciel Linhares*
44. *Veronica Lockett Ruiz*
45. *José Alexandre Monteiro*
46. *Sara Lima*
47. *Jorge Lasarte Sanz*
48. *Alejandra Consejo*
49. *M-Carmen Martinez-Garcia*
50. *Victor Rodriguez Lopez*
51. *Jessica Gomes*
52. *Yaiza Garcia Sanchez*
53. *Petros Papadogiannis*
54. *Patrícia Oliveira*
55. *Dayan Flores Cervantes*
56. *Pablo Perez Merino*
57. *Miriam Casares López*
58. *Anabel Martínez Espert*
59. *Gonzalo Velarde*
60. *Juan Manuel Bueno*
61. *Cátia Magalhães*
62. *Iñaki Blanco*
63. *Judith Birkenfeld*
64. *María Mechó García*
65. *Sara Silva-Leite*
66. *André Rino Amorim*
67. *Francisco Avila*
68. *Laura Remon*
69. *Pablo Artal*
70. *Oscar del Barco*
71. *Sara Perches*
72. *Valentin Guadaño*

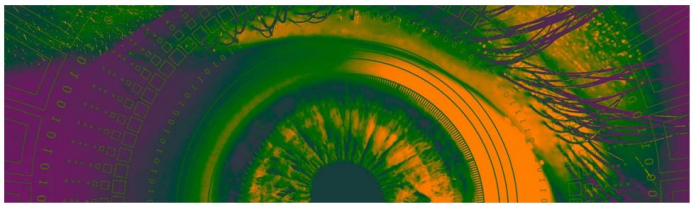

SOME BER2023 MOMENTS

BER2023 group picture

Early careers session

Keynote session


2007
Universidad
Zaragoza


The interest in the eye's optical quality has been focussed in the central part (fovea)
150x130 deg

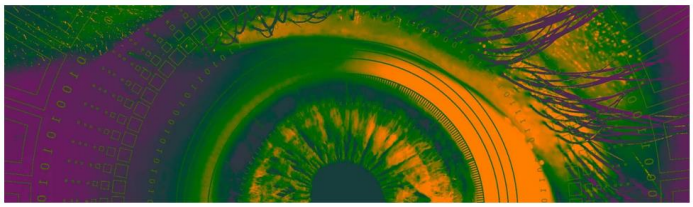

Dinner with the experts









Scientific sessions


Universidad
Zaragoza

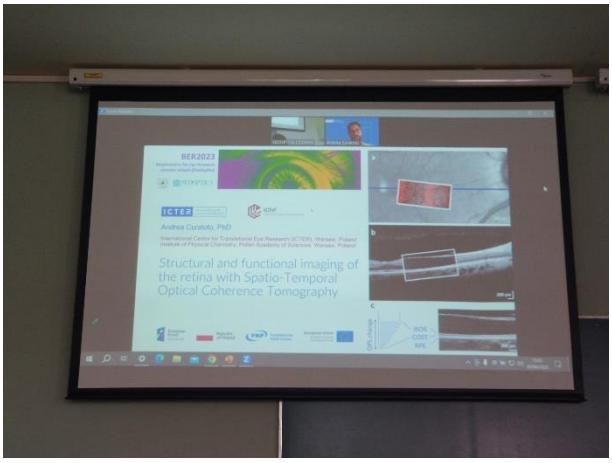
BER2023
Structural and functional imaging of the retina with Spatio-Temporal Optical Coherence Tomography


Universidad
Zaragoza


Simulation and validation of multifocal lenses with SimVis technology
Universidad
Zaragoza


Universidad
Zaragoza


Universidad
Zaragoza


Universidad
Zaragoza


Universidad
Zaragoza

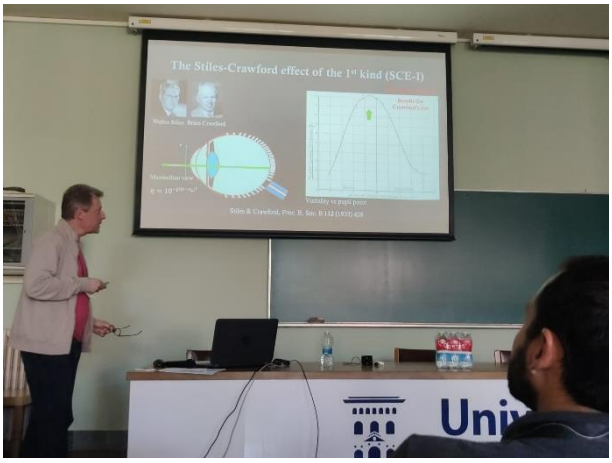
The Stiles-Crawford effect of the 1st kind (SCE-I)


THANK YOU!
Universidad
Zaragoza


Universidad
Zaragoza


Universidad
Zaragoza


imTOPscanner: system design and customization

Young researchers session

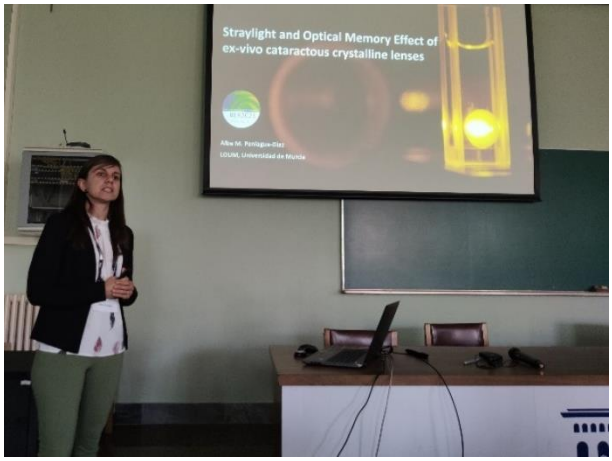

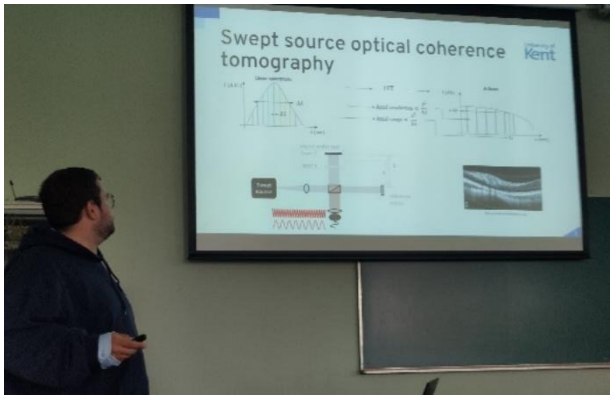
Swept source optical coherence tomography
Kent


BER2023
Biophotonics for Eye Research
summer school @Sedoptica
1-4 JUNE 2023 IACA, SPAIN
CLINICAL VALIDATION OF DAILY SOFT MULTIFOCAL CONTACT LENS SIMULATIONS USING SIMVIS GEKKO BASED ON IN-VITRO MEASUREMENTS

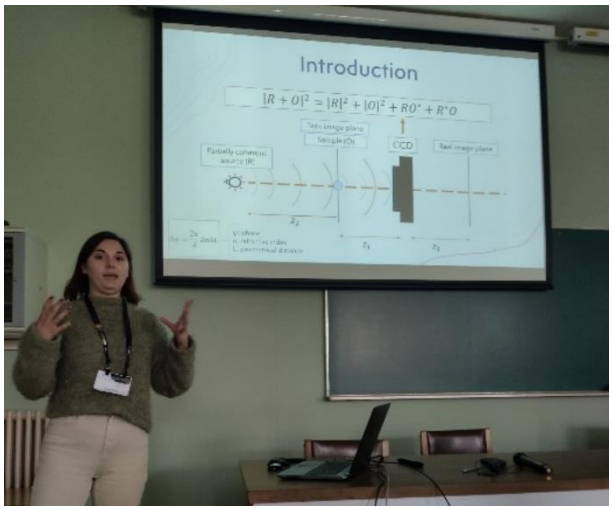
Introduction
CCD

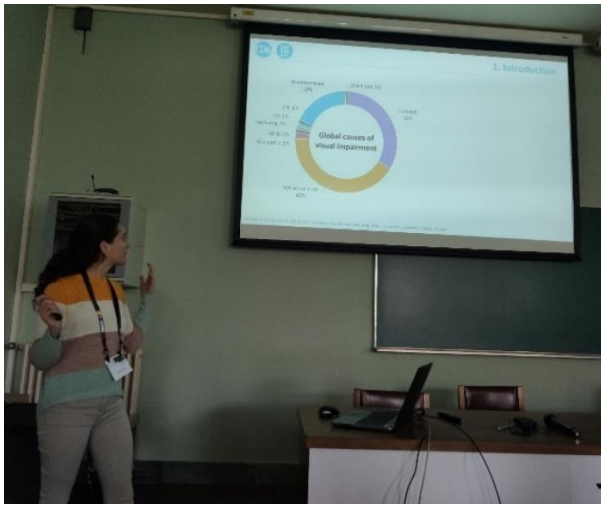
1. Introduction
Global causes of visual impairment

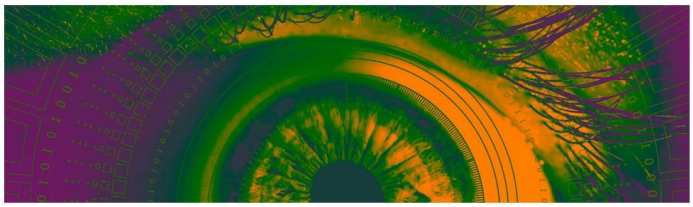


University of Kent

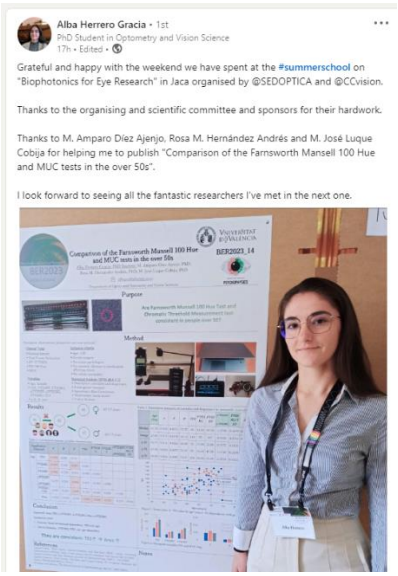
Alba Herrero Gracia • 1st
PhD Student in Optometry and Vision Science
17h • Edited •
Grateful and happy with the weekend we have spent at the #summerschool on "Biophotonics for Eye Research" in Jaca organised by @SEDOPTICA and @CCvision.
Thanks to the organising and scientific committee and sponsors for their hardwork.
Thanks to M. Amparo Díez Ajenjo, Rosa M. Hernández Andrés and M. José Luque Cobija for helping me to publish "Comparison of the Farnsworth Mansell 100 Hue and MUC tests in the over 50s".
I look forward to seeing all the fantastic researchers I've met in the next one.


Ines Baoud • 1st
Estudiante de doctorado y Msc en Optica y Optometría
1d •
What an amazing experience at the "BER2023 Congress" in Jaca (Spain)! I want to thank @SEDOPTICA and @CCVision for organizing this enriching event. I learned a lot, made new friends, and expanded my professional network. I'm thrilled about what I've learned and excited to apply it! #BER2023 #summerschool #Networking #ContinuousLearning


Rosa Vila • 1st
PhD-FPU student - Researcher at the University of Valencia. Optoelectronic ...
2d •
There was no better way to conclude this edition of Biophotonics for Eye Research than by receiving the honor of the Best Young Scientific Communication Award.
I cannot express with words how extraordinary it has been for me to have the opportunity to share the preliminary results of my PhD research with all the attendees. I'm very grateful to my PhD advisors Vicente Micó and Jose Juan Esteve Taboada for their great support and guidance.
I would like to extend my gratitude to the Scientific Committee, the Local Committee, and all the sponsors for their invaluable contributions towards organizing this exceptional event. I also deeply appreciate all the researchers who generously shared their remarkable findings, further enriching our knowledge. See you in the next edition!
Furthermore, I am truly grateful to OPTICA and SPIE for providing travel grants to early career assistants.

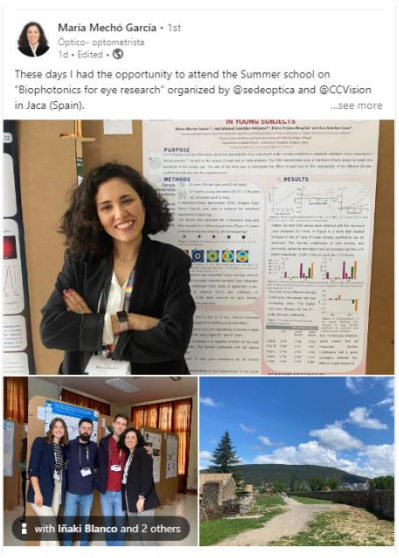
María Mechó García • 1st
Óptico- optometrista
1d • Edited •
These days I had the opportunity to attend the Summer school on "Biophotonics for eye research" organized by @sedeoptica and @CCVision in Jaca (Spain). ...see more
with Iñaki Blanco and 2 others

x

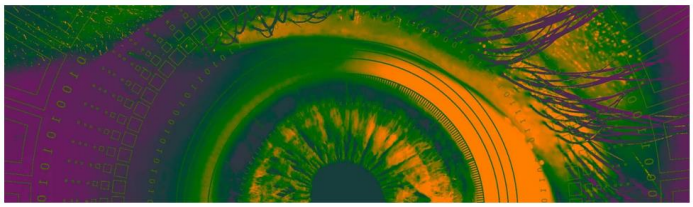

BER2023

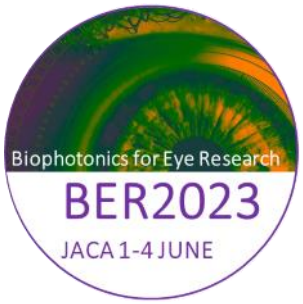

SmarThings4Vision

2EYESVISION

THORLABS

imagine eyes

SEDOPTICA
SOCIEDAD ESPAÑOLA DE ÓPTICA

Comité de Ciencias de la Visión

Universidad Zaragoza

SPIE.

OPTICA
Advancing Optics and Photonics Worldwide